공학박사 학위논문

A Study on Decision Making Procedures for Reduction of Carbon Emission and Energy Consumption of Process Systems

공정시스템의 이산화탄소 배출 및 에너지 소모 절감을 위한 의사결정 절차에 관한 연구

2012년 8월

서울대학교 대학원
화학생물공학부
김 승 혁

Abstract

A Study on Decision Making Procedures for Reduction of Carbon Emission and Energy Consumption of Process Systems

Seunghyok Kim

School of Chemical and Biological Engineering

The graduate school

Seoul National University

This thesis has presented the decision making procedures for mitigation of carbon dioxide (CO_2) emission and energy consumption of process systems, and its applications using various modeling, simulation, and optimization techniques. The conventional chemical processes, heretofore, are designed or revamped in terms of the efficiency of cost and energy. However, the management of chemical processes could not be treated as the matter of efficiency exclusively as the emission of greenhouse gas and the depletion of fossil fuel are becoming global issues. The sustainable development of chemical processes is inevitable, consequently. There are some phases of decision making for sustainable development. Namely, selection of feed, planning, and policy of

operation can be included in phases of decision making. Life cycle assessment can be introduced for appropriate decision making. Life cycle assessment is a technique to assess environmental impacts associated with all the stages of a product's life from-cradle-to-grave (i.e. from raw material extraction through materials processing, manufacture, distribution, use, repair and maintenance, and disposal or recycling). It can help avoid a narrow outlook on environmental concerns by compling an inventory of relevant energy and material inputs and environmental releases, evaluating the potential impacts associated with identified inputs and releases, and interpreting the results to help you make a more informed decision. While the conventional life cycle assessment is mainly concerned with a product, in this thesis, the whole processes for production are defined as a life cycle of chemical processes. Therefore, one can consider environmental impacts of chemical processes in terms of CO_2 emission and energy consumption.

First of all, the detailed description of life cycle assessment are introduced. The framework and procedure of life cycle assessment is presented. For life cycle assessment, the goal and scope of life cycle should be defined. The prime goal is to mitigate the emission of CO_2 to lessen environmental impact. The scope is subject to each case study. All processes included in the scope are simulated using process simulator (i.e. Aspen Plus) and numerical methods.

In the second place, Monte Carlo simulation are performed to con-

sider uncertainties existing in life cycle of processes. In real world, there are many uncertainties in chemical processes, the decision maker could not trust reliable results obtained by deterministic model. Thus, we introduce the stochastic model by Monte Carlo simulation. Monte Carlo simulation can show more reliable results through probabilistic outputs.

Lastly, for optimal management strategies, approximate dynamic programming is introduced. While the concept of the backward recursion of dynmaic programming is so powerful, one has to remind that its usefulness can be limited for practical problems due to the curses of dimensionality. Approximate dynamic programming is based on an algorithmic strategy that steps forward through time. In addition, post-decisition state based approximate dynamic programming is introduced to compensate the shortcomings that approximate dynamic programming has.

Case studies are presented to show the effectiveness of proposed methodologies. In first case, evaluation of potential raw materials for dimethyl ether (DME) production is performed. DME is one of the promising new-generation energy and can be synthesized by various feeds. The life cycle of DME production, from collecting raw materials to synthesizing DME, is simulated by a process simulator (Aspen Plus). Using simulation data, the impact assessment of whole scope of DME production is performed. In second case, the planning of energy systems is performed considering uncertainties. The capacity to be added

is optimized based on probabilistic model. Also, the sensitivity of uncertain factors is analyzed. In third case, the life cycle of CO_2-enhanced oil recovery and storage process is addressed. Using the proposed procedures, the optimal selection of potential reservoirs is made. Finally, the control schemes of oil recovery and CO_2 storage are provided, and this result supports decision making for CO_2 disposal.

Keywords: optimal decision making, life cycle assessment, decision making procedure, sustainability

Student Number: 2006-21334

Contents

Abstract **i**

Chapter 1 Introduction **1**

1.1 Life cycle assessment 2

1.2 Sustainable development and sustainability 8

1.3 Proposed procedures for decision making 11

1.4 Research scope 15

1.5 Outline of thesis 17

Chapter 2 Background Theory **19**

2.1 Monte Carlo simulation 19

2.2 Finite volume method 29

2.3 Approximate dynamic programming 33

2.3.1 Introduction to dynamic programming 33

2.3.2 The three curses of dimensionality 38

2.3.3 Introduction to approximate dynamic programming 41
2.3.4 Approximate dynamic programming using post-decision state variable 47

Chapter 3 Evaluation of Raw Materials for DME Production System 51

3.1 Problem description 51
3.2 Life cycle assessment of DME production system 55
3.2.1 Goal and scope definition 55
3.2.2 Inventory analysis 58
3.3 Results and impact assessment 79
3.4 Cost analysis 83

Chapter 4 Energy Planning Model Considering Uncertainties 87

4.1 Problem description 87
4.2 Mathematical modeling 91
4.2.1 Definition of production costs 91
4.2.2 Learning effects 93
4.2.3 Fuel and carbon prices for handling uncertainties 96
4.2.4 Monte Carlo simulation 97
4.3 Structure of the proposed model 98
4.3.1 Structure of the problem 98

4.3.2 Optimization of energy planning 100
4.4 Results and their implications 106

Chapter 5 Optimal Management for CO_2 Enhanced Oil Recovery **113**

5.1 Problem description 113
5.1.1 Enhanced oil recovery (EOR) 115
5.1.2 Basics of reservoir modeling 117
5.2 Numerical modeling: two point flux approximation 124
5.3 Numerical modeling: miscible flow 129
5.3.1 Pressure change 129
5.3.2 Saturation change 133
5.4 Optimal management of the CO_2-EOR 137
5.4.1 Selection of feasible reservoir for CO_2-EOR 139
5.4.2 Numerical results of reservoir modeling 142
5.4.3 The calculation of the amount of CO_2 149
5.4.4 The calculation of energy requirement 157
5.5 Results and their implications 163

Chapter 6 Conclusion **173**

Bibliography **177**

List of Figures

Figure 1.1 The phases of life cycle assessment 4

Figure 1.2 An example of simulation using Aspen Plus . . . 12

Figure 1.3 An illustrative example of numerical modeling . 13

Figure 1.4 Proposed procedure for decision making 14

Figure 2.1 Schematic concept of Monte Carlo simulation . . 21

Figure 2.2 Schmetic diagram of TPFA 32

Figure 2.3 Example of a shortest path problem 34

Figure 2.4 Schmetic diagram of dynamic programming . . . 37

Figure 2.5 Schmetic diagram of post-decision state variable 49

Figure 3.1 DME production system 53

Figure 3.2 The defined scope of DME production life cycle . 57

Figure 3.3 Block diagram of conversion process for DME production using NG 63

Figure 3.4 Block diagram of coal-based DME production . . 72

Figure 3.5 Block diagram of waste wood-based DME production 76
Figure 3.6 The comparision of CO_2 emission intensity of each raw material 81
Figure 3.7 The comparision of energy intensity of each raw material 82
Figure 3.8 The cost intensity of each raw material 84

Figure 4.1 Alternative energy sources for energy and environment 88
Figure 4.2 Structure of the proposed model 99
Figure 4.3 The distribution result of total cost using Monte Carlo simulation 107
Figure 4.4 Sensitivity analysis of each uncertain variable . . 108
Figure 4.5 The amount to be added in each scenario 111
Figure 4.6 The proportion of energy sources in 2011, 2030 . 112
Figure 4.7 The estimation supply of renewable energy sources 112

Figure 5.1 The defined CO_2 emission life cycle 114
Figure 5.2 The methods of enhanced oil recovery 117
Figure 5.3 Schematic scheme of solution 136
Figure 5.4 The block diagram of defined life cycle of CO_2 enhanced oil recovery 138
Figure 5.5 The flowchart for selection of profitable reservoir 141

Figure 5.6 Pressure profiles of ideal flooding 143
Figure 5.7 Saturation profiles of ideal flooding 144
Figure 5.8 Pressure profiles of water flooding 145
Figure 5.9 Saturation profiles of water flooding 146
Figure 5.10 Pressure profiles of CO_2 flooding 147
Figure 5.11 Saturation profiles of CO_2 flooding 148
Figure 5.12 Production profile of various floodings 151
Figure 5.13 Relation between oil production and CO_2 sequestration (a), the change of recoverable oil with respect to time (b) 154
Figure 5.14 Typical CO_2 enhanced oil recovery operation . . 160
Figure 5.15 Value iterations of using post-decision-state-based approximate dynamic programming 168
Figure 5.16 Change of optimal injection rate with respect to oil price 170
Figure 5.17 Change of optimal injection rate with respect to CO_2 price 171

List of Tables

Table 3.1 Properties of LPG and DME 52

Table 3.2 The adopted heating value of materials 59

Table 3.3 Energy consumption and CO_2 emission in NG extraction 60

Table 3.4 Energy consumption and CO_2 emission in NG liquefaction 60

Table 3.5 Transportation data of LNG by LNG carrier . . . 61

Table 3.6 Specification of imported NG at Incheon base . . 62

Table 3.7 Reactions in pre-reforming process 64

Table 3.8 Reactions in tri-reforming process 65

Table 3.9 The specification of two CO_2 absorption column . 66

Table 3.10 Reactions in DME reactor 67

Table 3.11 The specification of DME reactor and separator . 67

Table 3.12 Energy consumption and CO_2 emission for mining coal 68

Table 3.13 Data of coal transportation 69
Table 3.14 Composition of coal 70
Table 3.15 Particle size of coal 71
Table 3.16 Required energy for chipping and drying process . 74
Table 3.17 Data of waste wood transportation 75
Table 3.18 The reactor conditions of conversion of coal and biomass 77
Table 3.19 Simulation information of gas cleaning process . . 78
Table 3.20 The result of inventory analysis in DME production life cycle 79
Table 3.21 The comparison result of non-carbon capture and applying carbon capture system 80
Table 3.22 Price data for cost analysis 83

Table 4.1 Mean and standard deviation of learning rates of energy system 95
Table 4.2 Mean and standard deviation of fuel prices for electricity generation of each energy sources . . . 96
Table 4.3 Mean and standard deviation of CO_2 price 97
Table 4.4 The values of energy demand 102
Table 4.5 The values of growth rate, level of energy target, loss factor and discount rate 103

Table 4.6 Estimated target amount of CO_2 emission from 2011 to 2030 104
Table 4.7 The values of capital cost, emission rate, initial capacity, size limit and capacity factor 105
Table 4.8 The mean values of added capacities of energy sources 109

Table 5.1 Properties of major North Sea reservoirs 140
Table 5.2 Typical values of properties with respect to phases 142
Table 5.3 CO_2 emissions from the transportation 150
Table 5.4 Design basis of EOR process 155
Table 5.5 CO_2 emissions from the EOR 156
Table 5.6 Energy consumptions for CO_2-EOR 162
Table 5.7 Reservoir information for ADP 165
Table 5.8 Adopted cost parameters for EOR 166
Table 5.9 Optimal decision of operating state 167

Chapter 1

Introduction

Systems engineering is the study of analysis of entire process systems, including chemical processes, in terms of design and management. There are a number of subordinate concepts to interpret systems engineering such as system analysis, decision making, optimization, modeling, and safety/reliability etc. This thesis focuses on the procedures how to decision-making. Recently, a decision making is required to be rigorous and sustainable since the design and management of process must observe the regulation of greenhouse gas emission, reduction of energy uses, and mitigation of environmantal harmful materials. The aim of the decision making procedure is to achieve sustainable development and enhance sustainability. Sustainable development and sustainability include mitigation of CO_2 emission and energy consumption. Hence, this thesis has mainly presented the life cycle asseessment (LCA)-based de-

cision making procedures. As applications, evaluation of potential raw materials, planning of energy system, and CO_2 enhanced oil recovery (EOR) process are considered to show the efficiency of the proposed decision making procedure.

1.1 Life cycle assessment

A life cycle assessment is a technique to assess environmental impacts associated with all the stages of product's life from-cradle-to-grave (i.e. from raw material extraction through materials processing, manufacture processing, manufacture, distribution, use, repair and maintenance, and disposal or recycling) [1, 2]. While life cycle assessment, heretofore, is primarily used for evaluation of environmental influences of 'a product', the usefulness of life cycle assessment can be expanded to enhance sustainability of a product's or process' life. In this thesis, we are to introduce the life cycle assessment as a decision-making strategy for improving process sustainability. Life cycle assessment can help avoid a narrow outlook on environmental concerns by compiling an inventory of relevant energy and material inputs and environmental releases, evaluating the potential impacts associated with identified inputs and releases, and interpreting the results to help you make a more informed decision [3]. Life cycle assessment has emerged as a valuable decision-support tool for both policy makers and industry in assessing the cradle-to-grave impacts of a product or process. Recently, industrial

responses to environmental issues are taking a progressive approach (e.g. eco-efficient manufacturing and integrated tools for environmental design) while those are compliant and proactive (e.g. pollution control and environmental standards) [4]. Therefore, we focus on the progressive approach for environmental considerations relating process design and optimization. Three forces are supporting this movement. First, government regulations are moving in the direction of 'life-cycle accountability'; the notion that a manufacturer is responsible not only for direct production impacts, but also for impacts associated with product inputs, use, transport, and disposal. Second, business is participating in voluntary initiatives which contain life cycle assessment and product stewardship components. These include, for example, ISO 14000 and the Chemical Manufacturer Association's Responsible Care Program, both of which seek to foster continuous improvement through better environmental management systems. Third, environmental 'preferability' has emerged as a criterion in both consumer markets and government procurement guidelines. Together these developments have placed life cycle assessment in a central role as a tool for identifying cradle-to-grave impacts both of products and the materials from which they are made. There are four phases of lfie cycle assessment, goal and scope definition, inventory analysis, impact assessment, and interpretation (Figure 1.1).

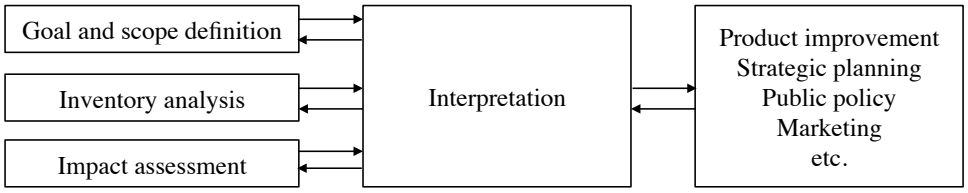

Figure 1.1 The phases of life cycle assessment

A life cycle assessment starts with an explicit statement of the goal and scope of the study, which sets out the context of the study and explains how and to whom the results are to be communicated. Basically, the goal of life cycle assessment is to compare the full range of environmental effects assignable to products and services in order to improve processes, support policy and provide a sound basis for informed decisions.

The goal and scope includes technical details that guide subsequent work [5, 6]: the functional unit, which defines what precisely is being studied and quantifies the service delivered by the product system, providing a reference to which the inputs and outputs can be related; the system boundaries; any assumptions and limitations; the allocation methods used to partition the environmental load of a process when several products or functions share the same process; and the impact categories chosen.

Inventory analysis involves creating an inventory of flows from and to nature for a product or process system. Inventory flows include inputs of water, energy, and raw materials, and releases to air, land, and

water. To develop the inventory, a flow model of the technical system is constructed using data on inputs and outputs. The flow model is typically illustrated with a flow chart that includes the activities that are going to be assessed in the relevant supply chain and gives a clear picture of the technical system boundaries. The input and output data needed for the construction of the model are collected for all activities within the system boundary, including from the supply chain. The data must be related to the functional unit defined in the goal and scope definition. Data can be presented in tables and some interpretations can be made already at this stage. The result of the inventory analysis provides information about all inputs and outputs in the form of elementary flow to and from the environment from all the unit processes involved in the study.

Then, impact assessment follows. This phase of life cycle assessment is aimed at evaluating the significance of potential environmental impacts based on the inventory flow results. Classical impact assessment consists of the following mandatory elements: selection of impact categories, category indicators, and characterization models; the classification stage, where the inventory parameters are sorted and assigned to specific impact categories; and impact measurement, where the categorized inventory flows are characterized, using one of many possible inventory analysis methodologies, into common equivalence units that are then summed to provide an overall impact category total. In many life

cycle assessments, characterization concludes the impact assessment; this is also the last compulsory stage according to [5]. In addition to the above mandatory inventory analysis steps, other optional elements, normalization, grouping, and weighting, may be conducted depending on the goal and scope of the life cycle assessment study. In normalization, the results of the impact categories from the study are usually compared with the total impacts in the region of interest. Grouping consists of sorting and possibly ranking the impact categories. During weighting, the different environmental impacts are weighted relative to each other so that they can then be summed to get a single number for the total environmental impact.

Interpretation is a systematic technique to identify, quantify, check, and evaluate information from the results of the inventory analysis and/or the impact assessment. The results from the inventory analysis and impact assessment are summarized during the interpretation phase. The outcome of the interpretation phase is a set of conclusions and recommendations for the study. The interpretation should include the identification of significant issues based on the results of the inventory analysis, the evaluation of the study considering completeness, sensitivity and consistency checks, and conclusions, limitations and recommendations. A key purpose of performing interpretation is to determine the level of confidence in the final results and communicate them in a fair, complete, and accurate manner. Interpreting the results of

an life cycle assessment starts with understanding the accuracy of the results, and ensuring they meet the goal of the study. This is accomplished by identifying the data elements that contribute significantly to each impact category, evaluating the sensitivity of these significant data elements, assessing the completeness and consistency of the study, and drawing conclusions and recommendations based on a clear understanding of how the life cycle assessment was conducted and the results were developed.

A life cycle assessment is only as valid as its data. Therefore, it is essential that data used for the completion of a life cycle assessment are accurate and up-to-date. There are two basic types of life cycle assessment data, unit process data and environmental input-output data. Unit process data are derived from direct surveys of plants producing the product of interest, carried out at a unit process level defined by the system boundaries for the study. This can be obtained by simulation or modeling of processes of interest. Following chapters will show the detailed methodologies.

Life cycle assessment has some variants with its scope, cradle-to-grave, cradle-to-gate, cradle-to-cradle, gate-to-gate, and wheel to wheel. Cradle-to-grave is the full Life Cycle Assessment from resource extraction ('cradle') to use phase and disposal phase ('grave'). This life cycle assessment is somewhat difficult to realize because all inputs and outputs are considered. Cradle-to-gate is an assessment of a partial product

life cycle from resource extraction (cradle) to the factory gate (i.e., before it is transported to the consumer). The use phase and disposal phase of the product are omitted in this case. Cradle-to-gate assessments are sometimes the basis for environmental product declarations [7]. This method are to be used for evaluation of processes. Cradle-to-cradle is a specific kind of cradle-to-grave assessment, where the end-of-life disposal step for the product is a recycling process. It is a method used to minimize the environmental impact of products by employing sustainable production, operation, and disposal practices and aims to incorporate social responsibility into product development [8]. Gate-to-gate is a partial life cycle assessment looking at only one value-added process in the entire production chain. Gate-to-gate modules may also later be linked in their appropriate production chain to form a complete cradle-to-gate evaluation [9, 10]. Well-to-wheel is the specific life cycle assessment used for transport fuels and vehicles.

1.2 Sustainable development and sustainability

Life cycle assessment will eventually lead to sustainable development and improvement of sustainability of process since it is able to consider environmental, economical, and energy impacts of processes. There are some perspectives of sustainable development and sustainability. The general definition of sustainable development is a pattern of growth in which resource use aims to meet human needs while pre-

serving the environment so that these needs can be met not only in the present, but also for generations to come. It contains within it two key concepts, the concept of 'needs', in particular the essential needs of the world's poor, to which overriding priority should be given, and the idea of limitations imposed by the state of technology and social organization on the environment's ability to meet present and future needs [11]. The general definition of sustainability is slightly different from that of sustainable development. Sustainability is the capacity to endure. For humans, sustainability is the long-term maintenance of responsibility, which has environmental, economic, and social dimensions, and encompasses the concept of stewardship, the responsible management of resource use. It is studied and managed over many scales (levels or frames of reference) of time and space and in many contexts of environmental, social and economic organization. The focus ranges from the total sustainability of Earth to the sustainability of economic sectors, ecosystems, countries, municipalities, neighbourhoods, home gardens, individual lives, individual goods and services, occupations, lifestyles, behaviour patterns and so on. Sustainability creates and maintains the conditions under which humans and nature can exist in productive harmony, that permit fulfilling the social, economic and other requirements of present and future generations [11, 12]. It is important to making sure that we have and will continue to have, the water, materials, and resources to protect human health and our environment. Recently, CO_2

emission and energy consumption can be issues. In short, it can entail the full compass of biological and human activity or any part of it [13]. Applying this definition to process systems, the process sustainability indicates the long-term management with the concept of design, planning, operation, and stewardship.

Reflecting sustainability in process systems requires an appropriate decision-making methodology. Grossmann group [14] suggests that the decision-making should cover from the process design stage to the molecular computing. And there are a number of decision-making techniques. In this thesis, we adopt life cycle assessment as a decision-making methodology to enhance process sustainability, which is defined as the mitigation of CO_2 emission and energy consumption.

Process systems including chemical processes has widespread hierarchy. If we have a sort of chemical processes or plants, the goal may be minimization of cost, energy, and risk etc. or maximization of profit and sustainability. Conceptual design and process synthesis are required to achieve the goal. Those are methods for strategic planning. Then, we make our decision how to obtain desired product properly/efficiently. Life cycle assessment is included in this step. Various modeling, simulation, and optimization methodologies can be used to perform life cycle assessment.

1.3 Proposed procedures for decision making

In this section, the procedures for decision making is basically presented using life cycle assessment. These follow the conventional procedures of life cycle assessment and the proposed strategies would be modified pertinent to chemical processes of interest. At first, the goal and scope of the processes to be assessed should be defined. We mentioned that the goal is to enhance process sustainability, which described in Section 1.2. The mitigation of CO_2 emission and energy consumption of the chemical processes (or plants) is now regarded as significant factors for sustainability. Thus, we consider the amount of CO_2 emission and energy consumption as impact factors.

For inventory analysis, the processes (or plants) of interest should be modeled and simulated using some methods (e.g. compter-aided software, numerical modeling etc.). As a simple example, Aspen Plus can be introduced. Aspen Plus is one of the most popular process simulators (Figure 1.2). It is a kind of computer-aided software, which calculates physical relationships, such as material and energy balances, reaction, thermodynamic equilibrium. It shows performance of processes composed of units and streams. There are several advantages of Aspen Plus simulator (including computer-aided simulator) [15]:

· it allows the designer to easily test the performance of process flowsheets and can provide feedback to the process design/synthesis activ-

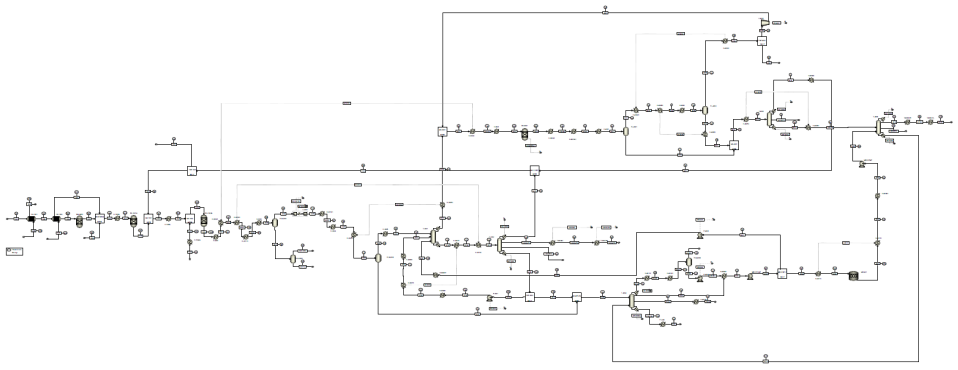

Figure 1.2 An example of simulation using Aspen Plus

ities.

· it can be coordinated with process synthesis to develop optimum integrated designs.

· it minimizes experimental efforts.

· it gives the result of sensitivity analysis.

· it models the process quantitatively.

Numerical modeling and simulation is also useful tool to realize the processes or plants. There are too many methods for solving the problems to describe all of them in this thesis. The description pertinent to the adopted case would be presented in case study section. An illustrative example, which is modeled in this thesis, can be shown (Figure 1.3).

In this way, all inventories and flows included in the defined scope are simulated. When the defined scope covers the practical processes, it is properly simulated using process simulator or numerical model-

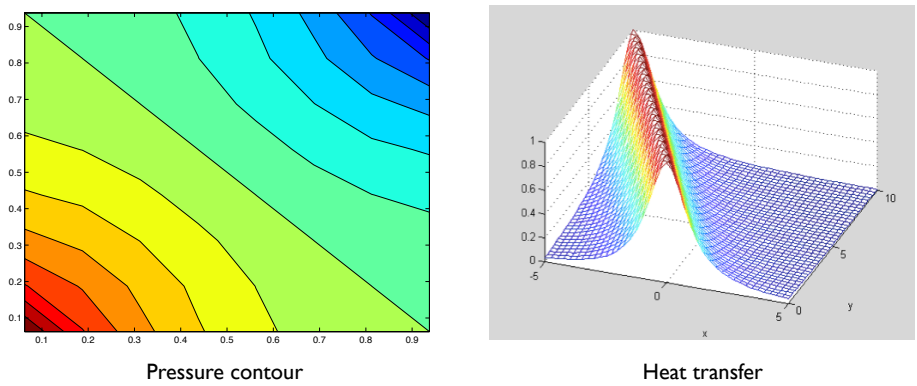

Figure 1.3 An illustrative example of numerical modeling

ing. However, when the scope is defined as a framework, not a process, the mathematical formulation would be more useful to handle inventories. The case study would show the procedure using mathematical formulation for energy planning. Input data can be obtained by the conventional researches. There are some uncertain variables to affect the results. To handle uncertain parameters or variables, we would introduce the mathematical optimization method such as Monte Carlo simulation. It allows us the robust analysis. Output data obtained from modeling and simulation is used for inventory analysis. Through inventory analysis, the impact assessment can be conducted. The adopted impact factors (CO_2 emission and energy consumption) would be assessed. This impact can give a decision maker valuable results of which should be determined. Following Figure 1.4 shows the proposed procedure for decision making.

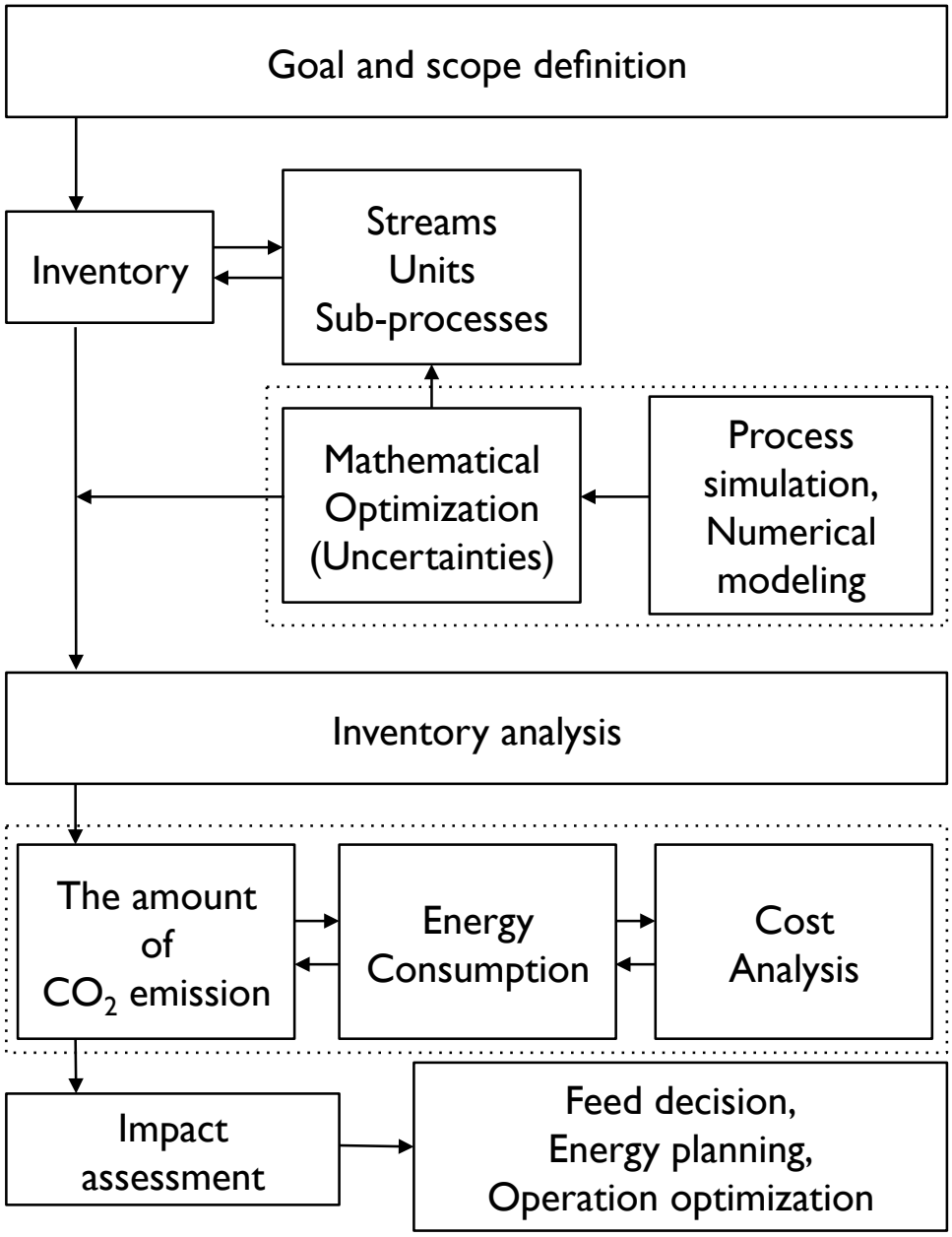

Figure 1.4 Proposed procedure for decision making

1.4 Research scope

Based on mentioned above, this thesis proposes the procedures of decision-making for process planning and management and presents some applications. Each application follows the proposed procedures and involves the methodologies of modeling, simulation, and optimization. At first, life cycle assessment-based procedures are performed by using the data from process simulation. This can be the simplest and the most basic method when life cycle assessment is applied to chemical processes. The commercial process simulator (Aspen Plus) is used for inventory analyses. Dimethyl ether (DME) production system is adopted as a case study. As defined in Section 1.1, up-to-date process design schemes are adopted. Dimethyl ether is one of the most promising energy sources because it is a clean synthetic fuel and can be used as a substitute for liquefied petroleum gas (LPG) and diesel. It can be produced from various materials such as natural gas (NG), coal, and waste wood. The application is focused on the evaluation of raw materials. Life cycle assessment of each raw material is performed and the amount of CO_2 emission and energy consumption are analyzed. In addition, cost intensity of life cycle is introduced for impact assessment. From the results, the most competitive feed can be determined.

Secondly, the proposed procedures are applied to energy planning under uncertainties that changes of external conditions. Mathematical

modeling can be introduced to analyze inventories related to case of interest. Energy planning is a very complicated task and a greater number of issues should be considered. Especially, the mitigation of greenhouse gas emission is the key issue. Thus, the optimization model is proposed to determine how much the capacities of energy systems should be added. The price of fuel and CO_2, and the learning rate of technology are considered to reflect uncertainties. Uncertain inputs have their distributions and the model becomes stochastic model. Monte carlo simulation technique is adopted to solve this stochastic model. Probabilistic inputs draw probabilistic outputs through the model. These outputs show the mean, standard deviation, skewness, and confidence level of solutions. Also, sensitivity analysis of uncertain factors can present more reliable results.

In third case, the proposed procedures are applied to process design and management using numerical modeling methods. CO_2 storage/sequestration process is adopted as a case study. This is the last stage of carbon capture and stroage (CCS) chain. The captured CO_2 is, heretofore, sequestrated by the simple injection under the ground, because the amount of captured CO_2 is small and the technology of storage/sequestration has not been developed yet. The captured CO_2 can be used for enhanced oil/gas recovery. Twin challenges of increasing oil/gas recovery and reducing emissions of CO_2, the topic of CO_2 enhanced oil recovery has received increased attention [16]. The reason

that CO_2 enhanced oil recovery was not popular was the supply price of CO_2. The existence of captured CO_2 makes the CO_2 enhanced oil recovery more realizable. This case models the behavior of oil and CO_2, which passes thorugh reservoir, and proposes the methodologies for optimal management to enhance sustainability. Based on the methodologies, we can obtain the strategies for optimal management of CO_2 enhanced oil recovery.

1.5 Outline of thesis

This chapter provided the motivation and basic research scope presented in this thesis. Hereafter, background theories, which is introduced in this thesis (Monte Carlo simulation, finite volume method, and approximate dynamic programming), is reviewed for life cycle assessment pertinent to each case study in Chapter 2. Chapter 3 shows the procedure and results of life cycle assessment for DME production system. A number of simulations are demonstrated to determine an appropriate raw material. Chapter 4 shows the results of procedures that applied to energy planning model under uncertainties. The method to handle uncertain variables is presented and, the results and their implications are discussed. Chapter 5 shows the results of procedures that applied to CO_2 enhanced oil recovery and sequestration process. Numerical modeling procedure is presented to realize the behavior of oil and CO_2 in reservoir. Based on this, approximate dynamic program-

ming is used to analyze optimal management strategies. Finally, the conclusion of this thesis is adressed and future directions are suggested in Chapter 6.

Chapter 2

Background Theory

2.1 Monte Carlo simulation

Monte Carlo simulation can be classified as a sampling method, since the inputs are randomly generated from probability distributions to simulate the sampling process from an actual population. Thus, we are able to choose a distribution for the inputs that most closely matches data we already have, or best represents our current state of knowledge. The generated data from the Monte Carlo simulation can be expressed as probability distributions (histograms) or converted to error bars, reliability predictions, tolerance zones, and confidence intervals [17]. Monte Carlo simulation stems from the concept of Monte Carlo method. Monte Carlo method (or Monte Carlo experiment) is a class of computational algorithms that depend on repeated random

sampling to calculate their results. Monte Carlo method can be used in the simulations of physical and mathematical systems using computer. These method is the most appropriate to calculation by a computer and can be used when it is infeasible to compute an exact result with a deterministic algorithm due to uncertainties [18]. Monte Carlo simulation are especially useful for simulating systems with many coupled degrees of freedom (e.g. fluids, disordered materials, strongly coupled solids, and cellular structures). In addition, they are useful tool to model phenomena with significant uncertainty in inputs (Figure 2.1), such as the calculation of risk in business or change of prices. They are also used in mathematics, for example to evaluate multidimensional definite integrals with complicated boundary conditions. When Monte Carlo simulations have been applied in space exploration and oil exploration, they would give better prediction results of failure, cost and schedule than human intuition or soft methods such as history matching [19]. In this thesis, we would apply Monte Carlo simulation to handle uncertainties for planning strategies. There are many ways to conduct Monte Carlo simulation, but it follows a particular step [20]:

Step 1. Define possible inputs (uncertain variables).

Step 2. Generate inputs randomly from a probability distribution over the domain.

Step 3. Perform a deterministic computation on the inputs.

Step 4. Aggregate the results.

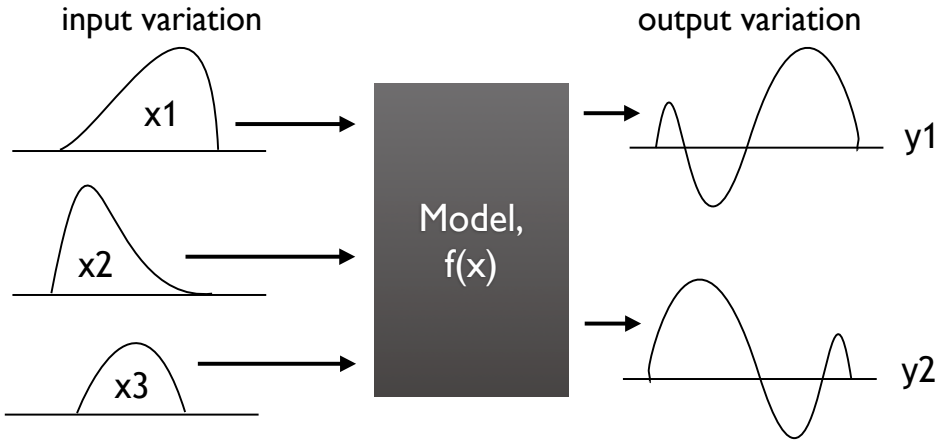

Figure 2.1 Schematic concept of Monte Carlo simulation

The definition of Monte Carlo has not been specified. There are some definitions addressed: Ripley defines most probabilistic modeling as stochastic simulation, with Monte Carlo being reserved for Monte Carlo integration and Monte Carlo statistical tests [21]. Sawilowsky distinguishes between a simulation, Monte Carlo method, and a Monte Carlo simulation: a simulation is a fictitious representation of reality, a Monte Carlo method is a technique that can be used to solve a mathematical or statistical problem, and a Monte Carlo simulation uses repeated sampling to determine the properties of some phenomenon [22, 23]. For example, a simulation is that drawing one pseudo-random uniform variable from the interval [0,1] can be used to simulate the

tossing of a coin [20]. If the value is less than or equal to 0.50 designate the outcome as heads, but if the value is greater than 0.50 designate the outcome as tails. This is a simulation, but not a Monte Carlo simulation. Monte Carlo method is the area of an irregular figure inscribed in a unit square can be determined by throwing darts at the square and computing the ratio of hits within the irregular figure to the total number of darts thrown. This is a Monte Carlo method of determining area, but not a simulation. Monte Carlo simulation is that drawing a large number of pseudo-random uniform variables from the interval [0,1], and assigning values less than or equal to 0.50 as heads and greater than 0.50 as tails, is a Monte Carlo simulation of the behavior of repeatedly tossing a coin. Kalos point out that such distinctions are not always easy to maintain. For example, the emission of radiation from atoms is a natural stochastic process. It can be simulated directly, or its average behavior can be described by stochastic equations that can themselves be solved using Monte Carlo methods. In fact, the same computer code can be viewed simultaneously as a natural simulation or as a solution of the equations by natural sampling [24].

Monte Carlo simulation does not always require truly random numbers to be useful - while for some applications, unpredictability is inevitable [25]. Many of the most useful techniques use deterministic, pseudorandom sequences, making it easy to test and re-run simulations. The only quality usually necessary to make good simulations is

for the pseudo-random sequence to appear random enough in a certain sense [20]. This means that the practical simulation depends on the application, however typically they should pass a series of statistical tests and samples. Testing that the numbers can be uniformly distributed or follow another desired distribution when a large enough number of samples (or elements) of the sequence are considered is one of the simplest, and the most common ones. Sawilowsky lists the characteristics of a high quality Monte Carlo simulation [22, 23]:

· the (pseudo-) random number generator has certain characteristics (e.g. a long period before the sequence repeats)

· the (pseudo-) random number generator produces values that pass tests for randomness

· there are enough samples to ensure accurate results

· the proper sampling technique is used

· the algorithm used is valid for what is being modeled

· it simulates the phenomenon in question.

(Pseudo-) Random number sampling algorithms are used to transform uniformly distributed (pseudo-) random numbers into numbers that are distributed according to a given probability distribution. Low-discrepancy sequences are often used instead of random sampling from a space as they ensure even coverage and normally have a faster order of convergence than Monte Carlo simulations using random or pseudo-random sequences. Methods based on their use are called quasi-Monte

Carlo methods [20].

There are ways of using probabilities that may be definitely not Monte Carlo simulations. For example, consider a deterministic modeling using single-point estimates. Each uncertain variable within a model can be assigned a best-guess estimate. Scenarios (e.g. best, worst, or most likely case) for each uncertain input variable are chosen and the results stored. By contrast, Monte Carlo simulation collects samples from probability distribution for each variable to produce hundreds or thousands of possible outcomes. The results are analyzed to get probabilities of different outcomes [26]. Monte Carlo simulation is especially useful for simulating phenomena with significant uncertainty in inputs and systems with a large number of coupled degrees of freedom. Thus, it widely used in engineering for sensitivity analysis and quantitative probabilistic analysis in process design. The key feature of a Monte Carlo simulation is that it can tell how you create the ranges of estimates and how likely the resulting outcomes are. The need arises from the interactive, co-linear and non-linear behavior of typical process simulations. Simple steps for Monte Carlo simulation are listed below [17]:

Step 1. Create parametric model ($y = f(x_1, x_2, \cdots, x_k)$)

Step 2. Generate a set of random inputs ($x_{1i}, x_{2i}, \cdots, x_{ki}$)

Step 3. Evaluate the model and store the results (y_i)

Step 4. Repeat 2 and 3 for $i = 1$ to n

Step 5. Analyze the results using histrograms, summary statistics, con-

fidence level, etc.

Another powerful and popular application for random numbers in numerical simulation is in numerical optimization [27]. The problem is to minimize (or maximize) functions of some vector that often has a large number of dimensions. Many problems can be phrased in this way: for example, a computer chess program could be seen as trying to find the set of, say, 10 moves that produces the best evaluation function at the end. In the traveling salesman problem the goal is to minimize distance traveled. There are also applications to engineering design, such as multidisciplinary design optimization. The traveling salesman problem is what is called a conventional optimization problem. That is, all the facts (distances between each destination point) needed to determine the optimal path to follow are known with certainty and the goal is to run through the possible travel choices to come up with the one with the lowest total distance. However, assuming that instead of wanting to minimize the total distance traveled to visit each desired destination, we wanted to minimize the total time needed to reach each destination. This goes beyond conventional optimization since travel time is inherently uncertain (traffic jams, time of day, etc.). As a result, to determine our optimal path we would want to use simulation - optimization to first understand the range of potential times it could take to go from one point to another (represented by a probability distribution in this case rather than a specific distance) and then opti-

mize our travel decisions to identify the best path to follow taking that uncertainty into account.

In this way, Monte Carlo simulation provides a much more comprehensive view of what may happen. It furnishes the decision-maker with a range of possible outcomes and the probabilities they will occur for any choice of action. Monte Carlo simulation performs uncertainty analysis by building models of possible results by substituting a range of values (a probability distribution) for any factor that has inherent uncertainty. It then calculates results over and over, each time using a different set of random values from the probability functions. Depending upon the number of uncertainties and the ranges specified for them, Monte Carlo simulation could involve thousands or tens of thousands of recalculations before it is complete. Monte Carlo simulation produces distributions of possible outcome values. By using probability distributions, variables can have different probabilities of different outcomes occurring. Probability distributions are a much more realistic way of describing uncertainty. Common probability distributions include [27]:

· Normal - The user simply defines the mean or expected value and a standard deviation to describe the variation about the mean. Values in the middle near the mean are most likely to occur. It is symmetric and describes many natural phenomena. Examples of variables described by normal distributions include inflation rates and energy prices.

· Lognormal - Values are positively skewed, not symmetric like a nor-

mal distribution. It is used to represent values that don't go below zero but have unlimited positive potential. Examples of variables described by lognormal distributions include real estate property values, stock prices, and oil reserves.

· Uniform - All values have an equal chance of occurring, and the user simply defines the minimum and maximum. Examples of variables that could be uniformly distributed include manufacturing costs or future sales revenues for a new product.

· Triangular - The user defines the minimum, most likely, and maximum values. Values around the most likely are more likely to occur. Variables that could be described by a triangular distribution include past sales history per unit of time and inventory levels.

· PERT - The user defines the minimum, most likely, and maximum values, just like the triangular distribution. Values around the most likely are more likely to occur. However, values between the most likely and extremes are more likely to occur than the triangular, that is, the extremes are not as emphasized. An example of the use of a PERT distribution is to describe the duration of a task in a project management model.

· Discrete - The user defines specific values that may occur and the likelihood of each. An example might be the results of a lawsuit: 20% chance of positive verdict, 30% change of negative verdict, 40% chance of settlement, and 10% chance of mistrial.

In addition, Monte Carlo simulation provides a number of advantages over deterministic [27]:

· Probabilistic results - Results show not only what could happen, but how likely each outcome is.

· Graphical results - Because of the data a Monte Carlo simulation generates, it is easy to create graphs of different outcomes and their chances of occurrence. This is important for communicating findings to other stakeholders.

· Sensitivity analysis - With just a few cases, deterministic analysis makes it difficult to see which variables impact the outcome the most. In Monte Carlo simulation, it's easy to see which inputs had the biggest effect on bottom-line results.

· Scenario analysis - In deterministic models, it's very difficult to model different combinations of values for different inputs to see the effects of truly different scenarios. Using Monte Carlo simulation, analysts can see exactly which inputs had which values together when certain outcomes occurred. This is invaluable for pursuing further analysis.

· Correlation of inputs - In Monte Carlo simulation, it's possible to model interdependent relationships between input variables. It's important for accuracy to represent how, in reality, when some factors goes up, others go up or down accordingly.

2.2 Finite volume method

The finite volume method (FVM) is a discretization method for the approximation of a system of partial differential equations, which are called conservation laws (e.g. elliptic, parabolic, or hyperbolic).

1. Elliptic : $-\nabla \cdot (c\nabla u) + au = f$

2. Parabolic : $du_t - \nabla \cdot (c\nabla u) + au = f$

3. Hyperbolic : $du_{tt} - \nabla \cdot (c\nabla u) + au = f$

It has been extensively used in several engineering fields, such as fluid mechanics, heat and mass transfer, or petroleum engineering [28]. They describe the relations between partial derivatives of unknown variables such as temperature, concentration, pressure, molar fraction, density, or probability density function, with respect to variables within the domain (space or time) under consideration. The values are calculated at discrete places on a meshed geometry. The term, finite volume, indicates the small volume surroudning each node point on a mesh. In the finite volume method, volume integrals in a partial differential equation that contain a divergence term are converted to surface integrals, using the divergence theorem. These terms are then evaluated as fluxes at the surfaces of each finite volume. Because the flux entering a given volume is identical to that leaving the adjacent volume, these methods are conservative. For using finite volume methods, a mesh is required, which consists in a partition of the domain where the space variable

lives. The elements of the mesh are called control volumes. The integration of the partial differential equations over each control volume results in a balance equation. The set of balance equations is then discretized with respect to a set of discrete unknowns. The main issue is the discretization of the fluxes at the boundaries of each control volume.

Finite volume methods have the similar way of fundamentals of finite difference methods. In finite difference methods, partial differential equations are approximated by replacing the partial derivatives with appropriate divided differences between point values on a discrete set of points in the domain. On the other hand, finite volume methods have a more physical motivation and are derived from conservation of quantities over cell volumes. Thus, in a finite volume method, the unknown functions are represented in terms of average values over a set of finite volumes[1] [29]. There are a number of schemes to solve the partial differential equations by using the finite volume methods. Depending on the characteristic of partial differential equations (i.e. elliptic, parabolic, and hyperbolic), the appropriate schemes exist, respectively. General finite volume methods approximates the average integral value on a volume of interest. Suppose a region $V_i = [x_{i-1/2}, x_{i+1/2}]$ and

$$\int_{x_{i-1/2}}^{x_{i+1/2}} u_t dx + f(u_{i+1/2}) - f(u_{i-1/2}) = 0 \tag{2.1}$$

[1]This manuscript is extracted from the references, 'An introduction to the numerics of flow in porous media using Matlab' by J. E. Aarnes.

where we have applied Gauss' theorem and integrated analytically the resulting term

$$\int_{x_{i-1/2}}^{x_{i+1/2}} f_x(u)dx. \tag{2.2}$$

We can apply a quadrature rule, for example midpoint, to the remaining integral to get a semi-discrete form:

$$(x_{i+1/2} - x_{i-1/2})u_t(x_i) + f(u_{i+1/2}) - f(u_{i-1/2}) = 0. \tag{2.3}$$

For example, consider an elliptic equation $u_{xx} = f(x)$ on a control volume $V_i = [x_{i-1/2}, x_{i+1/2}]$, then

$$\int_{x_{i-1/2}}^{x_{i+1/2}} u_{xx}dx = \int_{x_{i-1/2}}^{x_{i+1/2}} f dx. \tag{2.4}$$

Evaluating the left hand side analytically and the right via midpoint gives

$$u_x(x_{i+1/2}) - u_x(x_{i-1/2}) = (x_{i+1/2} - x_{i-1/2})f_i. \tag{2.5}$$

Using centered differences on the remaining derivatives yields

$$\frac{u_{i+1} - 2u_i + u_{i-1}}{h} = hf_i \tag{2.6}$$

for $h = x_{i+1/2} - x_{i-1/2}$.

Using the methods, the diffusion fluxes can be calculated at the interfaces of control volumes [30]. A control volume formulation in reservoir simulation, which would be treated as a case study in this thesis, involves computing the flux [31]. We introduce a cell-centered finite

volume method, two point flux approximation (TPFA) scheme (Figure 2.2). This scheme is one of the discretization techniques for elliptic equations, and widely used in the oil industry [29]. More detailed ex-

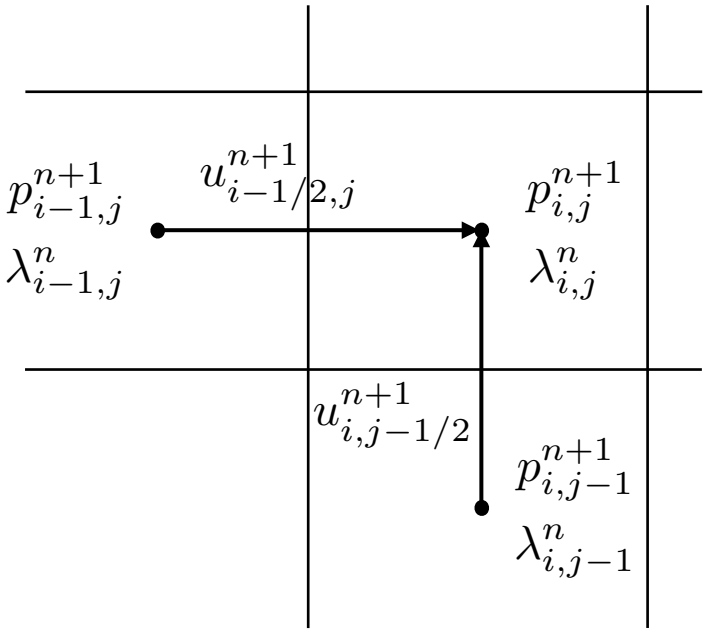

Figure 2.2 Schmetic diagram of TPFA

planation of TPFA would be shown in case study section.

In summary, finite volume method can be applied to integral form of conservation law and handles discontinuities in solutions. When heterogeneous materials are considered, each grid cell can be assigned different material parameters.

2.3 Approximate dynamic programming

2.3.1 Introduction to dynamic programming

[2]Dynamic programming is a method for solving complex problems by breaking them down into simpler subproblems. It is applicable to problems exhibiting the properties of overlapping subproblems which are only slightly smaller and optimal substructure [32]. The key idea behind dynamic programming is quite simple. In general, to solve a given problem, we need to solve different parts of the problem (subproblems), then combine the solutions of the subproblems to reach an overall solution. Often, many of these subproblems are really the same. Top-down dynamic programming simply means storing the results of certain calculations, which are later used again since the completed calculation is a sub-problem of a larger calculation. Bottom-up dynamic programming involves formulating a complex calculation as a recursive series of simpler calculations. The optimization of problems over time arises in many settings, ranging from the control of heating systems to managing entire economics in chemical processes [33, 34]. Examples are including landing aircraft, purchasing new equipmentk scheduling fleets of vehicle, selling assest, and investing money in portfolios. These problems involve making decisions, then observing information, after

[2]The contents of this section are summarized and re-arranged based on "Approximate Dynamic Programming - Solving the Curses of Dimensionality" by W. B. Powell, pp1-5, 54, 91-106. The manuscript is extracted and quoted from this reference.

which we make more decisions, and then more information, etc. Known as sequential decision problems, they can be straightforward to formulate, but solving them is another matter. Dynamic programming has its roots in several fields. Engineering and economics tend to focus on problems with continuous states and decisions. On the other hand, the fields of operations research and artificial intelligence work primarily with dicrete states and decisions. Most of this work focuses on deterministic problems using tools such as linear, nonlinear, or interger programming, but ther is a subfield known as stochastic programming which considers uncertainty [35]. Here is a simple example of dynamic programming, a shortest path problem (Figure 2.3).

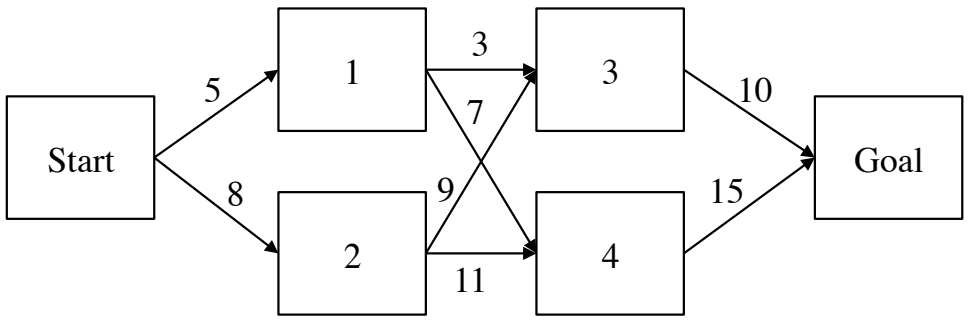

Figure 2.3 Example of a shortest path problem

Dynamic programming is both a mathematical optimization method and a computer programming method. In both methods, it refers to simplifying a complicated problem by breaking it down into simpler subproblems in a recursive manner. While some decision problems can-

not be taken apart this way, decisions that span several points in time do often break apart recursively; Bellman called this the 'Principle of Optimality' [36]. Likewise, in computer science, a problem that can be broken down recursively is said to have optimal substructure. If subproblems can be nested recursively inside larger problems, so that dynamic programming methods are applicable, then there is a relation between the value of the larger problem and the values of the subproblems [37]. In the optimization literature this relationship is called the Bellman equation (Equation (2.7)).

$$\begin{aligned} V_t(S_t) &= \max(C_t(S_t, x_t) + \gamma \mathbb{E} V_{t+1}(S^M_{t+1}(S_t, x_t, W_{t+1})|S_t)) \\ x^*_t(S_t) &= \arg\max_{x_t}(C_t(S_t, x_t) + \gamma V_{t+1}(S_{t+1})) \end{aligned} \tag{2.7}$$

A Bellman equation writes the value of a decision problem at a certain point in time in terms of the payoff from some initial choices and the value of the remaining decision problem that results from those initial choices. This breaks a dynamic optimization problem into simpler subproblems. Almost any problem which can be solved using optimal control theory can also be solved by analyzing the appropriate Bellman equation. However, the term, Bellman equation, usually refers to the dynamic programming equation associated with discrete time optimization problems. In continuous time optimization problems, the analogous equation is a partial differential equation which is usually

called the Hamilton-Jacobi-Bellman equation [35].

This usually refers to simplifying a decision by breaking it down into a sequence of decision steps over time. This is done by defining a sequence of value functions V_1, V_2, $\cdots$, V_n, with an argument y representing the state of the system at times i from 1 to n. The definition of $V_n(y)$ is the value obtained in state y at the last time n. The values V_i at earlier times $i = n-1, n-2, \cdots, 2, 1$ can be found by working backwards, using a recursive relationship called the Bellman equation. For $i = 2, \cdots, n, V_{i-1}$ at any state y is calculated from V_i by maximizing a simple function (usually the sum) of the gain from decision $i-1$ and the function V_i at the new state of the system if this decision is made. Since V_i has already been calculated for the needed states, the above operation yields V_{i-1} for those states. Finally, V_1 at the initial state of the system is the value of the optimal solution. The optimal values of the decision variables can be recovered, one by one, by tracking back the calculations already performed (Figure 2.4).

Here is an algorithm of backward dynamic programming [35].

Step 0. Initialization: Initialize the terminal value $V_T(S_T)$.

Set t= T-1

Step 1. Calculate

$V_t(S_t) = \max_{x_t}(C_t(S_t, x_t) + \gamma \sum_{s' \in S} \mathbb{P}(s'|S_t, x_t) V_{t+1}(s'))$

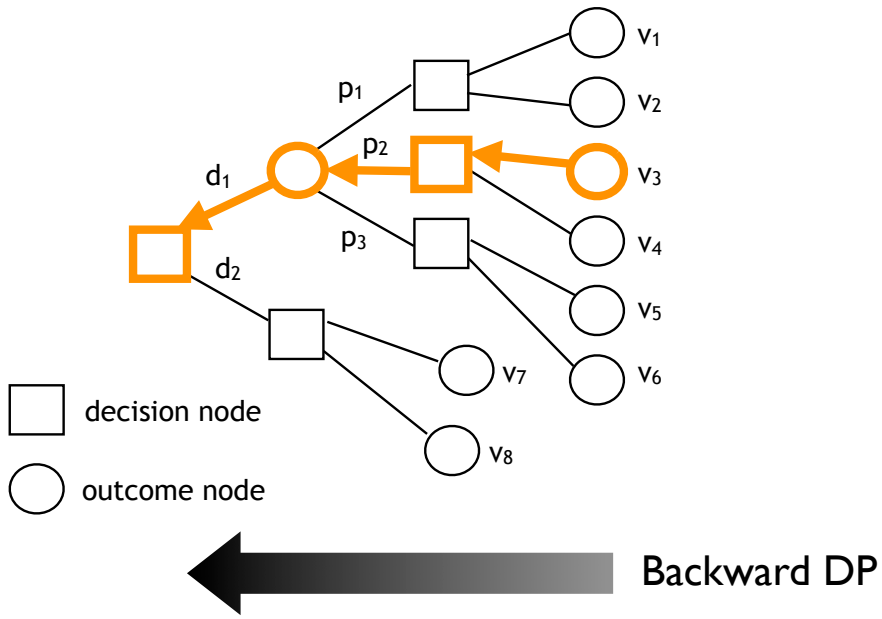

Figure 2.4 Schmetic diagram of dynamic programming

for all $S_t \in S$

Step 2. If $t > 0$, decrement t and return to step 1. Else, stop.

The difference between the backward dynamic programming algorithm and the decision tree in Figure 2.4 is primarily notational. Decision trees are visual and tend to be easier to understand. However, decision tree problems tend to be always presented in the context of problems with relatively small numbers of states and actions. And the difference between the algorithm and Equation (2.7) is transition of states. In the algorithm, we introduced one-step transition matrix, $\mathbb{P}$, while the expectation of states of next time in Equation (2.7). To com-

pute the one-step transition matrix, let Ω be the set of possible outcomes of $\hat{D}_t$, and let $\mathbb{P}$ be the probability. The one-step transition matrix is computed using

$$\mathbb{P}(s'|s,x) = \sum_{\omega \in \Omega} \mathbb{P}(\hat{D}_{t+1} = \omega) \mathbf{1}_{(s'=[s+x-w]^+)} \tag{2.8}$$

where Ω is the set of outcomes of the demand $\hat{D}_{t+1}$.

2.3.2 The three curses of dimensionality

The curse of dimensionality refers to various phenomena that arise when analyzing and organizing high-dimensional spaces (often with hundreds or thousands of dimensions) that do not occur in low-dimensional settings such as the physical space commonly modeled with just three dimensions. There are multiple phenomena referred to by this name in domains such as sampling, combinatorics, machine learning and data mining. The common theme of these problems is that when the dimensionality increases, the volume of the space increases so fast that the available data becomes sparse. This sparsity is problematic for any method that requires statistical significance. In order to obtain a statistically sound and reliable result, the amount of data you need to support the result often grows exponentially with the dimensionality. Also organizing and searching data often relies on detecting areas where objects form groups with similar properties; in high dimensional data

however all objects appear to be sparse and dissimilar in many ways which prevents common data organization strategies from being efficient.

All dynamic programs can be written in terms of a recursion that relates the value of being in a particular state at one point in time to the value of the states that we are carried into at the next point in time [35]. For deterministic problems, this equation can be written

$$V_t(S_t) = \max_{x_t}(C_t(S_t, x_t) + V_{t+1}(S_{t+1})) \tag{2.9}$$

where S_{t+1} is the state we transition to if we are currently in state S_t and take action x_t. As mentioned above, Equation (2.9) is Bellman equation, Hamilton-Jacobi equation, or Hamilton-Jacobi-Bellman equation. Most of the problems that we address in this volume involve some form of uncertainty. For example, in a simple inventory problem, assume the amount of inventory,S_t, in stock. Then, assume the amount of order, x_t after which satisfying a random demand $\hat{D}_{t+1}$ which follows some probability distribution. The state variable, S, would be described by the transition equation

$$S_{t+1} = \max[0,\ S_t + x_t - \hat{D}_{t+1}] \tag{2.10}$$

Assume that $C_t(S_t, x_t)$ is the contribution at time t, given by

$$C_t(S_t, x_t, \hat{D}_{t+1}) = p_t \ \min[S_t + x_t, \hat{D}_{t+1}] - cx_t. \tag{2.11}$$

To find the best decision, we need to maximize the contribution from x_t plus the expected value of the state that we end up at. We should to solve

$$V_t(S_t) = \max_{x_t}[C_t(S_t, x_t, \hat{D}_{t+1}) + V_{t+1}(S_{t+1})|S_t] \tag{2.12}$$

This equation is not too hard to solve for now. Assume we know V_{t+1}, we have to compute Equation (2.12) for each value of S_t, which then gives us $V_t(S_t)$. We can keep stepping 'backward' in time to compute all the value functions.

For the majority of problems, the state of the system is a vector. If we have to track the inventory of N different products, where we might have $0, 1, \cdots, M-1$ units of inventory of each product, then we would have M^N different states. The size of the state space increases very quickly as the number of dimensions grows. This is a kind of curses of dimensionality of dynamic programming. In fact, there are three curses of dimensionality [35]:

1. The state space - If the state variable $S_t = (S_{t1}, S_{t2}, \cdots, S_{ti}, \cdots, S_{tI})$ has I dimensions, and if S_{ti} can take on L possible values, then we might have up to L^I different states.

2. The outcome space - The random variable

$W_t = (W_{t1}, W_{t2}, \cdots, W_{tj}, \cdots, W_{tJ})$ might have J dimensions. If W_{tj} can take on M outcomes, then our outcome space might take on up to M^J outcomes.

3. The action space - The decision vector $x_t = (x_{t1}, x_{t2}, \cdots, x_{tk}, \cdots, x_{tK})$ might have K dimensions. If x_{tk} can take on N outcomes, we might have up to N^K outcomes.

However, not all problems suffer from the three curses of dimensionality. Some problems have small sets of actions (active, inactive, decommissioned), easily computable expectations, and small state spaces. The field of dynamic programming has identified problems, some with genuine industrial applications, which avoid the curses of dimensionality.

2.3.3 Introduction to approximate dynamic programming

There are still problems which have many states, outcomes, and actions in real world. Even small problems may be hard because we lack a model of the information process, or we may not know the transition function of states. Also the optimality equations are themsevles computationally intractable due to the curses of dimensionality as mentioned. Approximate dynamic programming offers a set of starategies for problems that are hard. The concept of the backward recursion of dynamic programming is so powerful, but its usefulness can be so limited for many problems as mentioned previous section, curses of dimensionality. The basis of approximate dynamic programming is based

on an algorithmic strategy that steps forward through time. If we solve a problem using classical dynamic programming (backward dynamic programming), we would have to find the value function $V_t(S_t)$ using

$$\begin{aligned} V_t(S_t) &= \max_{x_t \in X_t} [C(S_t, x_t) + \gamma \mathbb{E}(V_{t+1}(S_{t+1})|S_t)] \\ &= \max_{x_t \in X_t} [C(S_t, x_t) + \gamma \sum_{s' \in S} \mathbb{P}(s'|S_t, x_t) V_{t+1}(s')] \end{aligned} \tag{2.13}$$

for each value of S_t. There is a maximization problem as one of choosing the best $x_t \in X_t$. X_t is the feasible region and captures the constraints on our decisions. X_t depends on our state variable. However, this problem cannot be solved easily using backward dynamic programming that we loop over all possible states. With approximate dynamic programming, we step forward in time. In order to simulate the process forward in time, we need to solve two problems. The first is that we need a way to randomly generate a sample of what might happen in terms of the various sources of random information. The second is that we need a way to make decisions.

When we solve exact dynamic programming, we stepped backward in time, exactly computing the value function which we then used to produce optimal decisions. When we step forward in time, we have not computed the value function, so we have to turn to an approximation in order to make decisions. Let $\bar{V}_t(S_t)$ be an approximation of the value function. This is easiest to understand if we assume that we have an

estimate $\bar{V}_t(S_t)$ for each state S_t, but since it is an approximation, we may use any functional form we wish. For example, there is a portfolio problem. We might create an approximation $\bar{V}_t(R_t)$ that depends on the number of shares, rather than the prices. Then, we can use a separable approximation of the form

$$V_t(S_t) \approx \sum_{k \in K} \bar{V}_{tk}(R_{tk}) \tag{2.14}$$

where $\bar{V}_{tk}(R_{tk})$ is a nonlinear function giving the value of holding R_{tk} shares of stock k. This structure surely has some errors. The challenge is finding approximations that are good enough for the purpose at hand.

Approximate dynamic programming proceeds by estimating the approximation $\bar{V}_t(S_t)$ iteratively. An initial approximation $\bar{V}_t^0$ for all t is given. Let $\bar{V}_t^{n-1}$ be the value function approximation after $n-1$ iterations. Assume that the iteration starts $t = 0$ in state S_0, then x_0 is solved by

$$\begin{aligned} x_0 &= \arg\max_{x \in X_0}(C(S_0, x) + \gamma \mathbb{E}(\bar{V}_1(S_1)|S_0)) \\ &= \arg\max_{x \in X_0}(C(S_0, x) + \gamma \sum_{s' \in S} \mathbb{P}_0(s'|S_0, x)\bar{V}_1(s')) \end{aligned} \tag{2.15}$$

where x_0 is the value of x that maximizes the right-hand side of Equation (2.15), $\mathbb{P}(s'|S_0, x)$ is the one-step transition matrix. We are going to step forward in time from S_0 to S_1. This starts by making the decision x_0. Giving a decision, we need to know the information that arrived between $t = 0$ and $t = 1$. At $t = 0$, this information is unknown, and

therefore random. The strategy will be to simply pick a sample realization of the information at random such as Monte Carlo simulation. As mentioned previous section, Monte Carlo simulation refers to the practice of generating random information. Since many computer language have a random number generator that produces a number that is uniformly distributed between 0 and 1, we can obtain random samples of information easily. Using random sample of new information, we can calculate the next state we visit, given by S_1. With a transition function, we present this equation

$$S_{t+1} = S^M(S_t, x_t, W_{t+1}) \tag{2.16}$$

where W_{t+1} is a set of random variables representing the information that arrived between t and $t+1$. From $\bar{V}_t$ for all t, we simply repeat the process of making a decision by solving

$$x_1 = \arg\max_{x \in X_1}(C(S_1, x) + \gamma \sum_{s' \in S} \mathbb{P}_1(s'|S_1, x)\bar{V}_2(s')) \tag{2.17}$$

Once we determine x_1, we again sample the new information $(\hat{p}_2, \hat{d}_2)$, calculate S_2 and repeat the process. Whenever we make a decision based on a value function approximation (Equation (2.17)), this can be called a greed strategy. The basic to approximate dynamic programming is the idea of following a sample path. A sample path is a particular sequence of exogenous information. Let $W_t(\omega)$ be a particular sample realization in time period t. In an iterative algorithm, we might choose ω^n in iter-

ation n, and then follow the sample path $W_1(\omega^n), W_2(\omega^n), \cdots, W_t(\omega^n)$. In each iteration, we choose a new outcome ω^n.

Stepping forward through time following a single set of sample realizations would not produce anything of value. We have to approximate value functions over and over using a fresh set of sample realizations each time. Here is an approximate dynamic programming algorithm using the one-step transition matrix. It is similar to backward dynamic programming, except that we step forward in time.

Step 0. Initialization:

Step 0a. Initialize $\bar{V}_t^0(S_t)$ for all states S_t.

Step 0b. Choose an initial state S_0^1.

Step 0c. Set $n = 1$.

Step 1. Choose a sample path ω^n.

Step 2. For $t = 0, 1, 2, \cdots, T$ do:

Step 2a. Solve

$$\hat{v}_t^n = \max_{x_t \in X_t^n} (C_t(S_t^n, x_t) + \gamma \sum_{s' \in S} \mathbb{P}(s'|S_t^n, x_t) \bar{V}_{t+1}^{n-1}(s')) \tag{2.18}$$

and let x_t^n be the value of x_t that solves the maximization problem.

Step 2b. Update $\bar{V}_t^{n-1}(S_t)$ using

$$\bar{V}_t^n(S_t) = \begin{cases} \hat{v}_t^n & \text{if } S_t = S_t^n \\ \bar{V}_t^{n-1}(S_t) & \text{otherwise} \end{cases} \tag{2.19}$$

Step 2c. Calculate $S_{t+1}^n = S^M(S_t^n, x_t^n, W_{t+1}(\omega^n))$.

Step 3. Let $n = n + 1$. If $n < N$, go Step 1.

where n is iteration number, ω^n represents the specific value of ω that we sampled for iteration n. At time t, the state is S_t^n, and decision x_t^n is made by using the value function approximation $\bar{V}^{n-1}$. The reason why we index $n-1$ is that the value function was calculated using information from iteration $n-1$. After finding x_t^n, we would observe the information $W_{t+1}(\omega^n)$ to obtain S_{t+1}^n. When the calculation is achieved the end of horizon, we start over again. In this way, we have not to loop over all stages, but introduce a fresh set of problems. The problems are following [35]:

· Forward dynamic programming avoids the problem of looping over all possible states, but it still requires the uses of a one-step transition matrix, $\sum_{s' \in S} \mathbb{P}(s'|S_t^n, x_t)(\bar{V})$.

· We update the value of states we visit, and need the value of state we visit next time period, too. The method to estimate the value of being in states that we have not visited is needed.

· There are some good states that we never visited.

In addition, we have to calculate the expectation of the value if we do not calculate value function by one-step transition matrix (Equation (2.13)). However, the calculation of expectation is often intractable in many applications. We need to approximate the expectation using the concept of one-step transition matrix (Equation (2.20)).

$$\sum_{\omega_{t+1} \in \hat{\Omega}_{t+1}} p_{t+1}(\omega_{t+1}) \bar{V}_{t+1}^{n-1}(S^M(S_t, x_t, \omega_{t+1})) \tag{2.20}$$

where $p_{t+1}(\omega_{t+1})$ is the probability of outcome ω_{t+1}, if we choose N observations in the $\hat{\Omega}_{t+1}$, $p_{t+1}(\omega_{t+1}) = 1/N$.

2.3.4 Approximate dynamic programming using post-decision state variable

The calculation of expectation is more difficult within the max operator (Equation (2.13), (2.18)). In the practical application of approximate dynamic programming, finding the one-step transition matrix is impossible. We can circumvent this by introducing the post-decision state variable. It is possible to break down the effect of decisions and information on the state variable. From Equation (2.10), we can break this into two steps (Figure 2.5):

$$\begin{aligned} S_t^x &= S_t + x_t, \\ S_{t+1} &= \max(S_t^x - \hat{D}_{t+1}, 0) \end{aligned} \tag{2.21}$$

S_t is the state of the system immediately before we make a decision, while S_t^x is the state immediately after we make a decision. Therefore S_t can be called pre-decision state variable, while S_t^x is the post-decision state variable. Let $V_t(S_t), V_t^x(S_t^x)$ be the value of being in state S_t, S_t^x, respectively. A simple relationship between $V_t(S_t)$ and $V_t^x(S_t^x)$ can be

expressed [35]:

$$
\begin{aligned}
V_{t-1}^{x}(S_{t-1}^{x}) &= \mathbb{E}(V_t(S_t)|S_{t-1}^{x}), \\
V_t(S_t) &= \max_{x_t \in X_t}(C_t(S_t, x_t) + \gamma V_t^{x}(S_t^{x})), \\
V_t^{x}(S_t^{x}) &= \mathbb{E}(V_{t+1}(S_{t+1})|S_t^{x})
\end{aligned}
\tag{2.22}
$$

where $S_t = S^{M,W}(S_{t-1}^{x}, W_t)$, $S_t^{x} = S^{M,x}(S_t, x_t)$, and $S_{t+1} = S^{M,W}(S_t^{x}, W_{t+1})$. Then we can obtain the standard form of Bellman's equation [35]:

$$
V_t(S_t) = \max_{x_t \in X_t}(C_t(S_t, x_t) + \gamma \mathbb{E}(V_{t+1}(S_{t+1})|S_t^{x})) \tag{2.23}
$$

Also the optimality equations around the post-decision state variable

$$
V_{t-1}^{x}(S_{t-1}^{x}) = \mathbb{E}(\max_{x_t \in X_t}(C_t(S_t, x_t) + \gamma V_t^{x}(S_t^{x}))|S_{t-1}^{x}) \tag{2.24}
$$

Now the expectation is outside of the max operator. This gives us a computational advantage because $V_t(S_t)$ in Equation (2.22) is a deterministic optimization problem and does not need the use of approximation methods. Applying the post-decision state variable to approximate dynamic programming, we should solve the optimization problem first.

$$
\hat{v}_t^{n} = \max_{x_t \in X_t^{n}}(C_t(S_t^{n}, x_t) + \gamma \bar{V}_t^{n-1}(S^{M,x}(S_x^{n}, x_t))) \tag{2.25}
$$

where $\hat{v}_t^{n}$ is the optimum value of x_t. And then, the value function is updated by

$$
\bar{V}_{t-1}^{n}(S_{t-1}^{x,n}) = (1 - \alpha_{n-1})\bar{V}_{t-1}^{n-1}(S_{t-1}^{x,n}) + \alpha_{n-1}\hat{v}_t^{n} \tag{2.26}
$$

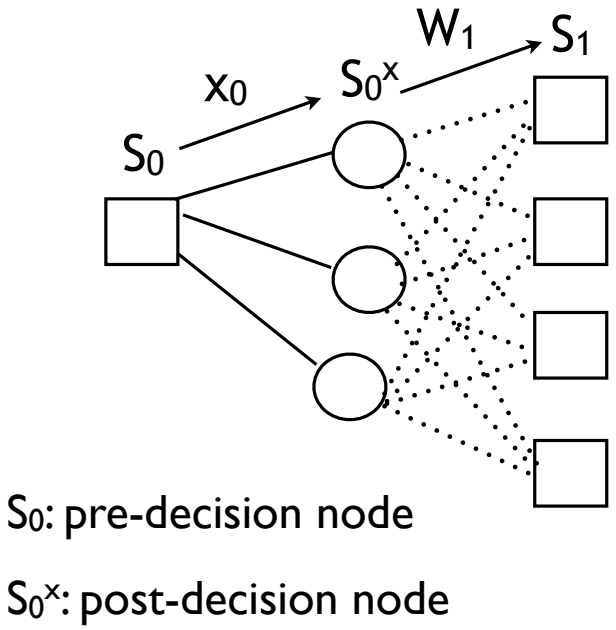

Figure 2.5 Schmetic diagram of post-decision state variable

Forward dynamic programming using the post-decision state variable is very useful when the optimization problem is an integer program, or a difficult linear or nonlinear program [35, 38].

Chapter 3

Evaluation of Raw Materials for DME Production System

3.1 Problem description

[1]Ensuring of energy security may be major challenges to secure national competitiveness. The current crisis regarding the depletion of oil resources around the world demands the development of a next generation energy system in many countries. Korea is no exception; actually Korean government has invested many efforts to control its energy situation for sustainable development [40]. There are some new energy resources, which can overcome the current crisis, including non-petroleum-based energy resources such as solar, wind, and geothermal energy, and synthetic energy resources such as biomass, fuel cell,

[1]This section is referred to the thesis, 'A study on the sustainability of DME production system from various energy feedstocks' [39]. Based on the thesis, this section shows that the case study would be revised and improved.

and coal gasification. Among the candidates for these energy resources, dimethyl ether (DME) is one of the most favorable because it can easily replace conventional fuels and is more eco-friendly than traditional fuels [41, 42]. Since the physical properties of DME are similar to those of liquefied petroleum gas (LPG), DME can replace LPG as an automotive and residential fuel. DME mixed with 20% LPG is now commercially used at a lower price without any modifications [43]. Also DME has a cetane number between 55 and 60. This value is very similar to that of diesel fuel, and the combustion of DME emits much less pollution than diesel [44]. Hence, DME can be a substitute for diesel fuel and widely used in transport sector [45] (Table 3.1).

Table 3.1 Properties of LPG and DME

	Propane	Butane	DME
Chemical formula	C_3H_8	C_4H_{10}	CH_3OCH_3
Molar weight (kg/mol)	44.11	58.13	46.07
Boiling point @ 1atm (°C)	-42.1	-0.5	-25.1
Vapor pressure @ 20°C (bar)	8.4	3.1	5.1
Liquid density @ 20°C (kg/m^3)	500	610	670
Ignition temperature (°C)	470	365	235
Cetane number	5	20	55-60
Explosion limit in air (vol%)	2.1-9.4	1.9-8.4	3.4-17

DME can be synthesized in at least two steps. The first is the synthetic gas (syngas) generation step; hydrocarbons obtained from natural gas, coal, or biomass are converted to synthetic gas (syngas), which is a combination of carbon monoxide (CO) and hydrogen gas. The second is the DME conversion step; the obtained syngas is converted to DME by several processes. DME conversion process has two different methods. These methods are indirect synthesis and direct synthesis (Figure 3.1). Indirect synthesis requires two reactors for methanol synthesis and dehydration whereas direct synthesis produces DME directly from syngas and does not include the intermediate steps of methanol production and purification [46]. Though there are two synthesis methods, the reforming process is essential to produce syngas. Syngas can be synthesized from many sources (e.g. natural gas, coal, waste wood, and agricultural products). Reforming process using natural gas and gasification process using coal, heretofore, are the most common methods for producing of syngas. The technology of reforming process using biomass has been developing, recently [47].

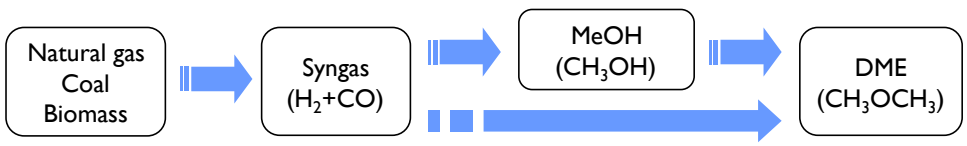

Figure 3.1 DME production system

There are various types of reactors and catalysts used in a DME pro-

duction system, and many studies on DME production have discussed DME reactors and catalysts, besides the production system [48, 49]. However, those studies focused on specific sections, and none analyzed the entire production process to assess a feasible feedstock for sustainability. Life cycle assessment can be a useful method to evaluate the competitiveness of raw materials of a target process [50, 51] and analyze the sustainability, since it is a tool to quantify environmental impacts. Life cycle assessment of DME production from biomass was performed, but this study focused on transportation process, and excludes coal and natural gas as raw materials [52, 53]. A study covers the life cycle assessment of coal-based DME production [54]. Gangadharan assessed sustainability of polygeneration processes based on syngas from coal and natural gas [55], but this study treated the conversion processes such as DME production and IGCC (Integrated Gasification Combined Cycle). While the previous researches do not cover the life cycle of various raw materials for DME production, this study has treated the evaluation of various raw materials which are potential for DME production, NG, coal, and waste wood.

Thus, the life cycle assessment of a DME production system from potential raw materials can be a modern method for designing DME production processes. Because the selection of a principal feedstock is a key factor for process design, the assessment of competitiveness of raw materials with respect to energy and the environment [56] is essential

for DME production. Also this assessment can be reflected to strategy of nationwide energy supply for sustainability [57, 58].

In this case study, the DME production systems from feasible raw materials such as natural gas, coal, and waste wood are analyzed to compare the amount of CO_2 and energy consumption through the defined life cycle. We introduce the intensities of CO_2 emission and energy to avoid tedious work, which calculates the amount of CO_2 emission from all energy sources for impact assessment. The life cycle of DME production includes the collection of raw materials, pretreatment of the collected raw materials, transportation to the DME production plant, and DME conversion. All processes for DME conversion are simulated using an process simulator (i.e. Aspen Plus). Recent technologies pertinent to practical plant in Korea and Korean energy situation data are introduced in the case study.

3.2 Life cycle assessment of DME production system

In this section, the proposed procedures based on life cycle assessment is followed to evaluate various raw materials for DME production.

3.2.1 Goal and scope definition

The goal of this study is to assess the environmental impact (i.e. CO_2 emission) and energy impact of the entire DME production processes, which are mentioned in the previous section. The prospective

raw materials in Korea are natural gas, coal, and waste wood. The scope of the DME production life cycle can be defined as pretreatment of raw material, transportation, and conversion. We introduce the confined life cycle (i.e. cradle-to-gate) since the prior and posterior steps of life cycle defined in this study are not significant consideration: all raw materials have no value in prior defined life cycle and the produced DME will be consumed identically in posterior step. The main structure of the system is shown in Figure 3.2.

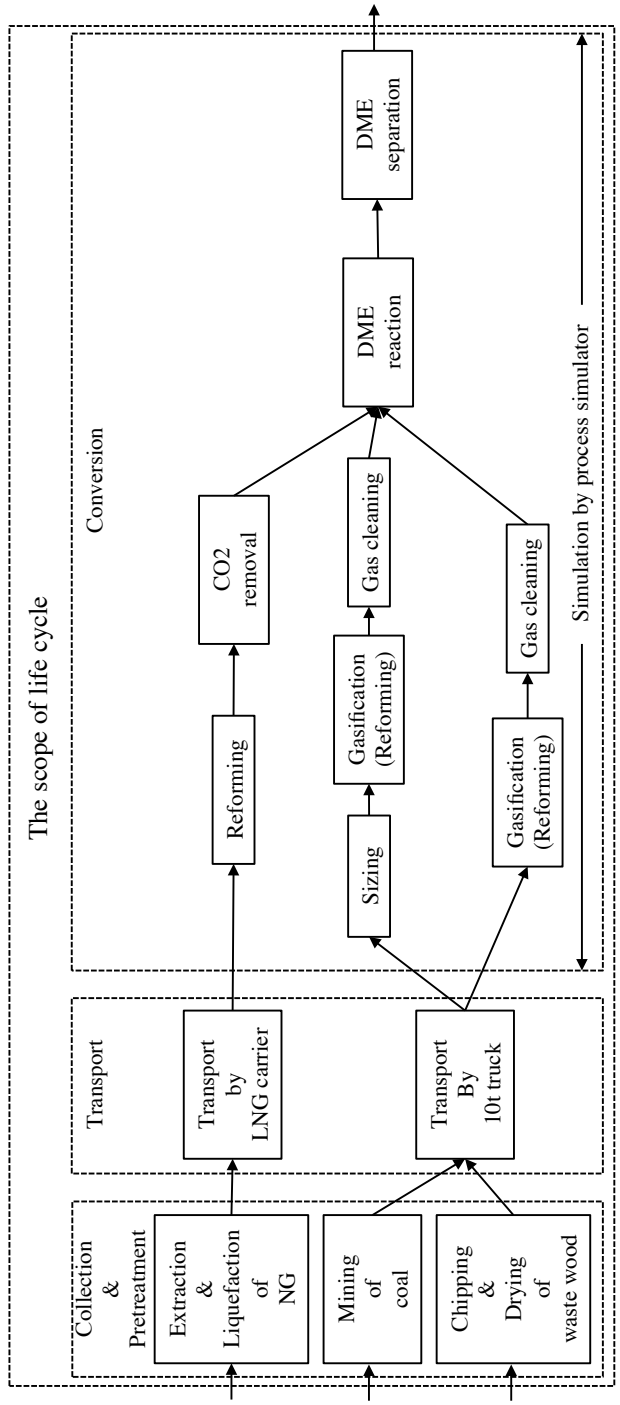

Figure 3.2 The defined scope of DME production life cycle

3.2.2 Inventory analysis

As previously mentioned, three raw materials are used in accordance with the defined scope. This scope is comprised of inventories such as collection of raw materials, pretreatment, transportation, and conversion [59]. The pretreatment section represents improvement of the quality of raw materials for DME conversion. The transportation section includes movement of materials to the DME production plant, and the conversion section includes syngas production and the DME reaction. In this study, the amount of CO_2 emission is considered as environmental impact and the all required energy in DME production is regarded as energy impact. The processes that are included in the pretreatment and transport section are calculated with some assumptions in terms of CO_2 emission and energy. The processes that are included in the conversion process are simulated using an process simulator (i.e. Aspen Plus). From simulation results, we can obtain the amount of CO_2 emission and consumed energy. The capacity of each DME plant is assigned as 1,000 t/day, which is the practical target in a Korea Gas Corporation (KOGAS) DME plant [60]. The amount of CO_2 emission and energy intensity is adopted to evaluate impacts for inventory analysis. The CO_2 emission and energy intensity can be defined by Equation (3.1) and (3.2).

$$\text{CO}_2 \text{ emission intensity}_{inv} = \frac{w_{CO_2,inv}}{\text{Total Energy}} \tag{3.1}$$

$$\text{Energy intensity}_{inv} = \frac{\sum_{inv}(FE + RE)}{PE_{DME}} \tag{3.2}$$

where *inv* represents each inventory. In the numerator terms of two parameters, w_{CO_2} indicates the amount of CO_2 emission while FE and RE are consumed fuel energy and required energy in process, respectively. In the denominator, PE_{DME} stands for total produced DME energy. For the calculation, the heating values used in this study are listed in Table 3.2.

Table 3.2 The adopted heating value of materials

	The adopted heating value [MJ/kg]
Natural gas	52.2
coal	34.1
waste wood	20.3
DME	31.7
Diesel	45.8

Natural gas

Imports of natural gas to Korea come mostly from Indonesia. Thus, natural gas for DME production is assumed to be extracted and liquefied in Indonesia, and transported to Incheon, Korea by a LNG carrier. The distance between the two locations is approximately 4,000 km. The required energy and the amount of CO_2 emission for the extrac-

tion process can be obtained from references [61], and the related values are shown in Table 3.3. The amount of CO_2 emission is mainly from the compressor for extraction and the flare stack for purge gas.

Table 3.3 Energy consumption and CO_2 emission in NG extraction

	Energy required [MJ/MJ NG]	CO_2 emission [gCO_2/MJ NG]
Extraction of natural gas	1.065	0.62

The liquefaction process has many sub-processes such as compression, purification, and refrigeration etc. Though the liquefaction process can be a significant topic, we adopted the existing data from references for the sake of brevity. The related values for liquefaction of NG are listed in Table 3.4 [62, 63].

Table 3.4 Energy consumption and CO_2 emission in NG liquefaction

	Energy required [MJ/MJ NG]	CO_2 emission [gCO_2/MJ NG]
Liquefaction of NG	9.05	6.95

In addition, the data for analysis of the transportation process is presented in Table 3.5 [64]. Based on the data, the amount of CO_2 emission can be calculated as 2.76 [gCO_2/MJ NG].

Table 3.5 Transportation data of LNG by LNG carrier

	Value	[unit]
Volume of carrier	138,000	[m^3]
Distance (round-trip)	8,000	[km]
Tanker speed	19.5	[knot]
CO_2 emission per distance	653,957	[gCO_2/km]
Fuel combustion rate (diesel)	11,320	[MJ/km]
Energy required	0.018	[MJ/MJ NG]
CO_2 emission	2.76	[gCO_2/MJ NG]

The conversion process is more complicated than the former processes because there are some sub-processes composing conversion process. The conversion process for DME production at the Incheon base in Korea was simulated using process simulator (i.e. Aspen Plus) in this thesis, and the detailed process block diagram is shown in Figure 3.3. The specification of feed stream is required to perform simulation, and it is listed in Table 3.6.

Table 3.6 Specification of imported NG at Incheon base

Condition		Component	Mole fraction
Temperature	20 [°C]	N_2	0.003
Pressure	3.601 [MPa]	CO_2	0.047
Mole flow	2,550 [kmol/hr]	CH_4	0.858
		C_2H_6	0.055
		C_3H_8	0.022
		n-butane	0.0055
		i-butane	0.0055
		i-pentane	0.004

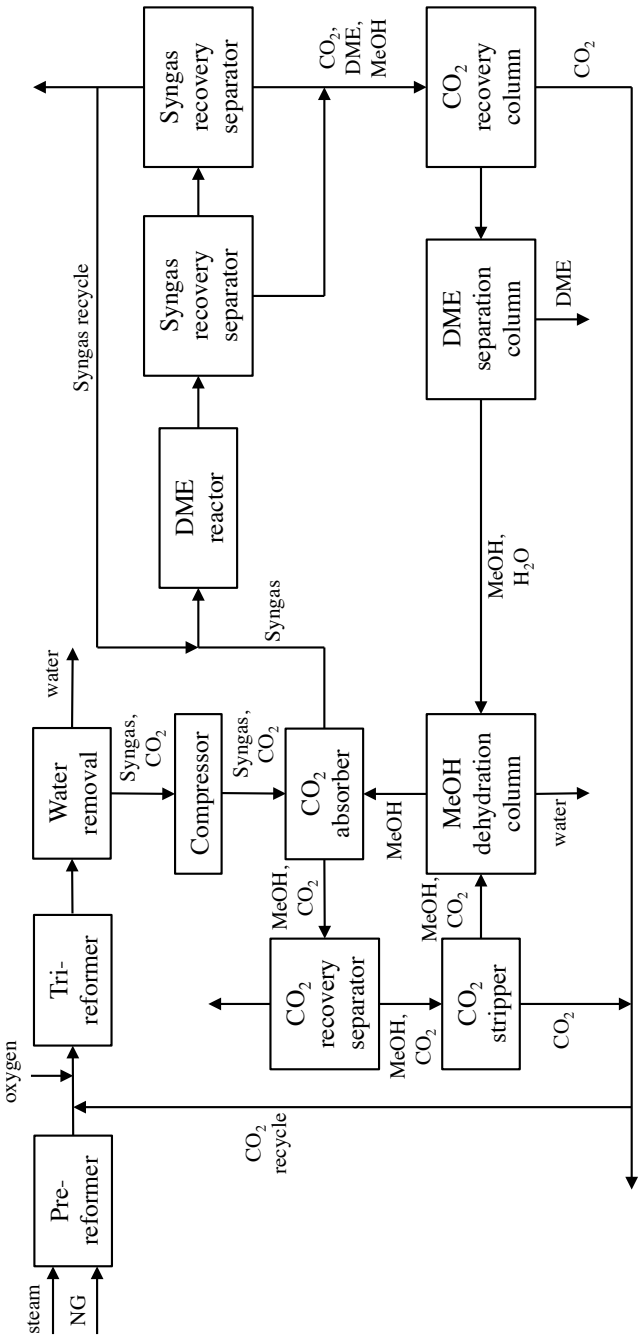

Figure 3.3 Block diagram of conversion process for DME production using NG

The conversion process involves two reforming processes, CO_2 absorption, DME synthesis, and DME separation process [65, 66]. In the reforming processes, pre-reformer cracks heavy hydrocarbons and tri-reformer generates syngas. Methane is generated after steam and NG pass through pre-reformer. The product stream of pre-reformer, which includes CO_2, H_2O, and methane, flows in tri-reformer with oxygen. The tri-reformer generates syngas from oxidation reaction. In detail, the pre-reformer converts heavy hydrocarbons into hydrogen, carbon monoxide, and carbon dioxide. Simulation information of the pre-reformer are shown in Table 3.7.

Table 3.7 Reactions in pre-reforming process

	Reaction
1	$3H_2 + CO \rightarrow CH_4 + H_2O$
2	$CO + H_2O \rightarrow H_2 + CO_2$
3	$C_2H_6 + 2H_2O \rightarrow 2CO + 5H_2$
4	$C_3H_8 + 3H_2O \rightarrow 3CO + 7H_2$
5	$n - butane + 4H_2O \rightarrow 4CO + 9H_2$
6	$i - butane + 4H_2O \rightarrow 4CO + 9H_2$
7	$i - pentane + 5H_2O \rightarrow 5CO + 11H_2$

Then the tri-reformer converts methane gas into carbon dioxide and carbon monoxide through steam reforming, water gas shift, and

combustion process (Table 3.8). The stream generated by tri-reformer

Table 3.8 Reactions in tri-reforming process

	Reaction
Steam reforming 1	$CH_4 + H_2O \rightarrow CO + 3H_2$
Steam reforming 2	$CH_4 + 2H_2O \rightarrow CO_2 + 4H_2$
Total combustion	$CH_4 + 2O_2 \rightarrow CO_2 + 2H_2O$
Partial oxidation	$CH_4 + 1/2O_2 \rightarrow CO + 2H_2$
Partial combustion	$CH_4 + O_2 \rightarrow CO_2 + 2H_2$
Steam reforming	$CH_4 + 1/2O_2 \rightarrow CO + H_2$
CO_2 reforming	$CH_4 + CO_2 \rightarrow 2CO + 2H_2$
Water gas shift	$CO + H_2O \rightarrow CO_2 + H_2$

moves to V-L separator via heat exchanger.

Water in the generated syngas is separated using a V-L (vapor-liquid) separator. The V-L separator recovers 99% of water in the stream. The CO_2 absorption block removes CO_2 in the generated syngas stream. To recover CO_2 in the generated syngas stream, CO_2 is absorbed using two columns. In these columns, methanol is used as an absorbent. The specification of two columns are shown in Table 3.9.

The DME reaction block is for DME synthesis, the direct method is used in this case, because the DME production process in Korea is now conducted by the direct method [60] (KOGAS, which operates pilot

Table 3.9 The specification of two CO_2 absorption column

	1st column	2nd column
Temperature	-36.5 °C	50 °C
Pressure	62 bar	34 bar
Stages	5	14
Feed stage	5	5
Condenser type	No condenser	Partial-vapor

plant for DME in Korea, proposed one step DME conversion.). Finally, the products of the DME reaction (i.e. DME, syngas, methanol, water, and CO_2) pass through the DME separation block. In this thesis, we assumed that syngas is re-circulated to the DME reaction block and CO_2 is recovered by the tri-reformer; finally, DME is separated. The DME conversion process contains one DME reactor and two separation units. Since the DME reactor model is very complicated and hard to analyze, the parameters for modeling such as CO conversion factor and selectivity were adopted by the data from KOGAS [60, 63]. The reaction formulars in DME reactor are presented in Table 3.10. The separation units are for CO_2 absorption and DME separation. The remained syngas and CO_2 are recycled by CO_2 separation unit, and DME separation unit recovers 99.99% of DME. The specification of DME reactor and separator are shown in Table 3.11. The property methods

Table 3.10 Reactions in DME reactor

	Reaction
DME synthesis 1	$3CO + 3H_2 \rightarrow CH_3OCH_3 + CO_2$
DME synthesis 2	$2CO + 4H_2 \rightarrow CH_3OCH_3 + H_2O$
Methanol synthesis	$2CO + 4H_2 \rightarrow 2CH_3OH$
Dehydration	$2CH_3OH \rightarrow CH_3OCH_3 + H_2O$
Water gas shift	$CO + H_2O \rightarrow CO_2 + H_2$

Table 3.11 The specification of DME reactor and separator

DME reactor		Separator	
Reactor type	Yield type	Stages	19
Pressure	60 bar	Feed stage	8
Temperature	260 °C	Pressure	35.2 bar
Phases	V-L	Condenser type	Partial-vapor

for simulation are SRK when substances have a vapor phase behavior and RKSMHV2 when substances have a vapor-liquid phase behavior [65, 67].

From the simulation result, the amount of feed and the heat duty of all units can be obtained for DME production of 1,000 t/day. Here, we assume that the total heat duty of conversion process reflects involved energy usage (e.g. fuel consumption, electricity), because this

case study put emphasis on energy intensity. Based on data and simulation results, the amount of CO_2 emission and the required energy per the produced DME energy can be obtained for inventory analysis.

Coal

Coal and waste wood as raw materials are treated by processes analogous to the treatment used for natural gas. They are assumed to be supplied by domestic production. Coal can be obtained by mining at Taebaek in Korea. The methods of mining are open-cut mining and underground mining. In Korea, most mines are in mountainous districts, and underground mining is favored. Table 3.12 shows the energy consumption and the amount of CO_2 produced by coal mining.

Table 3.12 Energy consumption and CO_2 emission for mining coal

	Coal mining	Unit
Electricity	19.4	[kWh/t coal]
Diesel	0.66	[L/t coal]
CO_2 emission for electricity	437.8	[gCO_2/kWh]
Energy required	0.488	[MJ/MJ coal]
CO_2 emission	0.228	[gCO_2/MJ coal]

Mined coal is moved to the Incheon base by 10t-trucks. For truck transportation, CO_2 emission and the required energy are related to the

fuel consumption of the truck, which can be expressed as a function of the loading rate of weight (λ) [52, 68] (Equations (3.3)-(3.5)).

$$f_{FC}(\lambda) = a\lambda + b \tag{3.3}$$

$$\lambda_{avg} = \frac{w_{material}}{10N_{material}} \tag{3.4}$$

$$N_{material} = (\frac{w_{material}}{24.7\rho}) + 1 \tag{3.5}$$

where f_{FC} indicates the rate of fuel consumption, a(=714 gCO_2/km) and b(=508 gCO_2/km) are constants on the fuel consumption, the loading platform of 10t-trucks is to be approximately 24.7m^3, ρ indicates bulk density of materials, and N is total number of transportation [52]. The data for coal transportation in Korea is listed in Table 3.13.

Table 3.13 Data of coal transportation

	Transportation	Unit
Bulk density (coal)	1,056	[kg/m^3]
Distance (round trip)	540	[km]
CO_2 emission	3.015	[gCO_2/g diesel]
Fuel efficiency	2.4	[km/L diesel]
Energy required	0.668	[MJ/MJ coal]
CO_2 emission	0.722	[gCO_2/MJ coal]

In conversion process, it is required that sizing, gasification, and gas cleaning process (i.e. desulfurization and CO_2 removal) for generating

syngas should be added to conversion process due to the characteristics of coal. Coal is mined in an irregular size, and should be sized uniformly. Also, it is necessary to make solid coal into gas [69]. Through the gasification process of coal, the syngas for DME synthesis is generated. The remainder of the energy conversion processes for coal are analogous to those used for natural gas [70]. A block diagram of coal based DME production is shown in Figure 3.4 [54]. For the simulation of process based on coal, the characteristics of coal should be defined, first. Those of coal can be assumed by data. The composition of coal can be assumed as shown in Table 3.14 and coal is assumed to be fractionated into particle size ranges listed in Table 3.15 [69].

Table 3.14 Composition of coal

Component	%
ash	9.66
C	74.455
H_2	4.955
N_2	1.585
Cl	0.065
S	2.44
O_2	6.84

Table 3.15 Particle size of coal

Mesh size	Weight fraction
0-20	0.11323618
20-40	0.04219685
40-60	0.05991239
60-80	0.09682933
80-100	0.1459255
100-120	0.1079199
120-140	0.0523056
140-160	0.04586571
160-180	0.0584937
180-200	0.27731484

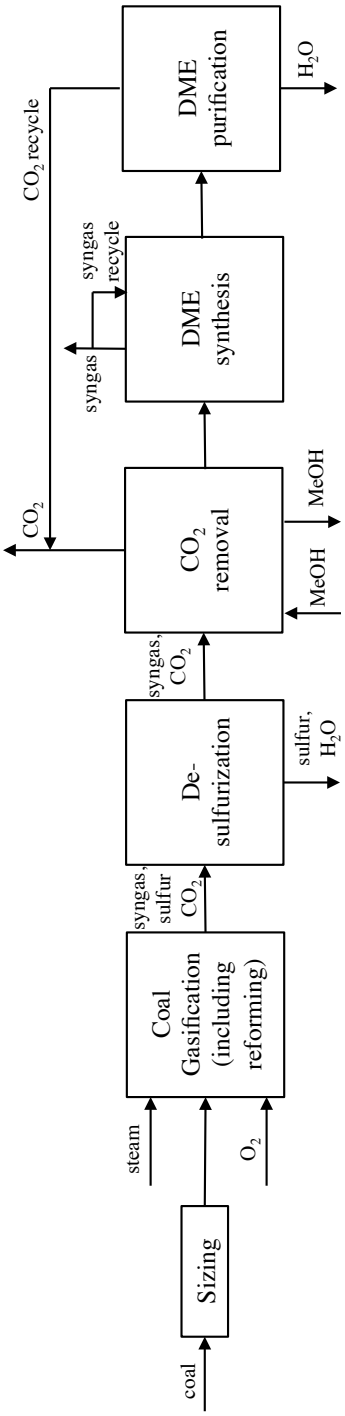

Figure 3.4 Block diagram of coal-based DME production

The coal is mixed with water and sent to a crusher that pulverizes the coal to a maximum particle diameter of 0.0002m. The Hardgrove Grindability Index is assumed to be constant at a value of 45. The pulverized coal is then sieved to obtain even sized coal, which moves to the gasification block. Among several gasification technologies, integrated gasification combined cycle is one of the most prospective technologies recently. We can therefore adopt this gasification technology among several alternatives in this study [71, 72]. In the gasification process, solid coal should be converted to a component which is able to react, and then syngas is generated under conditions of high pressure (475 psia) through a gasification process. The generated syngas stream has to undergo desulfurization and CO_2 removal processes such as in the case of natural gas. The purified syngas goes through the DME synthesis and purification blocks, which are identical to those of NG case. Through the simulation, the amount of CO_2 emission and the heat duty can be obtained from sizing to DME purification.

Waste wood

The inventories of DME production using waste wood are analogous to those of coal and include pretreatment, transportation, and conversion [52, 73]. Waste wood is assumed to be obtained in the domestic market in Gyeongsangbuk-do, Korea. As the local government tries to encourage the usage of waste wood for converting into useful

biomass [74], this assumption can be considered reasonable. The waste wood described in this study can be a kind of ligneous biomass. So, the pretreatment of waste wood includes chipping and drying processes. Similar to the case of coal, raw waste wood should be dehydrated and chipped into proper-sized pieces for gasification. The water content of waste wood should be decreased by at least 11%. The required energy for chipping and drying can be obtained as shown in Table 3.16 [52]. Additionally, Table 3.17 shows the data for transportation of waste wood.

Table 3.16 Required energy for chipping and drying process

	Chipping and drying	Unit
Electricity	13.6	[kWh/t waste wood]
Diesel	1.23	[L/t waste wood]
Energy required	0.414	[MJ/MJ waste wood]
CO_2 emission	0.162	[gCO_2/MJ waste wood]

The pretreated waste wood is moved to the Incheon production base. The distance between the repository in Gyeongsangbuk-do and Incheon base is approximately 300 km. The remaining assumptions are the same as those adopted for coal-based processes. The entire conversion process using waste wood is identical to the conversion process used for coal, except for the sizing process [75] (Figure 3.5).

Table 3.17 Data of waste wood transportation

	Transportation	Unit
Bulk density (waste wood)	294	[kg/m^3]
Distance (round trip)	600	[km]
CO_2 emission	3.015	[gCO_2/g diesel]
Fuel efficiency	2.4	[km/L diesel]
Energy required	0.207	[MJ/MJ waste wood]
CO_2 emission	1.22	[gCO_2 /MJ waste wood]

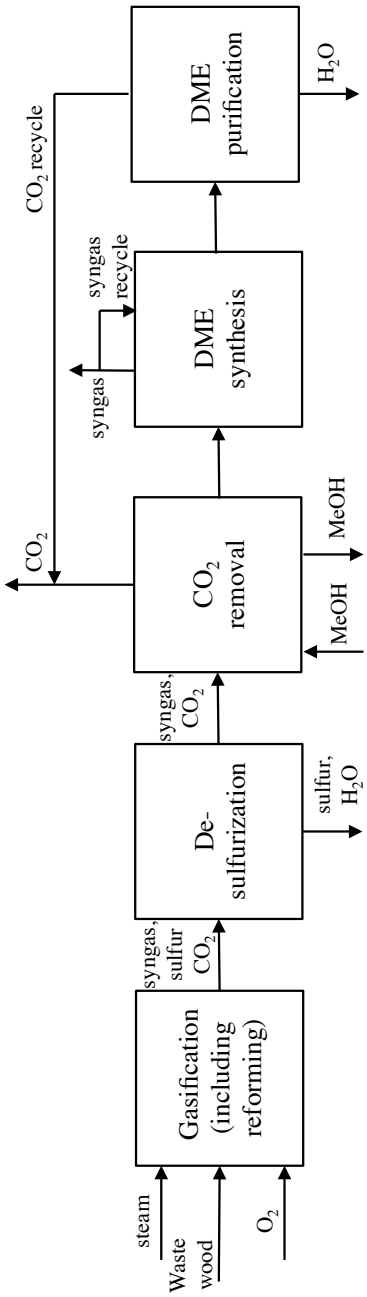

Figure 3.5 Block diagram of waste wood-based DME production

In detail, the DME production process using coal and biomass has identical processes except for pretreatment and sizing process [75, 76]. Prior to DME synthesis, gasification and cleaning (i.e. CO_2 removal and desulfurization) is essential to generate syngas. In this case study, a reactor is introduced to simulate the conversion (Table 3.18).

Table 3.18 The reactor conditions of conversion of coal and biomass

	Condition	
Reaction	coal/biomass	$\rightarrow H_2O + O_2 + N_2 + C + Ash$ $+S\ compounds + Cl_2 + H_2$
Pressure	0 bar	
Temperature	15.6 °C	

Then the converted materials moves to a gasifier. This is the main process to generate syngas. Then, H_2S and COS in the product stream should be removed, because they can cause corrosion of pipe or combustion unit and degradation of catalysts, seriously. It is difficult to remove COS, on the other hand, H_2S can be removed easily in gas cleaning process using acid gas removal (AGR) unit. Therefore, COS needs to be converted into H_2S and CO_2 using hydrolysis first. Next, the stream moves to the cleaning process. The cleaning process includes H_2S removal and CO_2 absorption. The simulation information of H_2S removal and CO_2 absorption are shown in Table 3.19.

Table 3.19 Simulation information of gas cleaning process

		H_2S removal	CO_2 absorption
Stages		20	10
Feed stages	Methanol	1	1
	Syngas	20	10
Pressure	Stage 1	400 psia	400 psia

3.3 Results and impact assessment

Table 3.20 shows simulation results. As previously mentioned, the plant in Incheon produces DME of 1,000 t/day. Energy efficiency means the produced DME energy per each potential energy of feed. The amount of methanol discharge as a waste stream is also presented since it can be harmful to environment.

Table 3.20 The result of inventory analysis in DME production life cycle

	Natural gas	Coal	Waste wood
DME [ton]	1,000	1,000	1,000
Feed [ton]	1,192	1,956	2,897
Total CO_2 [ton]	1,031.86	1,459.15	1,862.28
Methanol discharge [ton]	261.32	810.93	842.94
Required energy [MJ]	2,504,924	1,977,528	3,636,482
CO_2/DME [gCO_2/MJ]	32.79	48.23	62.55
Energy efficiency	0.518	0.475	0.539

Although waste wood-based DME plant has somewhat higher energy efficiency than either coal or natural gas, a large amount of waste wood is required for DME production due to its relatively lower chemical potential. In addition, the DME production process from waste wood emits large quantities of CO_2 and requires energy the most, therefore, waste wood is not competitive as a DME feedstock.

In terms of CO_2 emission, natural gas is the most favored. In this result, the practical CO_2 capture system was not applied to the all DME production processes, because it has not been developed for a 1,000 t/day DME plant yet. As some researchers suggest the carbon capture system in recent years [71], the chance of mitigation of CO_2 emission is increasing. Assuming that the CO_2 capture system is applied to the cases, the amount of CO_2 emission and required energy can be obtained to compare with non-capture cases. Table 3.21 shows the results. The amount of CO_2 is decreased dramatically, while the required energy is increased and carbon capture system needs more capital and fixed costs intrinsically; this topic is not treated in this study. This result will help a decision maker to decide the strategy of DME production.

Table 3.21 The comparison result of non-carbon capture and applying carbon capture system

		Natural gas	Coal	Waste wood
Non-Carbon capture system	Total amount of CO_2 [ton]	1,031.86	1,459.15	1,862.28
	Required energy [MJ]	2,504,924	1,977,528	3,636,482
With Carbon capture system	Total amount of CO_2 [ton]	413.54	936.35	1,137.91
	Required energy [MJ]	4,005,946	2,686,065	5,050,962

Each inventory analysis also is open to meaningful interpretation. Figure 3.6 and 3.7 show the resulting CO_2 emission intensity and energy intensity of the inventories for each raw material. The results were obtained without carbon capture system.

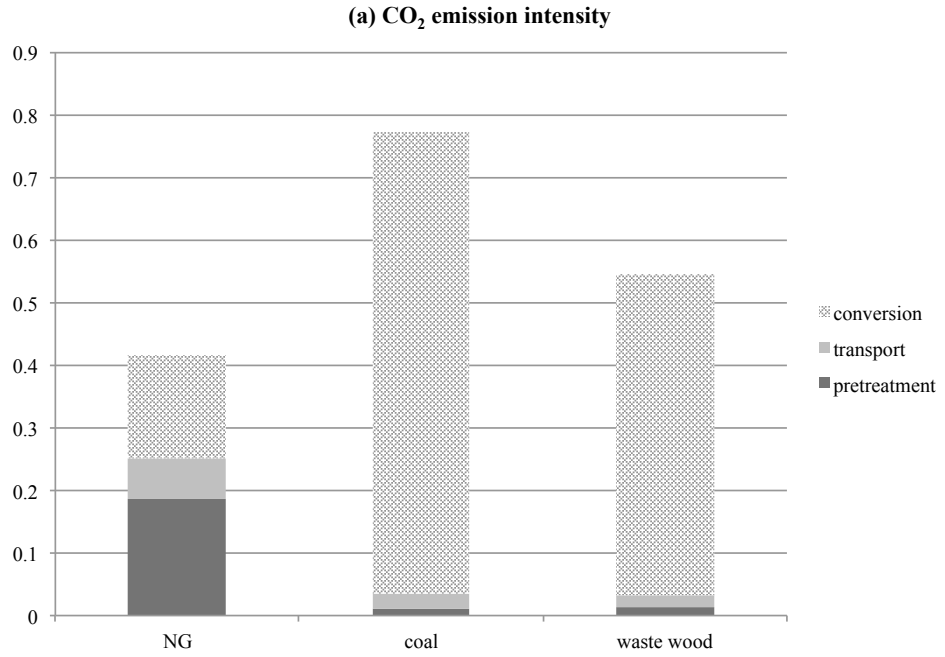

Figure 3.6 The comparision of CO_2 emission intensity of each raw material

The conversion process plays an important role in the amount of CO_2 emission. In the case of NG, the amount of CO_2 emission from pretreatment is slightly greater than that in the conversion process due to the use of complicated treatments such as liquefaction and regasification, and due to its long distance; the transportation process used for NG emits more CO_2 than the transportation process used for

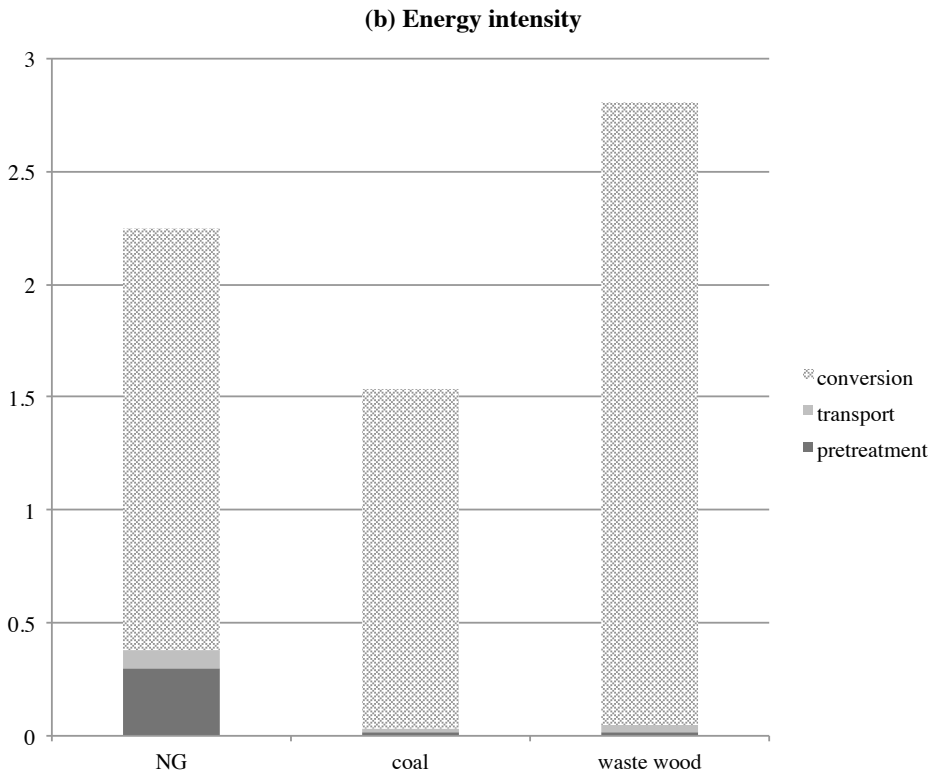

Figure 3.7 The comparision of energy intensity of each raw material

coal and biomass. When considering energy intensity, the conversion process is also the largest part of the entire process in all the cases. Especially, the process using NG has a disadvantage in that the difference of temperature is too great to save on energy consumption. In the conversion process used for NG, the temperature increases to 1,100°C (reformer) and decreases to -40°C (CO_2 separation).

3.4 Cost analysis

Based on the above obtained result, the concept of cost intensity can be introduced as Equation (3.6):

$$\text{Cost intensity} = \sum_{feed} \frac{(\text{FC} + \text{DC} + \text{EC})}{\text{PD}} \tag{3.6}$$

where FC, DC, and EC represent feed treatment, CO_2 disposal, and energy costs (except for energy consumption of feed treatment), respectively while PD is price of DME. This presents that the best potential material can be selected by considering feed supply, environmental, and energy cost. To reflect these costs, the price data are shown in Table 3.22. All values are regarded to be deterministic in spite of their uncer-

Table 3.22 Price data for cost analysis

	price	unit	References
NG	292.2	[$/ton]	[77]
Coal	106.8	[$/ton]	[20]
Biomass	220	[$/ton]	[78]
CO_2 disposal	20	[$/ton]	[61, 79]
Energy unit cost	0.0566	[$/kWh]	[62, 74]
DME	739.8	[$/ton]	[60, 74, 80]

tain fluctuations for simplicity in this case. Since a handling uncertainty becomes very complicated work, this should be addressed from a dif-

ferent perspective. The results of cost intensity analysis are shown in Figure 3.8.

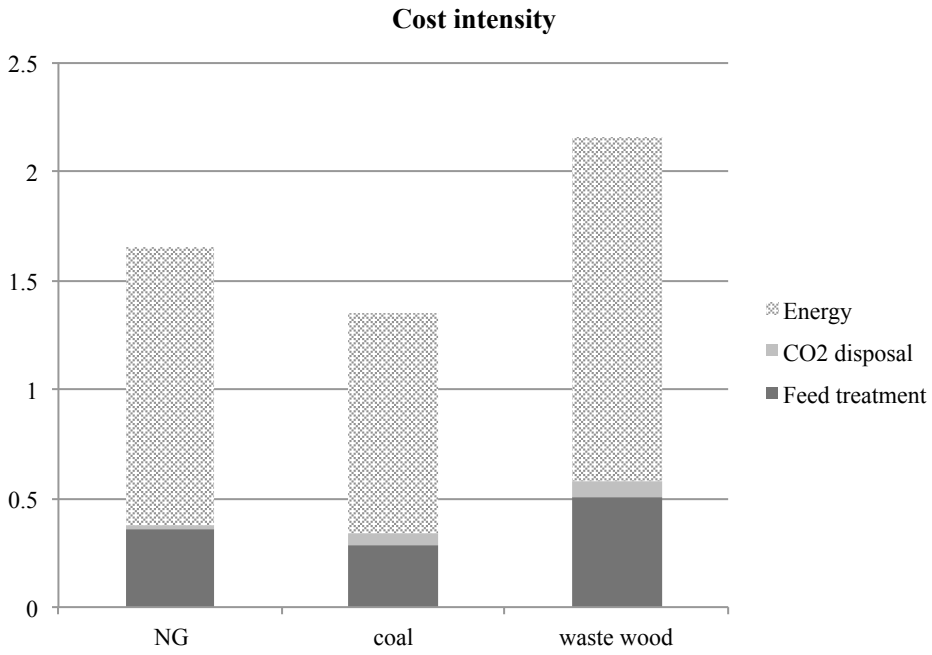

Figure 3.8 The cost intensity of each raw material

Analysis of cost intensity showed the same tendency as the result for energy intensity. Feed treatment and energy costs account for most of the cost intensity. The disadvantage of waste wood is the feed treatment cost as well as energy cost. The conversion of waste wood into useful biomass is still costly. This implies that the technology of making useful biomass should be improved to have its competitiveness.

On the contrary to this, coal may be the best prospective material to produce DME in Korea in terms of total cost. Although the coal-based

DME production emits the largest amount of CO_2, the cost of CO_2 disposal is insignificant. It is positive that coal from domestic mines can be used to stimulate a revival of the coal market in Korea. Many chances exist to improve the technologies used in coal gasification and carbon capture, because they have consistently developed over time. However, the values of cost intensity are all greater than one. This indicates that raw materials of interest are not still economical. It is inevitable that the price of DME should be increased for commercial supply. The selling prices of DME for sale are 1223.7 (NG), 998.4 (coal), and 1598.4 (waste wood) [$/ton], at least.

Chapter 4

Energy Planning Model Considering Uncertainties

4.1 Problem description

There is a trade-off between energy security and mitigation of greenhouse gas (GHG) [81]. According to CAFE (Corporate Average Fuel Economy) standards, we have to develop nuclear and renewable energy sources (Figure 4.1). Thus, energy planning model is needed to evaluate availability of potential energy sources (i.e. nuclear and renewable energy sources) including conventional energy sources such as coal, oil, natural gas, etc.

In this chapter, we construct the energy planning model[1]. Energy planning is difficult to be represented using the process simulator. Thus,

[1]This section is based on the research article, 'Optimization of Korean energy planning for sustainability considering uncertainties in learning rates and external factors' [82]. This is the published work of the author of this thesis.

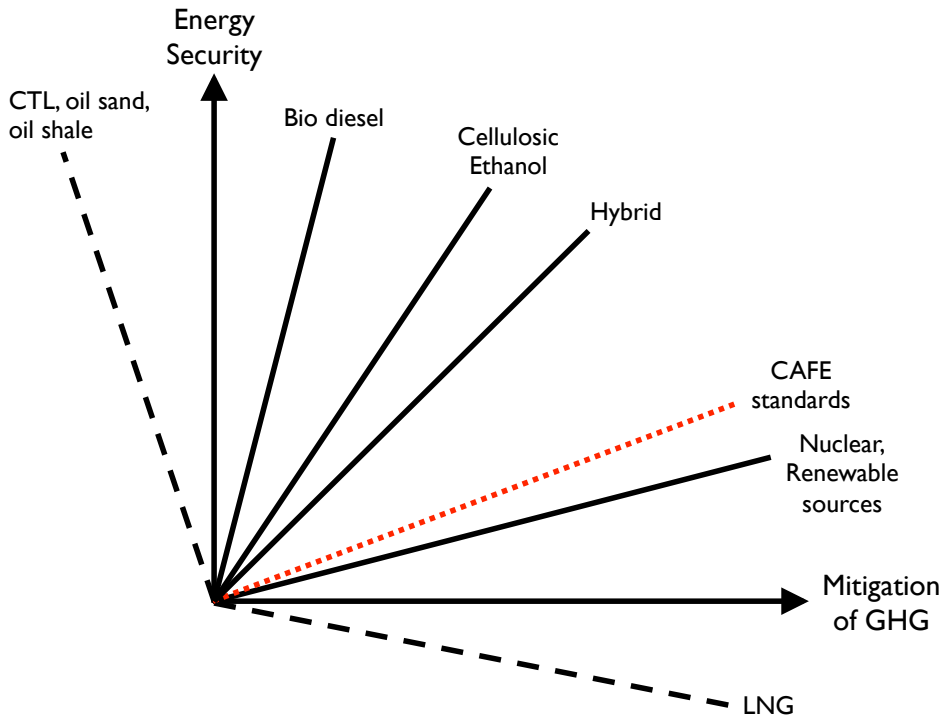

Figure 4.1 Alternative energy sources for energy and environment

the mathematical formulation would be introduced to identify the optimal energy planning model of interest. Also the uncertain variables would be considered using Monte Carlo method. Previously, a number of methodologies and schemes for energy planning have been studied and proposed for optimal energy planning. In terms of models, schemes have been introduced by the time-stepped energy system optimization model (TESOM) [83], market allocation model (MARKAL) [84, 85, 86], energy flow optimization model (EFOM) [87], and inexact community-scale energy model (ICS-EM) [88]. Each model reflects its own characteristics and optimization techniques but does not incorporate recent

changes in nature of renewable energy planning, and overall energy sources in large scale. Krukanont considered various uncertainties to analyze the near-term energy planning and suggested several policy regimes but covered limited renewable energy systems [89]. Evaluating feasibility various renewable energy systems have also been introduced. Viebahn compared costs and the contributions of carbon capture and storage (CCS) technologies and renewable energy systems in the long term [90]. Chatzimouratidis and Kaya evaluated some energy systems under several criteria with weights obtained by an analytical hierarchy process (AHP) [91, 92]. Krey incorporated uncertain energy prices into energy systems by including a stochastic risk function [93]. Similarly, Streimikiene conducted a long-term assessment of new electricity generation technologies for CO_2 price scenarios [94], and Koo studied scenario-based economic evaluation of renewable energy systems considering carbon capture and storage (CCS) and varying fuel prices [95]. Despite the recent works, energy planning needs to reflect the integration in terms of uncertainties in prices of fuel price for energy generation, expansion of carbon dioxide trading, and change of learning rates with various models to obtain optimal solution, because the governments which are interested in energy planning want to evaluate energy systems in many ways for robustness. While some previous works provided estimates of variables separately [96, 97], we suggest that the proposed method should apply the future prospects on cost

and learning effect.

Based on the previous works, a modified model can be introduced with supplementary information. The supplementary information discussed in the proposed method includes not only cost estimates at the present level but also prospects for the future. The uncertainties in the future situations will be considered with respect to the types of energy systems, and the proposed method presents several major uncertainties related to energy systems – the learning rate of the technologies, fuel prices, and carbon prices. The major uncertainties will affect the competitiveness of energy systems. The effects of learning rate and prices of an energy system may be unique attributes; we cannot anticipate exactly [98, 99, 100]. Thus, we have to estimate the unpredictable values. This study aims to integrate various uncertainties in growth rate scenarios and apply Monte Carlo simulation for handling uncertainties. The proposed method constructs the production and CO_2 emission trading costs as an objective function, which allows for economic evaluation of conventional and renewable energy systems taking into consideration the uncertainties. As a result, the optimal capacities of energy systems to be added can be obtained.

4.2 Mathematical modeling

The model is defined to reflect the integration of uncertainties in this section. As mentioned, the previous model needs to be modified by the supplementary information such as learning rate and prices. That makes our model consider the prospect for the future as well as estimation at the present level. The uncertainties are considered by Monte Carlo simulation to achieve robust optimization. Since the using of random input from sampling turns the model into a stochastic model, the inclusion of uncertainties would be reflected to decision-making that decides which energy system should be installed.

4.2.1 Definition of production costs

In this case study, energy system refers to power plants that generate electricity using a certain energy source. The aim of this study was to evaluate the production costs of possible energy supplies and optimize energy planning that included renewable energy systems. According to the method commonly practiced for economic evaluation, the total cost of the production can be expressed as the summation of the capital, fixed, variable, and external costs. Each cost can be calculated as follows [87, 95, 101, 102]:

$$\text{Capital cost} = \sum_{t=1}^{N_t} \frac{1}{(1+d)^t} KC \cdot I_t \tag{4.1}$$

$$\text{Fixed cost} = \sum_{t=1}^{N_t} \frac{1}{(1+d)^t} KF \cdot C_t \tag{4.2}$$

$$\text{Variable cost} = \sum_{t=1}^{N_t} \frac{1}{(1+d)^t} C_t \cdot PF_t \cdot \rho \cdot \tau \tag{4.3}$$

$$\text{External cost} = \sum_{t=1}^{N_t} \frac{1}{(1+d)^t} C_t \cdot PC_t \cdot R \cdot \tau \tag{4.4}$$

where N_t denotes the total years from 2011 to 2030; d is the discount rate; KC is the initial unit capital cost of the energy system; I_t is the capacity of the energy system installed in year t; KF is the unit fixed cost of the energy system in 2011; here, the unit fixed cost includes the operation and maintenance cost that are not dependent on the capacities. C_t is the cumulative capacity of the energy system in year t. Variable cost refers to expenses that change in proportion to the activity of a business; here, we assumed that the variable cost is limited to buying fuel. Thus, the variable cost is dependent on fuel price only, and PF_t is the required fuel price to operate the energy system in year t; ρ is the conversion ratio from the TOE to the MWh; τ is the capacity factor for the energy system, which represents the fraction of actual output produced over the maximum output achievable during a period of time. Lastly, PC_t is carbon price in year t; R is the emission rate with capacity C_t for the energy system.

4.2.2 Learning effects

The basic concept of learning is cost reductions as the result of learning-by-doing. It means that the performance improves as capacity or a product expands [98]. Learning can also be regarded as the cost-reducing effect in each energy system that might be used in economics to describe improvement in productivity [103]. The learning process can also be seen as a fundamental human characteristic. A person engaged in a task will improve his/her performance with experience and technological development. Many studies presents that the cost reduction is dependent on the industry, region, and time. Especially for renewable system, empirical studies show that learning is influenced by cumulative capacity, C_t [103, 104]. The cumulative capacity can be defined as following equation.

$$C_t = C_0 + \sum_{t=1}^{N_t} I_t \tag{4.5}$$

Reflecting the concept of learning effect, the total cost of each energy system over its life time can be modified as following equation.

Total cost =

$$\sum_{t=1}^{N_t} \frac{1}{(1+d)^t}((\frac{C_t}{C_0})^{\alpha_t} \cdot (KC \cdot I_t) + C_t(KF + PF_t \cdot \rho \cdot \tau + PC_t \cdot R \cdot \tau)) \tag{4.6}$$

C_0 stands for the initial capacity at the base year, α_t corresponds to learning effect term at year t. The learning effect is restricted to capital since the fixed, variable, and external costs do not depend on factors of experiences: the prices of fuel do not decrease with accumulated capacity, and the emission rate is assumed to remain unchanged throughout the studied period. And $\alpha_{e,t}$ depends on the particular energy system of interest, and can be expressed by following equation [101].

$$\alpha_{e,t} = \frac{\ln(1 - \beta_{e,t}/100)}{\ln 2} \tag{4.7}$$

Here, $\beta_{e,t}$ indicates the learning rate for the energy system of interest each at time t. Reliable estimates of learning rate are important if meaningful projections of cost reduction are to be sought under the application of the learning effect [103]. A dispute may occur; the differences between regional and global learning rates. Although the regional learning rate may not be same as the global learning rate, Korean effort can reflect the global movement to some degree because Korea is one of the countries that a lot of researches have been done in various energy systems. Thus, we assume that the regional learning rate is identical as the global learning rate in this case. We are to adopt the learning rates from previous works [103, 104]. For the reliable estimation of learning rate, the value is sampled using by Monte Carlo method and re-estimated every year. The method requires a model in order to use

properly, and we adopt Equation (4.7) instead of modeling the learning curves from the complicated techniques. Although many studies analyzing learning curves and/or learning rates have been done; these studies are profound and have a massive amount of information, in this study, the detailed theories on the prediction and estimation of learning curves for various energy systems have been omitted for the sake of brevity. If readers are interested in those works, the readers can refer to following works [105]. The mean and standard deviation values for Monte Carlo simulation in this study can be adopted by [101, 106, 107, 108, 109] (Table 4.1).

Table 4.1 Mean and standard deviation of learning rates of energy system

unit: [%]	Mean	Standard deviation
Coal	6.25	2.4
Oil	2.5	1.5
Natural gas	10.6	9.2
Nuclear	5.9	0.1
Hydro	3.8	1.9
Wind	13.1	5.2
Solar	28.2	6.6
Biomass	15	0.3

4.2.3 Fuel and carbon prices for handling uncertainties

As mentioned, the uncertain variables to be treated are the fuel prices and the carbon cost besides learning rates. The price of fuel (Table 4.2) and carbon (Table 4.3) are generated by Monte Carlo sampling [110, 111]. For hydro, wind, and solar energy system, fuel price for electricity generation is assumed to be zero. These values are renewed every year in the same way as learning rate.

Table 4.2 Mean and standard deviation of fuel prices for electricity generation of each energy sources

unit: [$/MWh]	Mean	Standard deviation
Coal	28	3
Oil	49	5
Natural gas	39	5
Nuclear	13	1
Hydro	0	0
Wind	0	0
Solar	0	0
Biomass	24	5

Table 4.3 Mean and standard deviation of CO_2 price

unit: [\$/tCO_2]	Mean	Standard deviation
CO_2 price	48.7	8.9

4.2.4 Monte Carlo simulation

Monte Carlo simulation is a method for iteratively evaluating a deterministic model using sets of random numbers as inputs and for analyzing uncertainty propagation. The goal is to determine how random variation and lack of knowledge of the system are modeled. Since the learning rate, fuel price, and carbon cost are hard to model accurately, this method can be an efficient approach to estimate uncertain variables stated in this study [112, 113]. The key to Monte Carlo method is generating the set of random inputs, which are uncertain variables in this study [114]. The uncertain variables are assumed to follow normal distribution. Related values are listed in Table 4.1-4.3. All values of each energy system are updated every year t. The number of the generated sample and function evaluation are set as 10,000. The results generated from the evaluation will be represented as histograms. Also we can see the distribution of values of feasible total cost, and the result can offer more reliable implications in the uncertain future.

4.3 Structure of the proposed model

4.3.1 Structure of the problem

Figure 4.2 shows the structure of the problem for the proposed methodology based on previous works [88, 101]. Although there are many renewable energy sources, which have been developed in Korea, it is assumed that four representative and potential ones will be adopted in this study. The generated energy is utilized by industries, transportation, residences, commerce, and public use. In addition, we assume that there will be emission allowance trading with foreign countries.

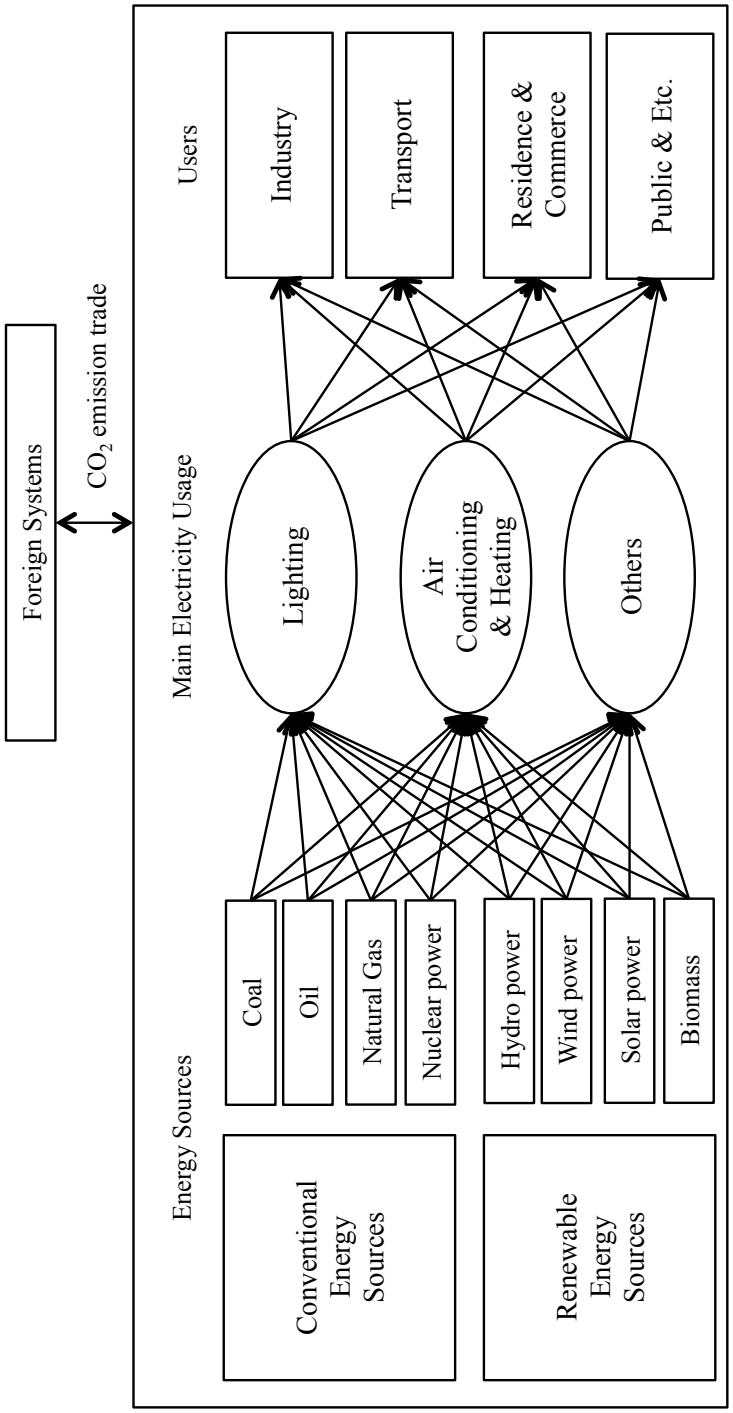

Figure 4.2 Structure of the proposed model

4.3.2 Optimization of energy planning

Objective function

The objective function for the proposed model can be expressed as the sum of the modified cost functions. The CO_2 trading term is added.

$$\begin{aligned}\min(\text{Total cost}) = \sum_{e=1}^{N_e}\sum_{t=1}^{N_t}\frac{1}{(1+d)^t}((\frac{C_{e,t}}{C_{e,0}})^{\alpha_{e,t}}\cdot(KC_e\cdot I_{e,t}) \\ + C_{e,t}(KF_e + PF_{e,t}\cdot\rho\cdot\tau_e + PC_t\cdot R_e\cdot\tau_e) - PC_t\cdot VT_t) \\ I_{e,t} = \arg\min_{\forall e,t}(\text{Total cost})\end{aligned} \tag{4.8}$$

The subscript e indicates the type of energy sources. In Equation (4.8), N_e indicates 8 (1: coal, 2: oil, 3: natural gas, 4: nuclear power, 5: hydro power, 6: wind power, 7: solar, and 8: biomass). $C_{e,0}$ denotes the initial capacity of each energy system. VT_t is the amount of CO_2 emissions treated in year t. At this point, the objective function is formulated as a nonlinear optimization because the learning effect term is nonlinear. And the uncertain variables such as learning effect ($\alpha_{e,t}$), fuel price ($PF_{e,t}$), and CO_2 cost ($PC_{e,t}$) are sampled using by Monte Carlo simulation. Then the sampled values are applied to objective function, and the optimization results reflect a robust handling of uncertainties.

Constraints

Renewable energy systems like hydro, wind, and solar energy cannot be constructed infinitely. Thus the size limit, SL_e, is set for the potential of the renewable energy sources. Since the biomass can usually be derived from timber, agriculture, and food processing waste; thus we need not restrict the size of this energy system. Equation (4.9) indicates the size limits of each energy system.

$$\begin{aligned} \sum_{hydro} \sum_{t=1}^{N_t} I_{e,t} + C_{hydro,0} &\leq SL_{hydro} \\ \sum_{wind} \sum_{t=1}^{N_t} I_{e,t} + C_{wind,0} &\leq SL_{wind} \\ \sum_{solar} \sum_{t=1}^{N_t} I_{e,t} + C_{solar,0} &\leq SL_{solar} \end{aligned} \tag{4.9}$$

The value of SL_e is based on the natural and technological conditions of the particular geographic region of interest such as Korea.

The energy planning should be able to satisfy the energy demand.

$$\psi\rho \sum_{t=1}^{N_t} \sum_{user} ((1+g)^t \cdot VD_{user,t}) \leq \sum_{e=1}^{N_e} \sum_{t=1}^{N_t} ((1+\kappa) C_{e,t} \cdot \tau_e) \tag{4.10}$$

In Equation (4.10), $VD_{user,t}$ denotes the energy demand from each user. To estimate the future energy demand, g and are introduced. g indicates

the energy demand growth rate and ψ the level of energy supply target. In this study, three scenarios of demand growth rate are applied to cover the energy fluctuation. Additionally, the level of energy supply target can be regarded as a buffer [95]. ψ is determined as 1.1, which means 10% buffer of target in this study. In right-hand side, κ denotes the loss factor, mainly due to the transmission loss and internal use of electricity in the energy systems. Those values for case study are shown in Table 4.4-4.5 [40, 115]. Each energy demand values are based on the Korean case.

Table 4.4 The values of energy demand

	Energy demand [TOE]
Industry	47,081,000
Transport	196,000
Residence & commerce	36,547,000
Public & etc.	4,084,000

And Korean government seeks to rely less on fossil fuels in supplying the necessary energy by expanding the renewable energy portfolio to 11% by 2030 [40, 116]. Thus the lower limit of the energy supplied by renewable energy systems should be considered as follows:

Table 4.5 The values of growth rate, level of energy target, loss factor and discount rate

	values
Energy growth rate	0.01 (low) 0.02 (normal) 0.03 (high)
Energy target level	1.1
Loss factor	0.06
Discount rate	0.05

$$(\sum_{e=5}^{8}\sum_{t=1}^{N_t} I_{e,t} + C_{e,0}) \geq 0.11 \times (\sum_{e=1}^{N_e}\sum_{t=1}^{N_t} I_{e,t} + C_{e,0}) \times \tau_e \tag{4.11}$$

In external cost, there is a term, VT_t, which is the amount of CO_2 emissions traded. CO_2 may be tradable to achieve the CO_2 emission target. A positive value of VT_t value implies that the amount of CO_2 emitted is lower than the target level; it allows the government to sell and the total cost can be reduced. Conversely, a negative VT_t, which means CO_2 emission is not satisfied with the target can increase the total cost.

$$VT_t = ET_t - \sum_{e=1}^{N_e}(C_{e,t} \cdot R_e \cdot \tau_e), \quad \forall t \tag{4.12}$$

ET_t indicates the emission target in year t. Some researches were studied CO_2 emission in various scenarios but, in this study, the value of the emission target by 2030 can be obtained in reports prepared by the Korean Ministry of Knowledge and Economy [40]. It is assumed that the value for each year is calculated with linear interpolation for simplicity. Table 4.6 shows the values.

Table 4.6 Estimated target amount of CO_2 emission from 2011 to 2030

t	ET_t [Mt]	t	ET_t [Mt]
2011	289.0	2021	211.0
2012	281.2	2022	203.2
2013	273.4	2023	195.4
2014	265.6	2024	187.6
2015	257.8	2025	179.8
2016	250.0	2026	172.0
2017	242.2	2027	164.2
2018	234.4	2028	156.4
2019	226.6	2029	148.6
2020	218.8	2030	140.0

Finally, the additional data for solving the problem are shown in Table 4.7. The values can be obtained by many sources [62, 74, 117, 118]. The capacity factor may vary with many disturbances, but the values are determined as constant in this study.

Table 4.7 The values of capital cost, emission rate, initial capacity, size limit and capacity factor

Energy sources	Capital cost [$/MW]	Fixed cost [$/MW]	CO_2 emission rate [t/MW]	Initial capacity [MW]	Size limit [MW]	Capacity factor [h]
Coal	1,218,750	237.5	1,965	18,678	-	6,132
Oil	603,750	78	1,496	6,128	-	6,132
Natural gas	765,000	125	1,154	10,049	-	6,132
Nuclear	1,987,500	375	631	17,932	-	6,132
Hydro	3,029,000	910	234	351	1,709	4,380
Wind	1,567,000	310	127	50	1,408.4	1,314
Solar	5,223,000	210	57	32	127,392	1,314
Biomass	2,089,000	760	793	-		4,380

4.4 Results and their implications

According to the Monte Carlo simulation, the total costs are around 1.887×10^{11}, 2.557×10^{11}, and 3.647×10^{11} [$] through scenarios. The dispersed total costs indicate that the uncertain variables, especially CO_2 emission cost and learning rate, have a considerable impact on total cost (Figure 4.3). A considerable portion of total cost distribution is within 5% and 95% confidence intervals. Also, we can see how sensitive the uncertain variables are to total cost using Monte Carlo simulation. Among three uncertain variables, two variables are fixed and the one variable is to be perturbed. In this way, the sensitivity of each uncertain variable can be obtained (Figure 4.4). The number of the generated sample and function evaluation were set as 1,000. In Figure 4.4, each standard deviation of results is 1.612×10^{7}, 2.036×10^{8}, and 1.766×10^{5}. It indicates that the fluctuation of carbon price contributes considerably to that of the total cost. It will be helpful to interpret the results. Since the carbon price is the most sensitive parameter, a decision maker should monitor the fluctuation of carbon price for installation of energy systems; if the carbon price is stable, the decision of installation can be made more reliably and not be affected by fluctuation. However, the carbon price applies to all over the energy systems as an independent term. The learning rate should be interpreted as an essential factor having a characteristic of each energy system for reliable solution.

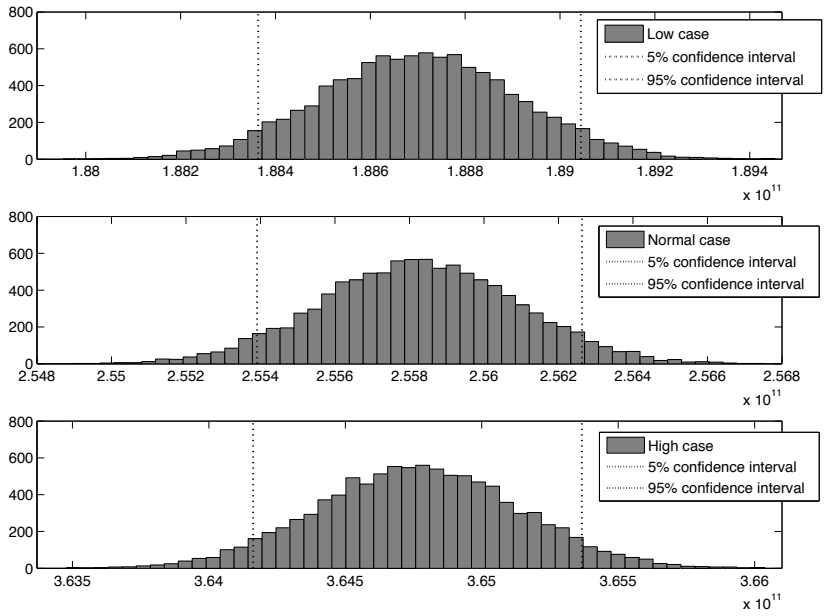

Figure 4.3 The distribution result of total cost using Monte Carlo simulation

The solutions of the case study, which were the capacities of each energy system to be added over the specified periods, are shown in Table 4.8. (L, N, and H indicates low, normal, and high energy growth rate scenarios, respectively) The mean values of capacities of energy system are listed. The result indicates that nuclear, solar, and biomass energy system should be mainly installed until 2030 while all conventional energy systems need no longer to be installed. Though some novel technologies such as Integrated Gasification Combined Cycle (IGCC), Integrated Gasification Fuel Cell (IGFC), and Advanced Ultra Supercritical power plant are emerging, these are confined to retrofitting con-

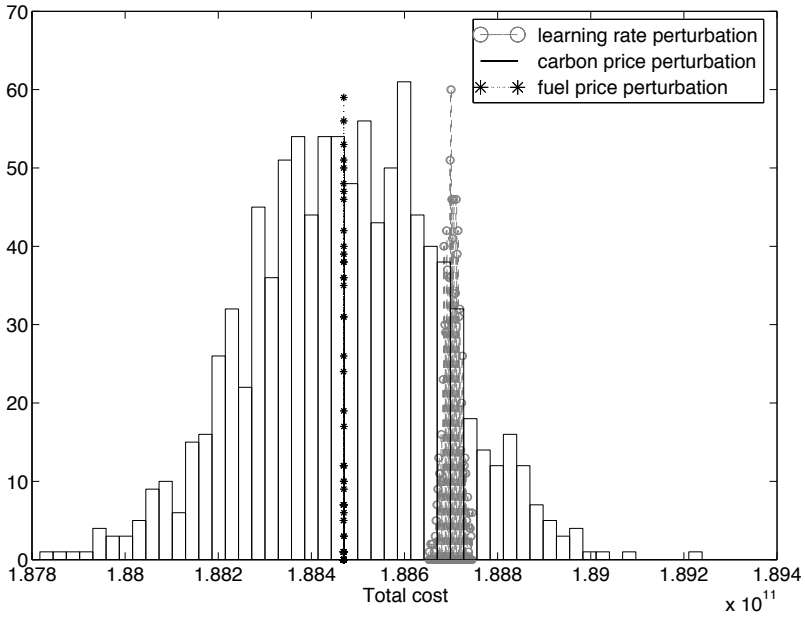

Figure 4.4 Sensitivity analysis of each uncertain variable

ventional energy systems, and will not affect the cost reduction of new construction favorably. This study accounts for newly added capacities of energy sources.

Figure 4.5 indicates nuclear energy will play an important role when the energy-demand increases. Overall the nuclear, solar, and biomass energy will make considerable contributions to the energy supply in the future due to their being not affected by uncertain fuel and carbon prices; although they have high capital and fixed cost, they seem to be enough to compensate. On the other hand, the conventional energy systems are unfavorable to be added because they are more sensitive to learning rate and CO_2 emission cost. The hydro and wind energy

Table 4.8 The mean values of added capacities of energy sources

unit: [MW]	Coal,oil,NG			Nuclear			Hydro			Wind			Solar			Biomass		
Scenario:	L	N	H	L	N	H	L	N	H	L	N	H	L	N	H	L	N	H
2011	-	-	-	-	-	-	-	-	-	-	-	-	-	-	-	-	-	-
2012	-	-	-	-	-	-	-	-	-	-	-	-	-	-	-	1148	-	3513
2013	-	-	-	828	1690	-	-	-	-	-	-	-	-	-	-	-	-	3618
2014	-	-	-	837	-	-	-	-	-	-	-	-	-	-	-	-	2413	3726
2015	-	-	-	845	1758	2742	-	-	-	-	-	-	-	-	-	-	-	-
2016	-	-	-	853	1793	2824	-	-	-	-	-	-	-	-	-	-	-	2326
2017	-	-	-	862	1829	2909	-	-	-	-	-	-	-	-	-	-	-	2395
2018	-	-	-	-	1865	2996	-	-	-	-	-	-	-	-	-	1219	-	2467
2019	-	-	-	-	1902	-	-	-	-	-	-	-	-	-	-	1231	-	4320
2020	-	-	-	888	1941	3178	-	-	-	-	-	-	-	-	-	-	-	-
2021	-	-	-	897	1980	3274	-	-	-	-	-	-	-	-	-	-	-	-
2022	-	-	-	906	2019	3372	-	-	-	-	-	-	-	-	-	-	-	-
2023	-	-	-	915	2059	3472	-	-	-	-	-	-	-	-	-	-	-	-
2024	-	-	-	924	2101	3577	-	-	-	-	-	-	-	-	-	-	-	-
2025	-	-	-	933	2143	3685	-	-	-	-	-	-	-	-	-	-	-	-
2026	-	-	-	943	2186	3795	-	-	-	-	-	-	-	-	-	-	-	-
2027	-	-	-	-	2229	3909	-	-	-	-	-	-	4443	-	-	-	-	-
2028	-	-	-	-	2273	-	-	-	1709	-	-	-	4488	-	12739	-	-	-
2029	-	-	-	971	2319	4147	-	-	-	-	-	-	-	-	-	-	-	-
2030	-	-	-	981	-	4271	-	-	-	-	-	-	-	11040	-	-	-	-
Added capacity	-	-	-	12583	32088	48149	-	-	1709	-	-	-	8931	11040	12739	3598	2413	15177

have disadvantages in terms of size limit and energy efficiency as well as learning rate despite they are advantageous to CO_2 emission. There may be some opinions on the contribution of nuclear energy system; it may sound absurd that high security risk inherent in nuclear energy should be endured. But Korea relies on imports for 97% of the energy sources and above 30% of the total electricity generation is dependent on a nuclear power already. Thus Korean government reported that it would not change the nuclear energy policy which plans constructions of twelve new nuclear power plants [111]. The matters of security and

risk should be viewed from a different standpoint. It is shown that the solar energy can play a role in the future by virtue of its high learning rate and low CO_2 emission; since the hydro and wind energy have strict size limit, they are not selected. From the model equations, we can see that the learning effect term is crucial in lowering the capital and fixed costs of energy systems. Thus, it implies that keeping the conditions that are exogenous to learning effect high is required. Allocating more budgets in R&D and strengthening the knowledge stock may support in successful reduction of capital and fixed costs via learning effects. And the low amount of CO_2 emission will bring about the stable cost variation of installation. This may offer the reliable strategy for decision makers.

Lastly, a few valuable and optimistic insights can be obtained. Figure 4.6 shows the proportion of the energy systems in 2011 and 2030. While the proportion of renewable energy sources in 2011 is just 0.9% in the total supply, it increases to about 16.5%, 13.7% and 22.9% in the case of low, normal, and high-energy growth rate. As the amount of energy demand increases, renewable energy systems will be a solution to satisfy the abatement of CO_2 emission. This satisfies one of the goals of the Korean National Energy Plan, which is to make renewable energy sources provide at least 11% of the total energy supply by the year 2030 [40]. From the results, we can also estimate the future supply of renewable energy sources (i.e. hydro, wind, solar, and biomass). Ac-

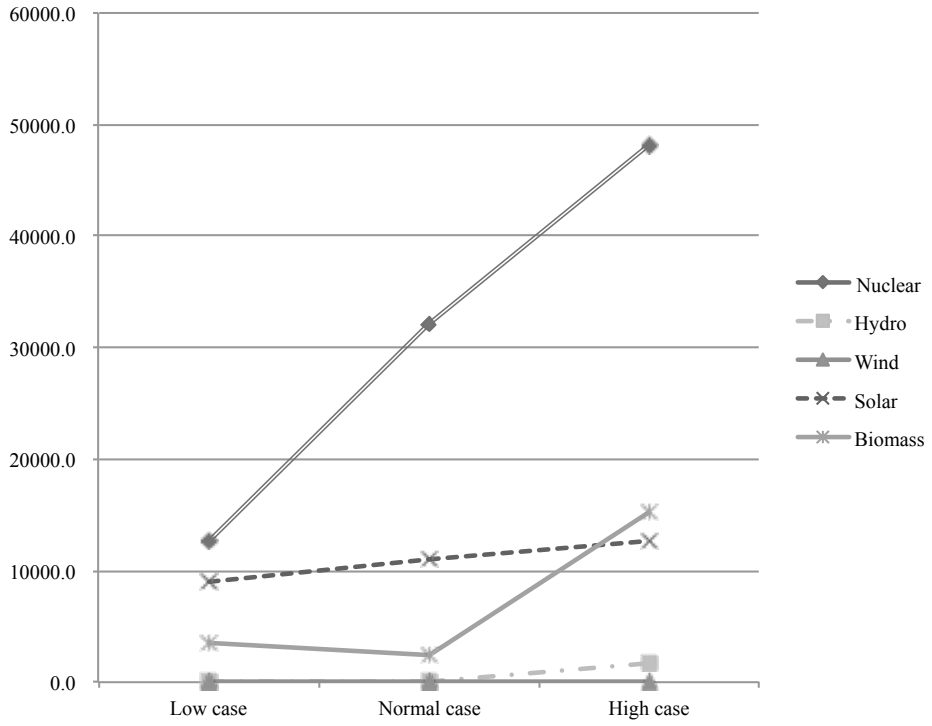

Figure 4.5 The amount to be added in each scenario

cording to [119], we are able to identify the supply of renewable energy sources until 2009. Figure 4.7 presents the estimated supply of renewable energy sources posterior to the year 2010 when the energy growth rate is assumed to be low, normal, and high. Figure 4.7 demonstrates applicability of the proposed model and directs a decision maker to future insight into energy plan, quantitatively.

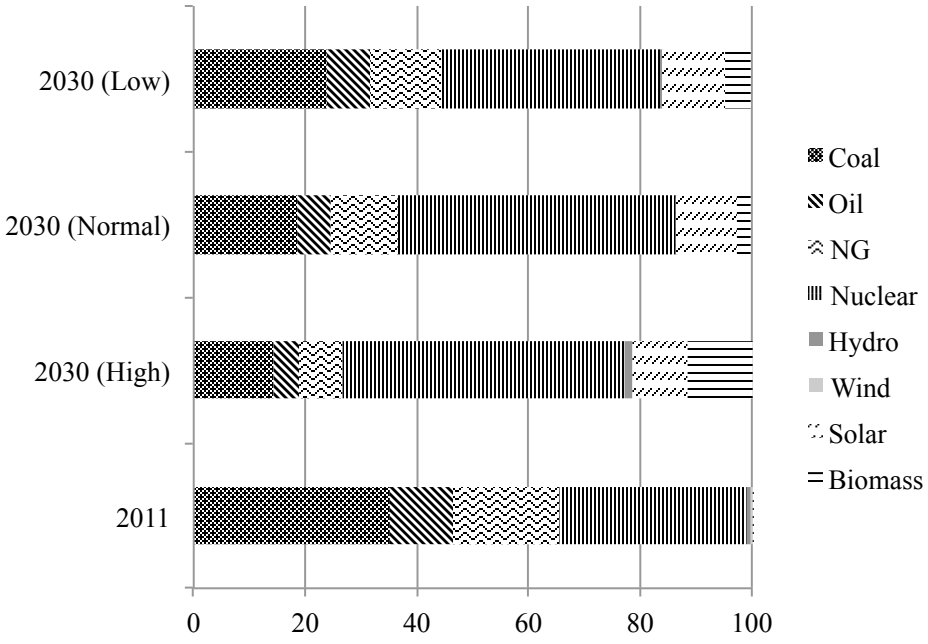

Figure 4.6 The proportion of energy sources in 2011, 2030

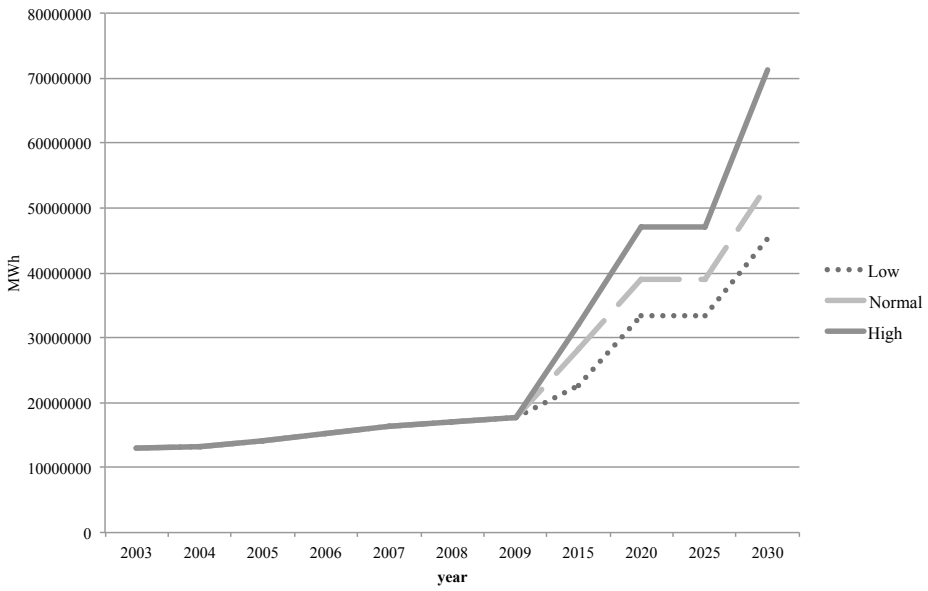

Figure 4.7 The estimation supply of renewable energy sources

Chapter 5

Optimal Management for CO_2 Enhanced Oil Recovery

5.1 Problem description

In this chapter, we present the methodology to obtain the optimal management strategy for CO_2 enhanced oil recovery (EOR). Although some previous works presented the methodology for exploration and life cycle assessment of CO_2 enhanced oil recovery [120, 121], their results have not treated the whole processes for CO_2 sequestration and enhanced oil recovery. For this reason, the direction of this study is to integrate reservoir modeling and CO_2 sequestration process. The flow of the miscible fluid, which is oil and CO_2 in porous media, would be modeled, numerically. Through the numerical modeling, we are to apply the numerical results to enhanced oil recovery process. CO_2 enhanced oil recovery process is one of the inventories of CO_2 life cycle.

Since CO_2 which is emitted by anthropogenic behaviors gives rise to serious global warming nowadays, the technology of Carbon Capture and Storage (CCS) is essential to mitigate CO_2 emission. Especially, carbon storage, which can be called as sequestration, is the direct removal and storage process of captured CO_2 [122]. We are to treat the direct carbon storage/sequestration of CO_2 through enhanced oil recovery process. In Carbon Capture and Storage chain (Figure 5.1), CO_2 enhanced oil recovery can be a final step to terminate CO_2.

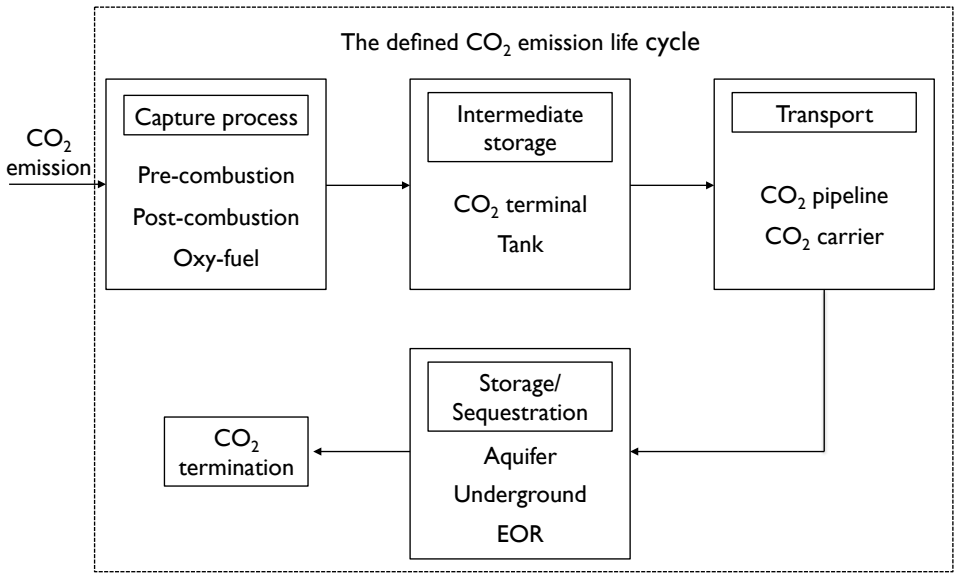

Figure 5.1 The defined CO_2 emission life cycle

Actually, CO_2 enhanced oil recovery is not a new phenomena [123]. Enhanced oil and gas recovery using CO_2 has been used since 1970s, however, the high cost of CO_2 supply and transport made decision makers avoid the method. At present, through the developing carbon

capture system, a good quality of CO_2 can be supplied and injected economically. From the first, the injection to aquifer or the underground injection has been used for storage or sequestration of CO_2, the injection to the matured oil/gas is now also focused because enhanced oil recovery has energy benefits. Enhanced oil recovery process using CO_2 can be cost effective due to revenues from oil and gas production [124]. Hence, enhanced oil recovery and carbon storage/sequestration can be treated as conjunct things. The aim of this case study is to 1) find optimal selection of appropriate reservoir for CO_2 enhanced oil recovery, and 2) find optimal management schemes to maximize oil recovery and CO_2 sequestration. It is clear that the suggestion of following procedure is novel approach for CO_2 sequestration and enhanced oil recovery.

5.1.1 Enhanced oil recovery (EOR)

Enhanced oil recovery is originated from oil recovery. It indicates improved oil recovery. Oil recovery is a generic term that means the amount of crude oil or natural gas that can be extracted from an oil/gas reservoir. Petroleum reservoir is a subsurface pool of hydrocarbons (i.e. crude oil or natural gas) contained in porous or fractured rock formations. Oil and gas recovery has several steps:

· Primary production - this process indicates that oil and gas are extracted by natural drives when a well is drilled into the reservoir. Oil is pushed up the well due to the pressure differences between a reser-

voir and ground. Natural drives include subsurface water displacing oil downward into the well, expansion of the natural gas, and gravity drainage from the movement of oil within the reservoir. About 5-20% of the hydrocarbons in the reservoir can be recovered at most.

· Secondary recovery - More of the oil may still be recovered by secondary recovery [125]. Secondary recovery depends on external energy into the reservoir to increase reservoir pressure. Usually, water and natural gas can be injected into the reservoir through one well. The injected water and natural gas can displace the oil to another well. Another 20-30% of the hydrocarbons in the reservoir can be recovered.

· Tertiary recovery - this is called enhanced recovery, in which we are interseted. Its objective is to obtain the greatest ultimate oil/gas recovery. It tries to increase the mobility of oil in order to increase extraction. Many methods can be used for enhancing oil recovery Figure 5.2. Typically, CO_2 flooding can reduce oil viscosity due to its miscibility with oil. There are two advantages of using CO_2 which is miscible with oil. Firstly, there are no surface-tension effects, and so the two fluids may more freely displace each other within the porous medium. Secondly, the injection of a miscible fluid, less viscous than the oil, leads to a mixture with a viscosity less than that of the oil, thus reducing the applied pressure gradient required to displace the oil, and aiding recovery [125]. When we inject CO_2 into an oil reservoir, it becomes mutually soluble with the residual crude oil as light hydrocarbons from

the oil dissolve in the CO_2 and CO_2 dissolves in the oil [16]. Through this process, the viscosity of oil is increased. However, below the miscible minimum pressure of CO_2, CO_2 and oil can no longer be miscible. The miscible minimum pressure would be a key factor to determine the feasibility and sustainability of a reservoir for CO_2 enhanced oil recovery. At typical reservoir conditions, CO_2 is a supercritical fluid, with the CO_2 fully miscible with the oil, and is less viscous than the oil, so the mixing region may spread faster than one might expect [125].

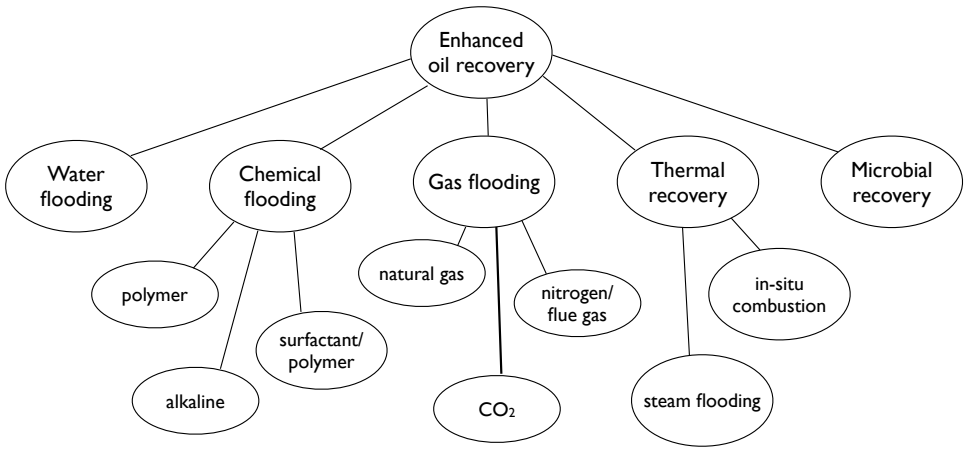

Figure 5.2 The methods of enhanced oil recovery

5.1.2 Basics of reservoir modeling

When CO_2 is injected into reservoir, there exists a miscible displacement in porous media. We have to model this phenomena. The physical forces holding the two phases apart would disappear. This makes the CO_2 to decrease the viscosity of oil and displace the oil from the rock

pores. The phase of injected CO_2 is supercritical phase and reservoir is assumed to be liquid phase. In general, supercritical CO_2 behaves like a liquid with respect to density, and like a gas with respect to viscosity [126]. Since the viscosity term is more effective term to enhance oil recovery, the injected CO_2 can be assumed to behave like a gas in the reservoir. Though reservoir is composed of crude oil, natural gas, and water, we consider the phase of reservoir as a liquid oil for brevity.

Displacement process in porous media has some characteristics. Fundamental among them is the momentum equation via Darcy's law and its multi-phase extension [127]. Miscible displacement can be defined as a single fluid for homogeneous porous medium, first. Saturation (or concentration) can be taken as independent variable [128]. On the other hand, the flow of multi-phase or multi-component fluids, whose characteristics are different between the flow-interacting components, through porous media are influenced by heterogeneities [129]. Fluids are interchangeable during the displacement process due to their miscibility [128].

The impact of heterogeneities precludes the use of classical convection-dispersion approach because the coupled fluid interactions are highly nonlinear and quite complex and the transport process can not be represented by superposition of a simple diffusive process. Fluid displacement in a petroleum reservoir is governed by the conservation of mass, momentum, and energy. In the simulation of flow in the reservoir, the

momentum equation is given in the form of Darcy's law [130]. Darcy's law is a simple proportional relationship between the instantaneous discharge rate through a porous medium, the viscosity of the fluid, and the pressure drop over a given distance [131].

$$Q = -\frac{\mathbf{K}A}{\mu}\frac{\Delta P}{L} \tag{5.1}$$

where Q is total discharge (volume per time), $\mathbf{K}$ is permeability of medium, A cross-sectional area, μ is viscosity of fluid, and ΔP and L are pressure drop and length between start point and end point, respectively. Dividing both sides of the equation by the area, the general form can be led:

$$q = -\frac{\mathbf{K}}{\mu}\nabla P \tag{5.2}$$

where q is flux (length per time), and ∇P is pressure gradient vector. The flux, q, can be called as Darcy flux. The pore velocity v is dependent on q and the porosity, ϕ (Equation (5.3)).

$$v = \frac{q}{\phi} \tag{5.3}$$

For miscible two-phase fluid, the above equations should be modified, appropriately. More detailed description would be presented in the

next section.

Prior to the proposal of numerical methods, some concepts of modeling flow in porous media should be considered [29]. The rock porosity, ϕ is the void volume fraction of the medium ($0 \leq \phi < 1$). The porosity is related on the pressure. If the rock is compressible, the rock compressibility can be expressed as:

$$c_r = \frac{1}{\phi}\frac{d\phi}{dp} \tag{5.4}$$

where p is the overall reservoir pressure. To simply the models, the rock compressibility can be neglected. Recent researches seek to identify the relation between flow models on pore scale and on reservoir scale. The permeability, which is denoted by $\mathbf{K}$, is a measure of the rock's ability to transmit a single fluid at certain conditions. The permeability is not proportional to the porosity, but still strongly correlated to the porosity. The unit is commonly Darcy (D) or milli-Darcy (mD). 1D is approximately $0.987 \times 10^{-12}(\mathrm{m}^2)$, means transmission of a 1 cp fluid through a homogeneous rock at a speed of 1 cm/s due to a pressure gradient of 1 atm/cm. Although the permeability in the different directions depends on the permeability in the other directions, it is expressed as horizontal and vertical permeability for most of models. The permeability may be changed during production, because the pressure and temperature of

reservoir is changed. In this thesis, we are to skip the detailed analysis of permeability.

Secondly, we look into the fluid properties, which is related to this case. Mostly, we can assume that the void in the porous medium is filled with the different phases. It can be called saturation (s) of the phase (Equation (5.5)).

$$\sum_{\text{all phases}} s_{component} = 1 \tag{5.5}$$

As usual, three phases can be considered: water, oil (oleic), and gas. Each phase contains one or more components. Because the aim of this case study is to model oil and CO_2 in two phases (liquid and gas), we would consider two phases: water in the reservoir is neglected in this case: in thermodynamic equilibrium, the mixture of CO_2 and oil in the reservoir would form two phases [132]. In the reservoir, the composition of oil and CO_2 would be changed during enhanced oil recovery. Let c_{ab} denote the mass fraction of component b (i.e. oil and CO_2) in phase a (i.e. liquid and gas), then

$$\sum_{Oil} c_{ab} = \sum_{CO_2} c_{ab} = 1. \tag{5.6}$$

Next, we need to introduce density (ρ) and viscosity (μ). These are related to phase pressure p_a and the composition of each phase.

$$\begin{aligned}\rho_a =& \rho^a_{Oil} + \rho^a_{CO_2} \\ &= \rho_a(p_a, c_{1a}, \cdots, c_{Na})\end{aligned} \tag{5.7}$$

where N indicates the number of different components. The density is important for CO_2. The compressibility of the phase can be expressed as:

$$c_i = \frac{1}{\rho_a}\frac{d\rho_a}{dp_a} \tag{5.8}$$

The compressibility is important for CO_2. Usually, we can neglect the compressibility of water. Then, we introduce the mass fractions [133]:

$$\begin{aligned}\omega^a_{Oil} = \frac{\rho^a_{Oil}}{\rho_a}, \quad \omega^a_{CO_2} = \frac{\rho^a_{CO_2}}{\rho_a} \\ \omega^a_{Oil} + \omega^a_{CO_2} = 1\end{aligned} \tag{5.9}$$

Although phases of interest do not mix, we assume that all phases may be present at the same location [29]. The permeability by one phase depends on the saturation of the other phases at specific location and interaction of phases. Thus, we should introduce relative permeability, k_r, to consider this concept.

$$k_r = k_r(s_b) \tag{5.10}$$

The effective permeability is $\mathbf{K} = \mathbb{K}k_r$. The relative permeability is nonlinear functions of the saturations, and the sum of the relative permeabilities at a location is not needed to be one. It is dependent on the pore-size distribution, fluid viscosity, reservoir temperature, and interfacial forces between fluids. The detailed explanation of the relative permeability is skipped.

5.2 Numerical modeling: two point flux approximation

The simplest model for two-phase flow in a porous medium is Darcy-Muskat law:

$$\begin{aligned} q_l &= -\mathbb{K}\frac{k_{rl}(s_l)}{\mu_l}(\nabla p_l - \rho_l \mathbf{G}) \\ q_g &= -\mathbb{K}\frac{k_{rg}(s_g)}{\mu_g}(\nabla p_g - \rho_g \mathbf{G}) \end{aligned} \tag{5.11}$$

where $\mathbb{K}$ is absolute permeability, k_r is relative permeability, the permeability we used is $\mathbf{K} = \mathbb{K}k_r$, and $\mathbf{G}$ is gravitationl acceleration. l and g denote liquid and gas phase, respectively. From the Equation (5.11), we can see that there are two driving forces in porous media flow, gravity and pressure gradient. Since the gravity is constant in the system of interest, we have to know the pressure of the reservoir. If we adopt the continuity equation which states that mass is conserved (Equation (5.12)) and combine it with Equation (5.11),

$$\frac{\partial(\phi\rho)}{\partial t} + \nabla \cdot (\rho v) = q \tag{5.12}$$

we can obtain the following elliptic equation (Equation (5.13)).

$$\nabla \cdot v_a = \nabla \cdot (-\frac{\mathbf{K}}{\mu_a}(\nabla p_a - \rho_a \mathbf{G})) = \frac{q_a}{\rho_a} \tag{5.13}$$

To solve elliptic equation, we have to specify boundary conditions.

Usually, no-flow boundary conditions are adopted in reservoir modeling. In this way, we can denote the reservoir boundary, $\partial\Omega$, and express $v_a \cdot n = 0$. n is the normal vector pointing out of the boundary, $\partial\Omega$.

Then, we introduce a cell-centered finite volume method, which can be called as two point flux approximation (we already described in Section 2.3). TPFA method is a common discretization technique in reservoir modeling. Finite volume method is derived from conservation of quantities over cell volumes. To derive a set of finite volume mass balance equations for Equation (5.13), we introduce the integral form over Ω_i, the reservoir domain:

$$\int_{\Omega_i} (\frac{q_a}{\rho_a} - \nabla \cdot v_a) dx = 0 \tag{5.14}$$

Using divergence theorem, Equation (5.14) can be transformed into following mass balance equation:

$$\int_{\partial\Omega_i} v_a \cdot n dv = \int_{\Omega_i} \frac{q_a}{\rho_a} dx \tag{5.15}$$

Here, n denotes the outward pointing unit normal on $\partial\Omega_i$. Then, approximating the pressure p_a with a cell-wise constant function $\mathbf{p} = p_{a,i}$ and estimating $v_a \cdot n$ across cell interfaces $\gamma_{ij} = \partial\Omega_i \cap \partial\Omega_j$ from a set of neighboring cell pressures [29], we are able to apply finit volume

method.

We can reformulate Equation (5.13) to apply two point flux approximation:

$$-\nabla \cdot \lambda \nabla u = f \tag{5.16}$$

where $\lambda = k_r/\mu$. This equation can be analyzed in two ways because $u = p + \rho \mathbf{G}$. We already mentioned the gravity term is constant, our interest is the pressure, p.

$$-\nabla \cdot \lambda \nabla u_a = \frac{q_a}{\rho_a} \tag{5.17}$$

Surely, two point flux approximation uses two points, u_i and u_j to estimate the flux, $v_{ij} = -\int_{\gamma_{ij}} (\lambda \nabla u) \cdot n d\nu$, where γ_{ij} is an interface between adjacent cells in the x-coordinate direction so that $n_{ij} = (1, 0, 0)^T$. Then ∇u on γ_{ij} can be expressed as:

$$\nabla u = \delta u_{ij} = \frac{2(u_j - u_i)}{\Delta x_i + \Delta x_j} \tag{5.18}$$

where Δx_i and Δx_j denote the respective cell dimensions in the x-coorditate direction. Finally, we can obtain equation for v_{ij}:

$$v_{ij} = \delta u_{ij} \int_{\gamma_{ij}} \lambda d\nu = \frac{2(u_j - u_i)}{\Delta x_i + \Delta x_j} \int_{\gamma_{ij}} \lambda d\nu \tag{5.19}$$

In many problems of reservoir modeling, we can assume that the permeability is cell-wise constant. However, the permeability is not well-defined at the interfaces. We should estimate λ on γ_{ij}. A distance-weighted harmonic average of the respective directional cell permeability is usually adopted in the two point flux approximation, $\lambda_{i,ij} = n_{ij} \cdot \lambda_i n_{ij}$ and $\lambda_{j,ij} = n_{ij} \cdot \lambda_j n_{ij}$. λ_{ij} on γ_{ij} can be computed as:

$$\lambda_{ij} = (\Delta x_i + \Delta x_j)(\frac{\Delta x_i}{\lambda_{i,ij}} + \frac{\Delta x_j}{\lambda_{j,ij}})^{-1} \tag{5.20}$$

Using this, we can approximate v_{ij},

$$v_{ij} = -|\gamma_{ij}|\lambda_{ij}\delta u_{ij} = 2|\gamma_{ij}|(\frac{\Delta x_i}{\lambda_{i,ij}} + \frac{\Delta x_j}{\lambda_{j,ij}})^{-1}(u_i - u_j) \tag{5.21}$$

After considering over all interfaces to adjacent cells, $\int_{\partial\Omega_i} v_\omega \cdot n dv$ is approximated. Also mass balance equation (Equation (5.15)) can be obtained.

If we introduce the transmissibility (t_{ij}) term to Equation (5.21), the equation is simplified.

$$t_{ij} = 2|\gamma_{ij}|(\frac{\Delta x_i}{\lambda_{i,ij}} + \frac{\Delta x_j}{\lambda_{j,ij}})^{-1}$$
$$v_{ij} = t_{ij}(u_i - u_j) \tag{5.22}$$

We should consider the whole domain, (Ω). In summary, we can obtain this equation (two point flux approximation), those phase fluxes across grid block are approximated by [29, 134]. Fluxes are discretized for all cells of grid block.

$$\sum_j t_{ij}(u_i - u_j) = \int_{\Omega_i} f dx, \quad \forall \Omega_i \tag{5.23}$$

5.3 Numerical modeling: miscible flow

In this section, we present the modeling method of miscible flow and solving method based on two point flux approximation. We mentioned the simple model for multi-phase flow briefly in the previous section. Miscible flow model can be modified based on the model.

5.3.1 Pressure change

Fundamental equations are the conservation equations for each component, oil and CO_2. And the phases are assumed to be liquid and gas as mentioned.

$$\frac{\partial}{\partial t}(\phi \sum_b c_{ab}\rho_b s_b) + \nabla \cdot (\sum_b c_{ab}\rho_b v_b) = \sum_b c_{ab} q_b, \qquad b = \mathrm{CO_2} \text{ and oil} \tag{5.24}$$

where c_{ab} is mass fraction of component b in phase a, ρ is the density of component a, s is the saturation, v_b is component velocity, and q_b is component source. v_b is same as q in Equation (5.11).

Because the sum of mass fraction in one phase equals to one, above conservation equation can be expressed as:

$$\frac{\partial(\phi\rho_b s_b)}{\partial t} + \nabla \cdot (\rho_b v_b) = q_b \tag{5.25}$$

Assumming the densities are constant, we can reformulate this equation.

$$\frac{\partial \phi}{\partial t} s_b + \phi \frac{\partial s_b}{\partial t} + \phi \frac{s_b}{\rho_b} \frac{\partial \rho_b}{\partial t} + \nabla \cdot v_b + \frac{v_b \cdot \nabla \rho_b}{\rho_b} = \frac{q_b}{\rho_b} \tag{5.26}$$

Using this equation, we can obtain the pressure and saturation equation for miscible flow through appropriate modifications. Summing the conservation equation for the CO_2 and oil, the equation can be expressed as:

$$\nabla \cdot (v_c + v_o) + \frac{\partial \phi}{\partial t} + \phi \frac{s_c}{\rho_c} \frac{\partial \rho_c}{\partial t} + \phi \frac{s_o}{\rho_o} \frac{\partial \rho_o}{\partial t} + \frac{v_c \cdot \nabla \rho_c}{\rho_c} + \frac{v_o \cdot \nabla \rho_o}{\rho_o} = q \tag{5.27}$$

where subscript c denotes CO_2 and o does oil. Combining with Equation (5.13), the equation is reformulated as follows,

$$\begin{aligned} &-\nabla \cdot (\mathbb{K}\lambda_c(\nabla p_c - \rho_c \mathbf{G}) + \mathbb{K}\lambda_o(\nabla p_o - \rho_o \mathbf{G})) \\ &+c_r \phi \frac{\partial p}{\partial t} - c_c(\nabla p_c \cdot \mathbb{K}\lambda_c(\nabla p_c - \rho_c \mathbf{G}) - \phi s_c \frac{\partial p_c}{\partial t}) \\ &-c_o(\nabla p_o \cdot \mathbb{K}\lambda_o(\nabla p_o - \rho_o \mathbf{G}) - \phi s_o \frac{\partial p_o}{\partial t}) = q \end{aligned} \tag{5.28}$$

where p denotes the pressure. There are two pressures; CO_2 pressure p_c, oil pressure p_o. Theser are variables that we have to obtain. This is

fundamental pressure equation in this thesis. Using some assumptions, we can conduct approximation as mentioned before. First, we assume that the compressibilities are zero, (i.e. $c_r, c_c, c_o = 0$). Because $\nabla \cdot v = q$, Equation (5.28) can be reduced,

$$v = -(\mathbb{K}\lambda_c(\nabla p_c - \rho_c \mathbf{G}) + \mathbb{K}\lambda_o(\nabla p_o - \rho_o \mathbf{G})) \tag{5.29}$$

Still, there are two unknown variables, p_c and p_o. To eliminate one of them, we introduce total pressure, p. Also we define the compensatory pressure (p_{com}) of oil, which compensates the oil pressure. The introduced pressures are dependent on the saturation of fluids and the capillary pressure p_{cap}. Assuming the total pressure is the difference between the oil pressure and compensatory pressure, $p = p_o - p_{com}$, where the saturation-dependent pressure is defined by [29]

$$\begin{aligned} p_{com}(s_c) &= \int_1^{s_c} f_c \frac{\partial p_{cap}}{\partial s_c}(\xi) d\xi, \\ f_c &= \frac{\lambda_c}{\lambda_c + \lambda_o} \end{aligned} \tag{5.30}$$

where f_c is fractional flow. From this equation, $\nabla p_{com} = f_c \nabla p_{cap}$ leads $v = v_c + v_o$ as a function of the total pressure (Equation (5.31)).

$$v = -\mathbb{K}(\lambda_c + \lambda_o)\nabla p + \mathbb{K}(\lambda_c \rho_c + \lambda_o \rho_o)\mathbf{G} \tag{5.31}$$

Letting $\lambda = \lambda_c + \lambda_o$, we can obtain more simpler elliptic equation.

$$q = -\nabla \cdot (\mathbb{K}\lambda\nabla p - \mathbb{K}(\lambda_c\rho_c + \lambda_o\rho_o)\mathbf{G}) \tag{5.32}$$

As we mentioned in the previous section, we assume no-flow boundary conditions to solve the elliptic equation.

Next, we should derive saturation equation to complete a reservoir model. Considering fluid properties (we treated this in the previous section), we can start using $s_c + s_o = 1$. From Darcy-Muskat law, the equation follows:

$$\lambda_o v_c - \lambda_c v_o + \mathbb{K}\lambda_c\lambda_o(\rho_o - \rho_c) - \mathbb{K}\lambda_c\lambda_o\nabla p_{cap} = 0 \tag{5.33}$$

Because $v = v_c + v_o$, we can arrange the equation divided by λ.

$$v_c = f_c(v + \mathbb{K}\lambda_o\nabla p_{cap} + \mathbb{K}\lambda_o(\rho_c - \rho_o)\mathbf{G}) \tag{5.34}$$

Introducing $\nabla p_{cap} = \frac{\partial p_{cap}}{\partial s_c}\nabla s_c$, we can obtain the saturation equation, finally.

$$\phi\frac{\partial s_c}{\partial t} + \nabla \cdot (f_c(s_c)(v + d(s_c) + g(s_c))) = \frac{q_c}{\rho_c} \tag{5.35}$$

where $f(s)v$ and $f(s)g(s)$ denotes viscosity and gravity forces, respectively. Intuitively, we can see that the pressure equation and saturation equation are very coupled system. This is main problem to model miscible flow.

To discretize the pressure equation (Equation (5.32)) using finite volume method, the equation can be reformulated.

$$-\int_{\partial\Omega_i} \mathbb{K}\lambda(s_c^k)\nabla p^{k+1} d\nu = \int_{\Omega_i} q\ dx - \int_{\partial\Omega_i} \mathbb{K}(\lambda_c(s_c^k)\rho_c + \lambda_o(s_c^k)\rho_o)\mathbf{G}\cdot n d\nu \tag{5.36}$$

where k denotes the step number. Two point flux approximation can be applied to this equation. The pressure is dependent upon changes of saturation (i.e. dynamic function). It is solved iteratively through many steps. The discretization scheme is presented as follows,

$$p_i^{k+1} = p_i^k + 2|\gamma_{ij}|(\frac{\Delta x_i}{\lambda_{i,ij}} + \frac{\Delta x_j}{\lambda_{j,ij}})^{-1} \tag{5.37}$$

5.3.2 Saturation change

Then the saturation equation of miscible flow should be presented. From Equation (5.35), we can rewrite the equation as follows,

$$\phi\frac{\partial s_c}{\partial t} + \nabla\cdot(f_c v - \mathbb{K}\lambda_c q_c \delta\rho g - D(s_c)\cdot\nabla s_c) = q_c \tag{5.38}$$

if we ignore gravity term $g = 0$, this equation can be divided two equations:

$$\phi\frac{\partial \bar{s}}{\partial t} + \frac{df^m(\bar{s})}{ds}\cdot\nabla\bar{s} = \phi\frac{d\bar{s}}{d\tau} = 0, \quad t_m \le t \le t_{m+1} \tag{5.39}$$

$$\phi\frac{\partial s}{\partial \tau} + \nabla\cdot(b^m(s)s) - \nabla(D(s)\nabla s) = q \tag{5.40}$$

where the diffusion term $D(s)$ is key factor to model the miscible flow. Equation (5.39) can be solved by the method, which is used for the pressure equation. Equation (5.40) should be handled somewhat differently [129, 135]. Again combining two equations and applying divergence theorem, Equation (5.39) and (5.40) can be changed.

$$\begin{aligned}
&\int_\Omega \phi s(x,t^{k+1})\omega(x,t^{k+1})dx + \int D\nabla s\cdot\nabla\omega\ dxdt \\
&+ \int_{J^{k+1}}\int_{\partial\Omega}(f_c v - D\nabla s)\cdot v\omega\ d\sigma dt \\
&- \int(\phi s_c + f_c\cdot v\cdot\nabla\omega)dxdt \\
&= \int_\Omega \phi s(x,t^k)\omega(x,t^k)dx + \int q_c\omega\ dxdt
\end{aligned} \tag{5.41}$$

where $f_c = \bar{f}(s) + b(s)s$ and $\omega(x,t)$ is constant along the characteristics determined by the directional derivative along τ with $\bar{f}$ defined from

the convex hull of f_c (we can assume $\bar{f}$ is very small enough to ignore). Substitute to Equation (5.38), Equation (5.41) is reduced.

$$\int_{\Omega_{ij}} \phi s(x,t^{k+1})\omega(x,t^{k+1})dx + \int D\nabla s - b(\tilde{s})vs\cdot\nabla\omega(x,t^{k+1})\ dxdt$$
$$= \int_{\Omega^*_{ij}} \phi s(x,t^{k})\omega(x,t^{k})dx + \int q_c\omega\ dxdt \tag{5.42}$$

where Ω^*_{ij} is the region at t^k spanned by the feet of the characteristics whose heads are in Ω_{ij}, $\tilde{s}^{k+1}$ is some approximation of s^{k+1}.

To discrete the saturation equation using finite volume method [135, 136, 137], we introduce θ-rule for temporal discretization, which approximates the partial derivatives ∂t. Then, the saturation equation is expressed as,

$$\frac{\phi_i}{\Delta t}(s_i^{k+1}-s_i^k) + \frac{1}{|\Omega_i|}\sum_{j\neq i}(\theta F_{ij}(s^{k+1}) + (1-\theta)F_{ij}(s^k)) = \frac{q_i(s_i^k)}{\rho},$$
$$s_i^k = \frac{1}{|\Omega_i|}\int_{\Omega_i} s(x,t_k)dx \tag{5.43}$$

for simplicity of equation, we can introduce F_{ij}. Surely, F_{ij} can be approximated as,

$$F_{ij}(s) = \int_{\gamma_{ij}} f_c(s)_{ij}(v_{ij} + d_{ij}(s)) \cdot n_{ij} d\nu \tag{5.44}$$

The saturation is updated each time step. The updated saturation would influence the pressures, too. The discretization of saturation equation can be presented as follows,

$$s_i^{k+1} = s_i^k + \frac{\Delta t}{\phi_i |\Omega_i|} \sum_j (q - f_c(s)_{ij}(v_{ij} + d_{ij}\Delta s_i)) \tag{5.45}$$

Finally, the diffusion term $D(s)$ is influenced by viscosity interchangeably, we should consider the change of viscosity [137, 138, 139, 140]. The illustration of this scheme can be expressed as following Figure 5.3.

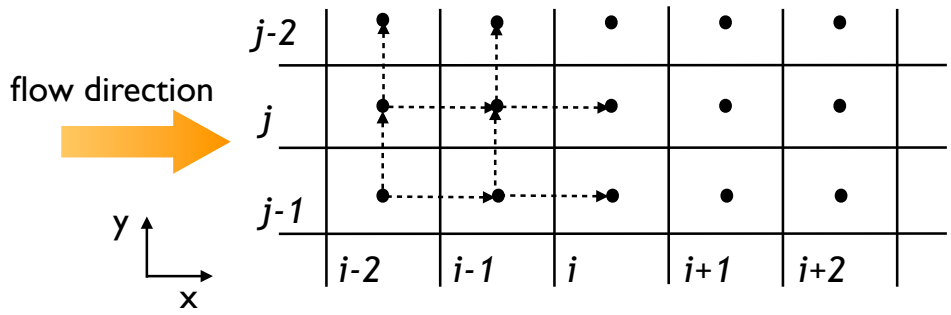

Figure 5.3 Schematic scheme of solution

5.4 Optimal management of the CO_2-EOR

Carbon dioxide originated from anthropogenic sources (e.g. the consumption of fossil fules) can be moved to a mature oil field and injected to injection well. At this stage, it is unavoidable to use energy. Then, the recovered oil is produced at the production well. The produced oil should be separated because it may contain impurities including CO_2. This process requires energy largely. Also the separated CO_2 is recycled back to the injection well. Some researches reported the life span of CO_2 enhanced oil recovery process is about 10-30 years [126, 141], depending on a variety of technical and economics (e.g. the ratio of CO_2 injection, oil price, CO_2 price, electricity cost, etc.). The defined life cycle of CO_2 enhanced oil recovery process includes CO_2 emission, capture process, compression, CO_2 injection to well, CO_2 sequestration to reservoir, oil production, and CO_2 recycle process (Figure 5.4). The detailed operation process are to be skipped in this thesis.

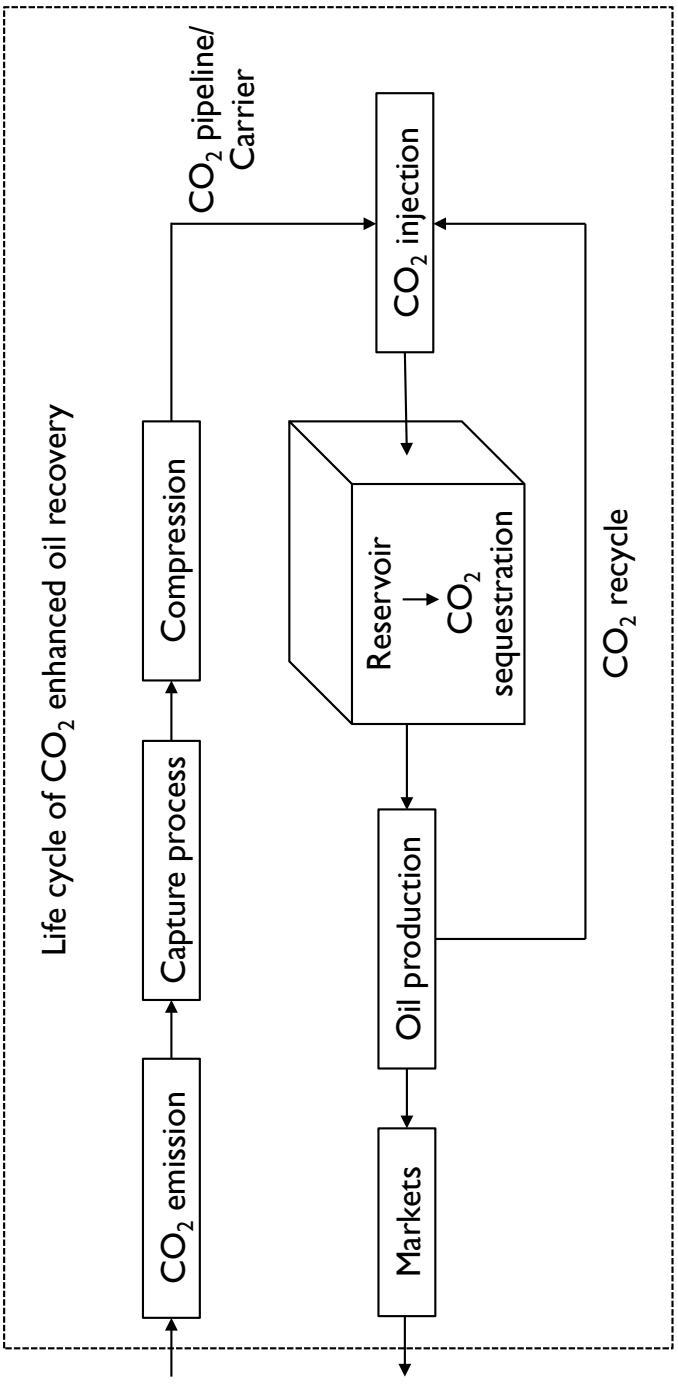

Figure 5.4 The block diagram of defined life cycle of CO_2 enhanced oil recovery

5.4.1 Selection of feasible reservoir for CO_2-EOR

Not all the reservoirs are used for enhanced oil recovery using carbon dioxide. For selection of reservoir for CO_2 enhanced oil recovery, minimum miscible pressure (MMP) should be introduced. Minimum miscible pressure means the pressure that CO_2/oil mixture is first reached completely miscible state. In the practical oil field, complete miscibility is a rare example, however, the minimum miscible pressure does give a guideline for the pressure at which the displacement of oil is efficient [132]. Some studies reported that the minimum miscible pressure is reached in reservoirs that are deep (>1000m) and/or hot (>50°C) and contain light oil (<870kg/m^3) at standard condition) [142]. Here are some examples of reservoir properties (Table 5.1) [132, 143]:

In addition to the minimum miscible pressure, we should identify that whether the reservoir is profitable or not. Usually, identifying profitable enhanced oil recovery is achieved by calculation of net present value (NPV) or profit [122, 144]. The choice of an operating state is dependent on net present value or expected future profit. This can be modeled as a Markov decision process [33]. Since a Markov decision process is expanded approximate dynamic programming, we would apply this method to the selection of feasible reservoirs. Figure 5.5 demonstrates the flow of life cycle assessment-based strategy for selection of profitable reservoirs.

Table 5.1 Properties of major North Sea reservoirs

	Forties	Brent	Ninian	Piper	Thistle
Initial pressure (MPa)	22	41	45	24	41
CO_2 MMP (MPa)	22	35	25	20	24
Temperature (°C)	90	93	102	80	102
Oil density at reservoir (kg/m^3)	750	570	790	750	760
CO_2 density (kg/m^3)	570	770	780	720	760
Oil viscosity (mPa·s)	0.82	0.28	1.35	0.73	1.05
CO_2 viscosity (mPa·s)	0.04	0.07	0.07	0.05	0.07

Although there are an immiscible CO_2 enhanced oil recovery process, the efficiency of the process is proved low. Thus, we assume that only CO_2 sequestration process can be implemented when the reservoir pressure is lower than minimum miscible pressure. Energy requirement can be calculated by the defined life cycle of enhanced oil recovery, and the amount of CO_2 injected, recycled, stored, and emitted can

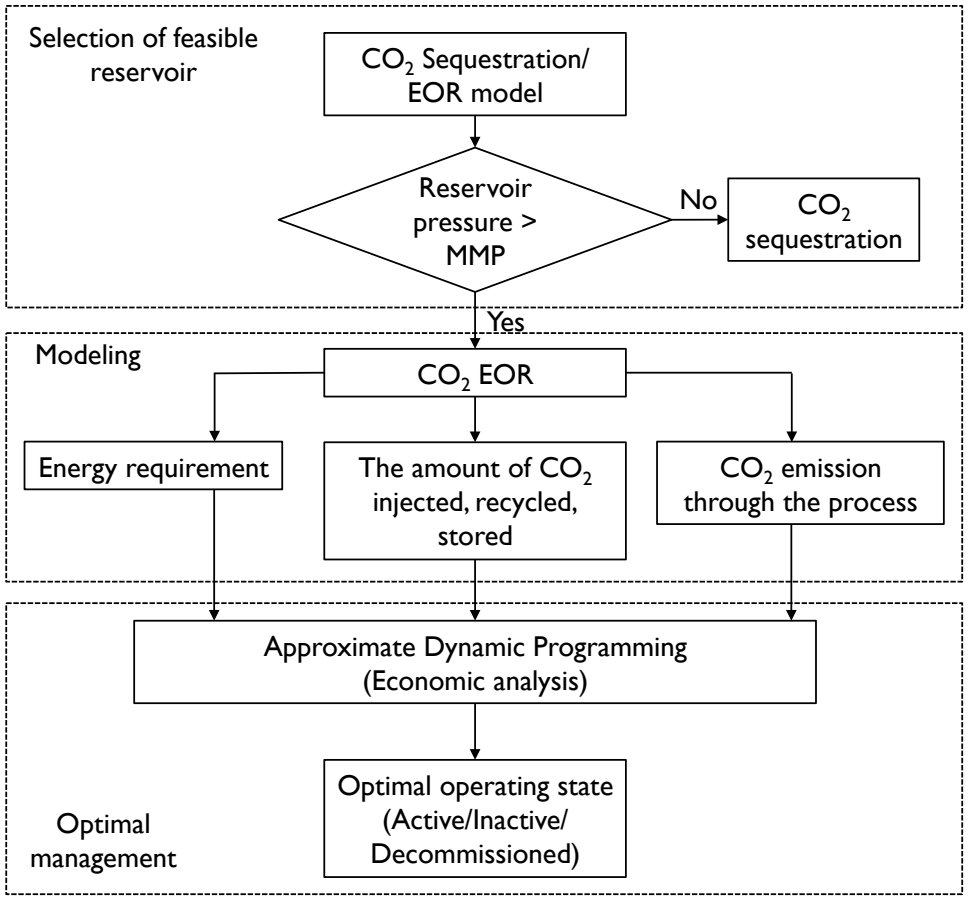

Figure 5.5 The flowchart for selection of profitable reservoir

be computed by numerical modeling as we mentioned before. Then, using approximate dynamic programming, we make a decision which reservoir operation state would be optimal (i.e. active, inactive, or decommissioned) with respect to profit.

5.4.2 Numerical results of reservoir modeling

Based on the Section 6.2 and 6.3, we can obtain the numerical results of reservoir modeling. To compare the results, we conducted the simulation three cases; immiscible ideal (oil) flooding, immiscible water flooding, and miscible CO_2 flooding. Due to the change of viscosities, the contour of saturation and pressure are shown differently [145]. Time duration is assumed to be 10 days and grid number of x and y-directions is 32. $(0, 0)$ is injection well and $(1, 1)$ is production well. The typical CO_2 property values of each phase can be referred as [146]:

Table 5.2 Typical values of properties with respect to phases

	Density (kg/m^3)	Viscosity (cP, 100°C)	Diffusivity (mm^2/s)
Gas phase	1-10	0.0185	0.0008-0.008
Supercritical phase	200-400	0.093-0.185	8×10^{-5}
Liquid phase	1000-	0.925-1.848	8×10^{-7}

First, Figure 5.6 and Figure 5.7 show the pressure and saturation profiles of ideal flooding, respectively. Ideal flooding means that oil is flooded to oil reservoir: same material is injected. The unit viscosity is used for the simulation because there are no differences between two fluids.

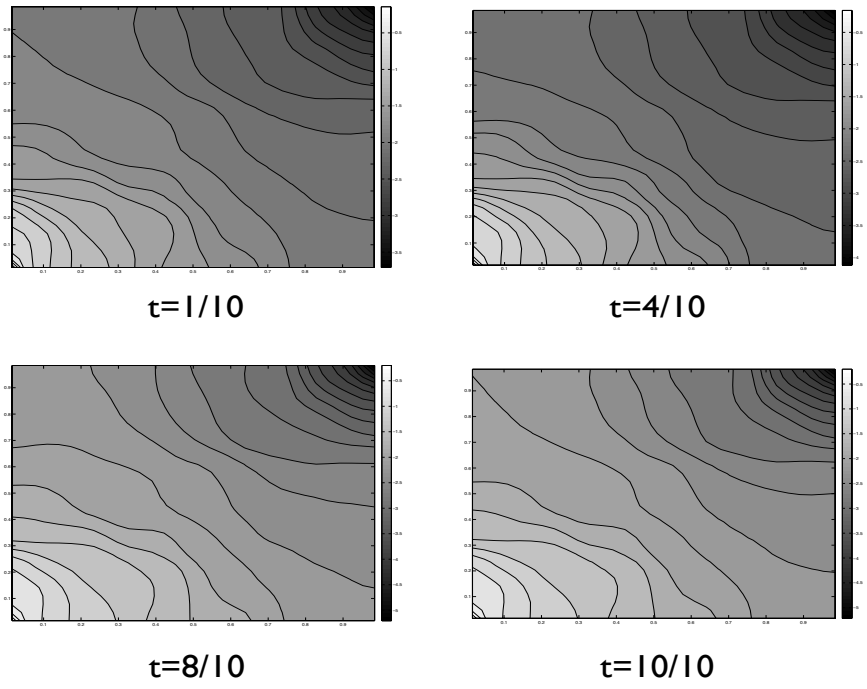

Figure 5.6 Pressure profiles of ideal flooding

Secondly, Figure 5.8 and Figure 5.9 show the pressure and saturation profiles of water flooding, respectively. Generally, the remaining oil have been recovered by water injection. In this simulation, the viscosities of fluids are 8.3 cP (oil) and 0.28 cP (water) at reservoir temperature, 100 °C [147].

Finally, Figure 5.10 and Figure 5.11 show the pressure and saturation profiles of CO_2 miscible flooding, respectively. We assume that the viscosity of CO_2 is 0.0185 cP [146]. The simulation includes the diffusion effect depends on the change of saturation and the reduction of viscosity of oil in the reservoir [138, 140].

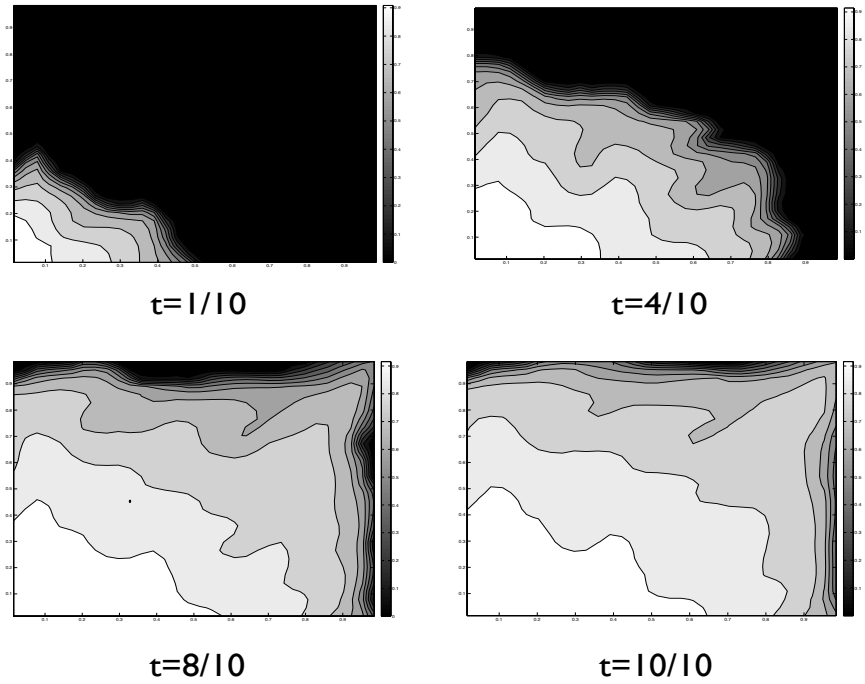

Figure 5.7 Saturation profiles of ideal flooding

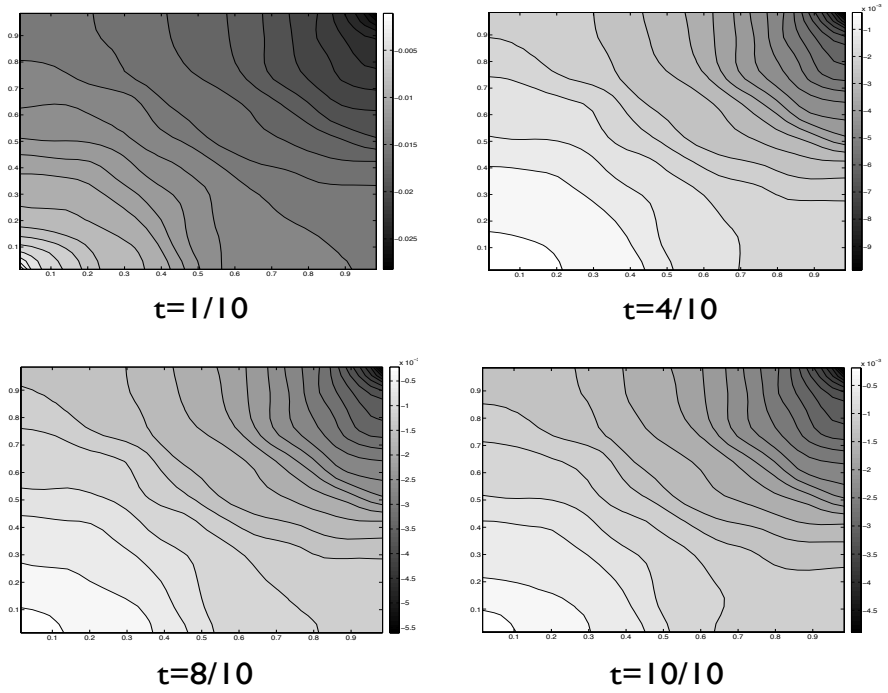

Figure 5.8 Pressure profiles of water flooding

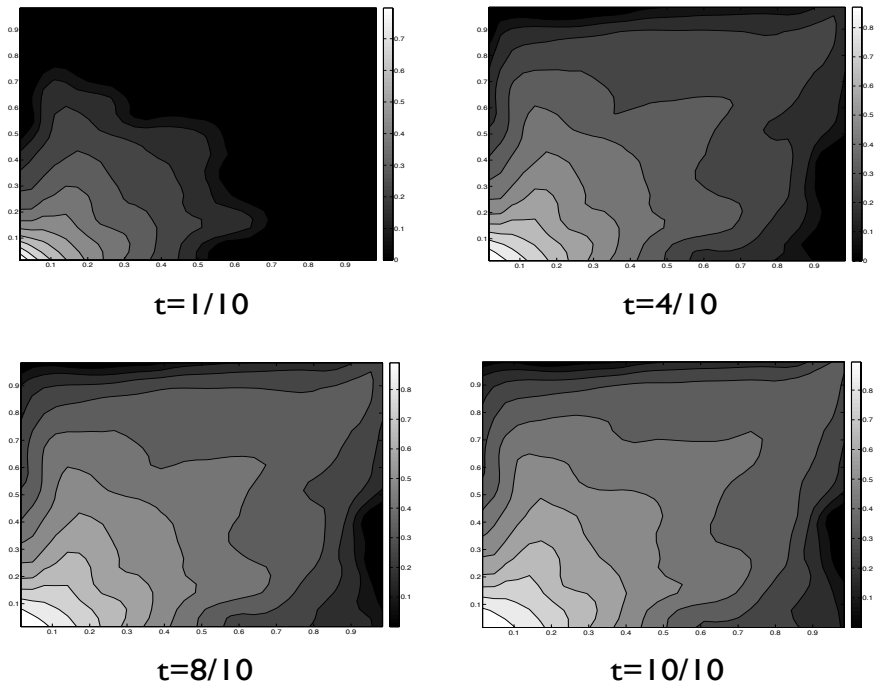

Figure 5.9 Saturation profiles of water flooding

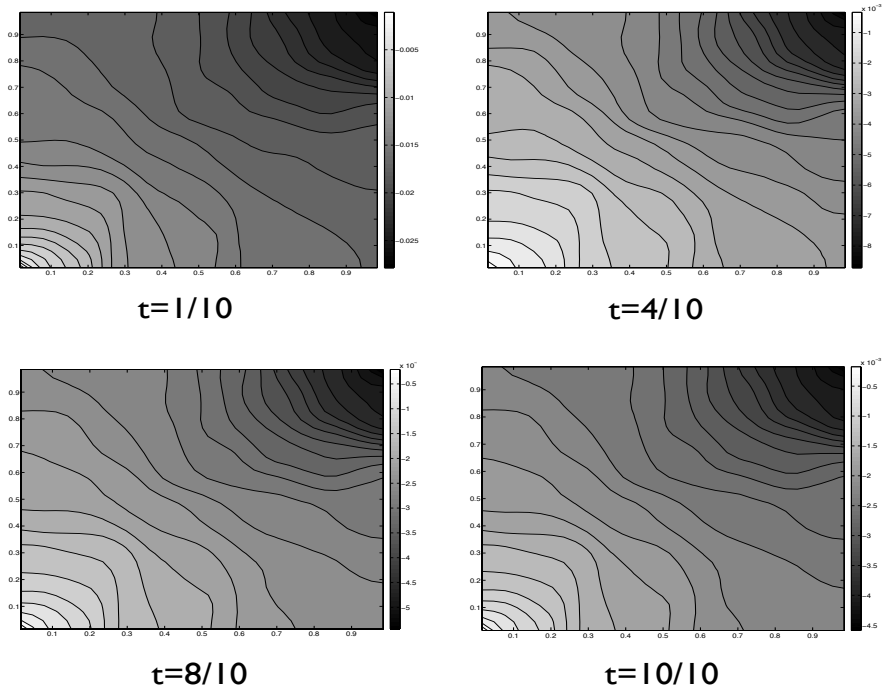

Figure 5.10 Pressure profiles of CO_2 flooding

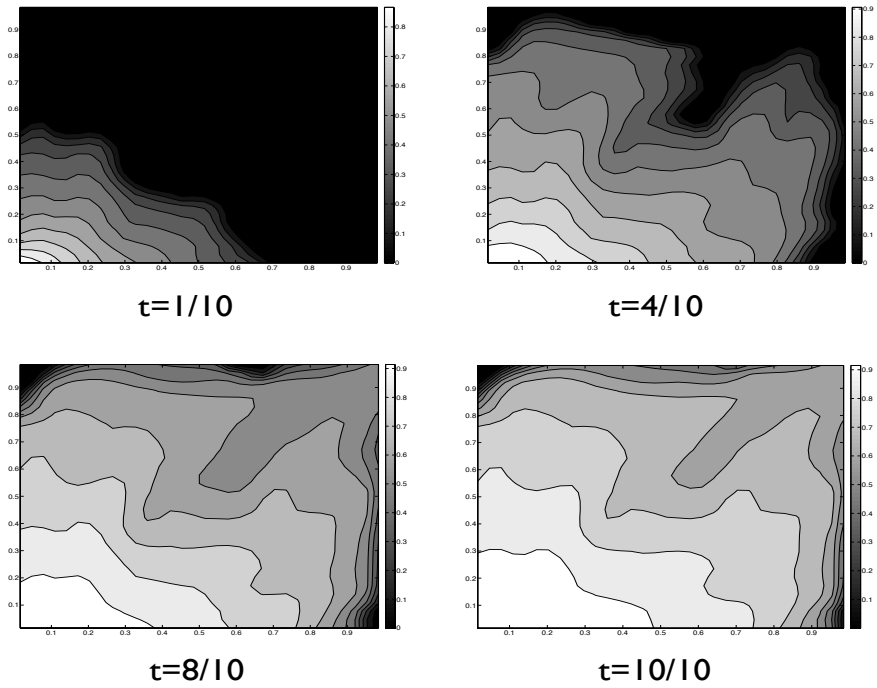

Figure 5.11 Saturation profiles of CO_2 flooding

5.4.3 The calculation of the amount of CO_2

Generally, the CO_2 for enhanced oil recovery is taken from CO_2 capture system of fossil fuel power plants. We assume that the CO_2 storage system is to be designed to handle 3.76 million standard cubic meter of new CO_2 per day [148].

Transportation of CO_2

Here, we should assume some parameters. It is assumed that the pipeline transports the captured CO_2 a distance of 100 km to the reservoirs pertinent to enhanced oil recovery. The transported CO_2 is mixed with recycled CO_2 and injected into the injection wells (Figure 5.4).

For transporation of CO_2, CO_2 should be compressed to bring up its pressure to the required pipeline inlet pressure. Although the pressure of CO_2 is depedent on the characteristics of the capture systems, we assume that the pressure of CO_2 from the sources is about 83 bar. The pressure should increase approximately 150-200 bar. Since the inlet pressure depends on the condition of wells (the conditions of wells can be different from the wells even in same reservoirs), we can adopt the value of inlet pressure as 153 bar. Also we assumed that the flow rate of CO_2 is 7,389 ton/day (3.76 Mm^3/day). And the emission by pipeline transportation is from the construction and decommissioning of compressors and steel pipeline. Thus, the CO_2 emission can be calculated as follows:

Table 5.3 CO_2 emissions from the transportation

	CO_2 emission (ton/yr)
Compression	1,598
Construction	6.1
Decommissioning	0.6
Pipeline construction	913
Pipeline decommission	91
Total	2,610

Enhanced oil recovery process

As mentioned, the amount of CO_2 in which we are interested encompasses a wide range of enhanced oil recovery processes. These are injection, recycling, sequestration to reservoir, and emission to the atmosphere. The amount of CO_2 injected is decision variable among them. From the prior numerical results, we can obtain the amount of CO_2 sequestrated (Figure 5.12 top). Supplementally, we are to present the production profiles of ideal flooding and water flooding to show the efficiency of CO_2 flooding: we can see that the longer duration of the production profile of CO_2 flooding than that of water flooding. We normalize that the amounts of injection and production equal as 1.

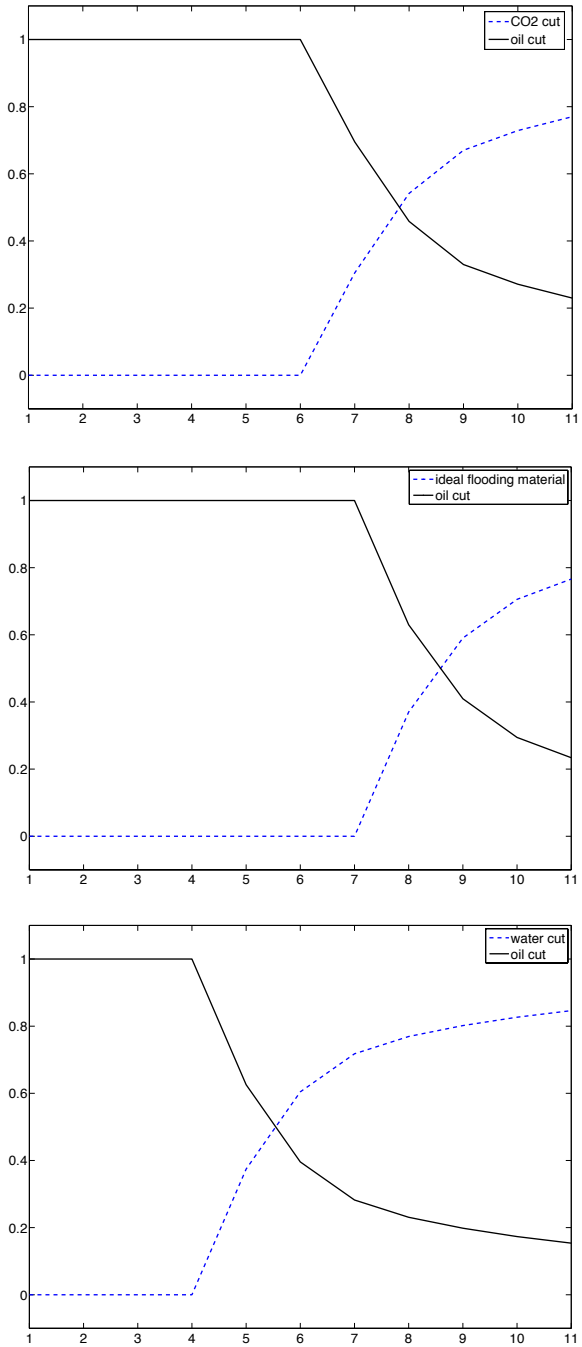

Figure 5.12 Production profile of various floodings

The amount of CO_2 injected equals the sum of the amount of CO_2 sequestrated (stored), recycled, and emitted.

$$\begin{aligned} q^c_{inj} &= q^c_{seq} + q^c_{re} + q^c_{emit} \\ q_{prod} &= q^c_{prod} + q^o_{prod} \\ q^c_{prod} &= q^c_{re} + q^c_{emit} \end{aligned} \tag{5.46}$$

where q denotes the amount of CO_2, and inj, seq, re and $emit$ denotes injection, sequestration, recycle, and emission, respectively. And the superscript c and o denote CO_2 and oil, respectively. Based on the basic equation, we can obtain optimal injection rate for CO_2 enhanced oil recovery and CO_2 sequestration. Setting the dynamic equation for sequestration, the change of the amount of CO_2 sequestration can be expressed:

$$\frac{dq^c_{seq}(t)}{dt} = \frac{dq^c_{inj}(t)}{dt} - \frac{q^c_{prod}(t)}{dt} \tag{5.47}$$

In this thesis, we assume that the amount of sequestration of CO_2 is proportional to the portion of the total injection.

$$\begin{aligned} \frac{dq^c_{seq}(t)}{dt} &= \frac{q^c_{inj}(t)}{q_{inj}(t)} \frac{dq^o_{prod}(t)}{dt} \\ c(t) &= \frac{q^c_{inj}(t)}{q_{inj}(t)} \end{aligned} \tag{5.48}$$

Also, the production of oil can be expressed by a decline rate, δ ($dq^o_{prod}/dt = \delta R(t)$). $R(t)$ is the amount of recoverable oil in the reservoir. The decline rate of overall oil production can be obtained from the historical data of mature reservoir because it is the properties of reservoir. We adopt that the decline rate can be calculated as[1] [144, 149]:

$$\delta(c) = 0.06 + \delta_1 c - \delta_2 c^2 \tag{5.49}$$

with parameters $\delta_1 = 0.2$ and $\delta_2 = 0.16$. Using this equation, we can identify the relation between oil production and CO_2 injection (Figure 5.13(a)). Also, we present the change of the amount of recoverable oil in the reservoir (Figure 5.13(b)).

From the result, we can see that the oil production increases to 0.625 of CO_2 injection. In the range over 0.625, the amount of sequestration increases, but the oil production decreases.

[1]This result is referred to 'Co-optimization of enhanced oil recovery and carbon sequestration' by A. Leach [144].

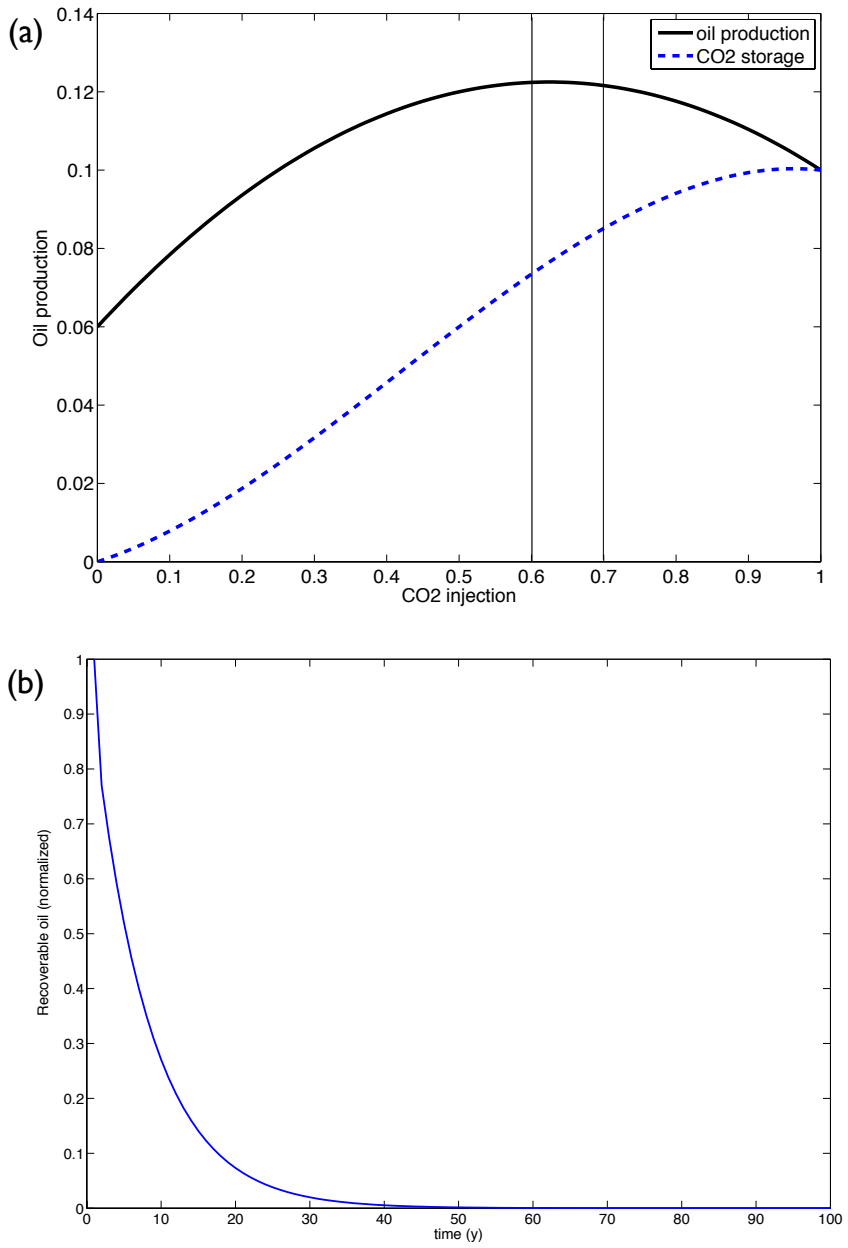

Figure 5.13 Relation between oil production and CO_2 sequestration (a), the change of recoverable oil with respect to time (b)

The amount of CO_2 sequestration and oil recovery can be calculated by introducing CO_2 effectiveness. CO_2 effectiveness is the required amount for recovery of 1 barrel of enhanced oil. It has scm/bbl or scf/bbl unit. CO_2 effectiveness of CO_2 enhanced oil recovery varies both one reservoir to another and within a reservoir itself [148]. In this thesis, we adopt the average value of CO_2 effectiveness, 170 (scm/bbl enhanced oil). Table 5.4 and Table 5.5 shows the design basis for enhanced oil recovery process and the amount of CO_2 emitted and sequestrated, respectively [148].

Table 5.4 Design basis of EOR process

	value	unit
CO_2 effectiveness	170	scm/bbl enhanced oil
Oil production per well	40	bbl/(day·well)
Total oil production	24,175	bbl/day
CO_2 flow rate	7,389	ton/day
Injector/producer	1.1	-
Maximum recycle ratio	3	-

Table 5.5 CO_2 emissions from the EOR

	CO_2 emission (ton/yr)
Power	128,378
Plant construction	343
Plant decommissioning	34
Recycle system	385
Sequestration	−1,968,456
Total	−1,839,316 (sequestrated)

5.4.4 The calculation of energy requirement

The complex procedures are needed to estimate the energy requirement for enhanced oil recovery. However, we simplify the model of enhanced oil recovery for our purpose. The energy requirement includes the work of pipeline transportation, electricity of equipments, and heat duty of units. Some rules of thumb have been derived to calculate energy requirements.

Transportation of CO_2

The captured CO_2 through various carbon capture processes should be moved to the reservoirs. There are two methods of the captured CO_2 transporation: pipeline and CO_2 carrier. In this thesis, we are to assume the CO_2 is moved by pipelines: the high-capacity CO_2 carrier has not developed yet. For life cycle assessment of transportation using pipelines, we need to know the diameter of the pipeline, the distance between CO_2 sources and reservoirs, the injection rate of CO_2, the efficiency of pumps, the temperature and pressure of CO_2 etc. Using these values, the velocity of CO_2 in pipeline can be calculated by [122]:

$$v = \frac{\dot{M}}{A \cdot \rho} \tag{5.50}$$

where v denotes velocity, $\dot{M}$ does mass flow rate, A does the cross-sectional area of pipeline, and ρ does the density of CO_2. The base

case design is based on a flow rate of 3.76 million standard cubic meter (approximately 7,389 ton) of CO_2 per day. It means that the amount of captured CO_2 is originated from about 400 MW CO_2 captured system in power plant such as intergrated gasification combined cycle, IGCC. We adopt that the diameter of pipeline is 12-inch [148] and the density of CO_2 at 200 bar, 20 °C is 770 kg/m^3. From Equation (5.50), the velocity of CO_2 in pipelines is approximately 5.483 km/h.

Then, the pressure drop can be obtained by:

$$\Delta P = \frac{2 \cdot f \cdot \rho \cdot v^2 \cdot L}{d} \tag{5.51}$$

where ΔP denotes the pressure drop, f does dimensionless Fanning friction factor, L does the length of the pipelines, and d does the diameter of pipe. It is assumed that the length between intermediate CO_2 terminal and injection well is 100 km. The dimensionless Fanning friction factor is one-fourth of the Darcy friction factor. Darcy friction factor represents the friction losses in pipe flow. When the flow in pipeline is laminar, Darcy friction factor equals $64/Re$, where Re is Reynolds number ($Re = \rho v d/\mu$). If the flow in pipeline is turbulent flow, Darcy friction factor is given by Colebrook equation.

$$\frac{1}{\sqrt{f}} = -2\log(\frac{\varepsilon}{3.7d} + \frac{2.51}{Re\sqrt{f}}) \tag{5.52}$$

where ε indicates roughness factor, we assume that this value is 0.000046

m. Since Re is greater than 4,000, we should adopt Equation (5.52) to obtain Fanning friction factor, f. As a result, we can calculate that f is approximately 0.013. Finally, we can calculate the work for transportation of CO_2. Using Bernoulli equation, the work is expressed as:

$$W_{trans} = \frac{\Delta P}{\rho} \tag{5.53}$$

Then, the pressure drop is about 152.3 bar and the work required for transportation in pipeline can be obtained approximately 19,787 J/kg.

Enhanced oil recovery process

Energy requirement of CO_2 enhanced oil recovery mainly includes compression for injection, transportatin of CO_2, separation of the produced oil, recycling of CO_2 (Figure 5.14) [126]. It is assumed that CO_2 capture process is excluded in the scope and pure CO_2 is supplied to life cycle of CO_2 enhanced oil recovery proecess.

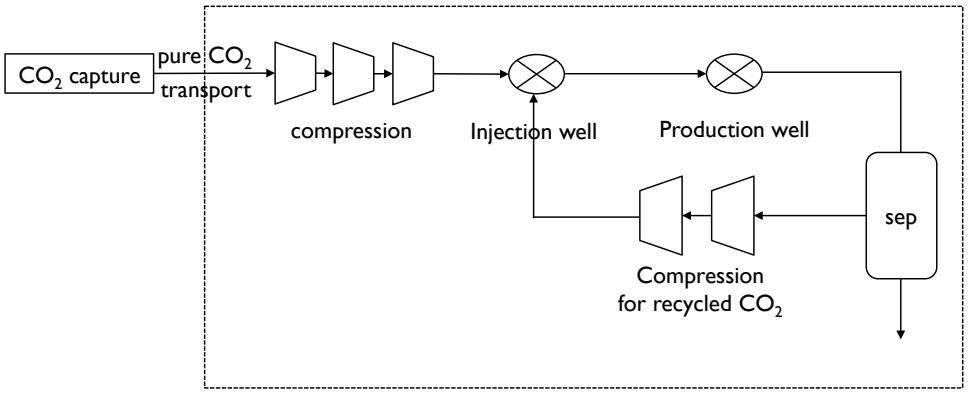

Figure 5.14 Typical CO_2 enhanced oil recovery operation

For the compression steps, the number of compression steps should be considered. The compression steps would require multi-stage compression process, stationary, adiabatic, and isentropic process etc [122]. In order to calculate the required energy in the compression work, every compression stage should have the same degree [122, 150]. The compression ratio can be calculated by:

$$\frac{P_i}{P_{i-1}} = (\frac{P_n}{P_0})^{\frac{1}{n}} \tag{5.54}$$

where P_i/P_{i-1} is compression ratio, P_n is discharge pressure, P_0 is intake pressure, and n is the number of stages. To identify mass, energy, and entropy balances of the compression system, we can adopt the simplified equations:

For mass balance;

$$\frac{dM_{in}}{dt} + \frac{dM_{out}}{dt} = 0 \tag{5.55}$$

For energy balance;

$$\frac{dM_{in}h_{in}}{dt} + \frac{dM_{out}h_{out}}{dt} + W = 0 \tag{5.56}$$

where h is specific enthaply and W denotes work.

For entropy balance;

$$\begin{aligned} \frac{dM_{in}S_{in}}{dt} + \frac{dM_{out}S_{out}}{dt} + W = 0 \\ S_{in} = S_{out} \end{aligned} \tag{5.57}$$

where S denotes the specific entropy.

We assume that the pressure of compressed CO_2 is 200 bar and the compressor efficiency is 85%. Then, we can obtain the required energy for CO_2 compression. From the calculation, we can obtain the result that we need three compressors. We adopt the compression ratio of 10 [151]. The number of compressors is highly dependent on the

pressure of the inlet stream. If the pressure drop is reduced by interim compressors during the transportation, the number of compressors for enhanced oil recovery can be reduced. We should consider the required energy for injection, sequestration, and recycle systems. To calculate these values, we adopt the data from [126] and simulation results. As results, the compressions of inlet CO_2 and recycled CO_2 consume the power of 24,023 kW, 6,489 kW, respectively, and CO_2 sequestration process including injection and separator requires the power of 25,142 kW (Table 5.6).

Table 5.6 Energy consumptions for CO_2-EOR

		unit: (kW)
CO_2 compression	inlet	24,023
	recycle	6,489
CO_2 sequestration		25,142

5.5 Results and their implications

A optimal decision to induce enhanced oil recovery or decommsion the reservoir can be made using approximate dynamic programming. Since we can not know the transition probability of reservoir state exactly, we should introduce the post-decision-state-based approximate dynamic programming and estimate value and decision. The algorithm avoids looping over all states and use of transition probability. It is assumed that only the mature (existing) reservoirs are used for enhanced oil recovery. Among the feasible reservoirs, those pressures are greater than the minimum miscible pressure, the profitable reservoirs should be selected and the future operating state also should be predicted. Moreover based on the numerical results and prediction of reservoir state, optimal strategies of operation state for CO_2 enhanced oil recovery can be achieved (e.g. decision of operation, CO_2 injection rate, and injection scheduling). The optimal strategy is dependent on the profit of enhanced oil recovery process and it is obtained by the profit from oil recovered, production cost including capital cost, O&M cost and energy consumption, and profit from CO_2 sequestration.

$$\text{Total profit} = \begin{cases} p_{1,oil} - c_1 + p_{1,CO_2} & \text{if } d = 1 \\ -c_2 - p_{1,CO_2} & \text{if } d = 2 \\ -c_3 - p_{1,CO_2} & \text{if } d = 3 \end{cases} \tag{5.58}$$

Here, d indicates the decision of operating state, active (1), inactive (2), decommissioning (3), respectively. $p_{1,oil}$ and p_{1,CO_2} means the profit from recovered oil and sequestrated CO_2. The profit from CO_2 sequestration is regarded as the product of the amount of CO_2 sequestrated and CO_2 price. c_1 denotes the sum of capital cost, O&M cost and energy consumption of processes. c_2 and c_3 denotes inactive fixed cost and decommissiong cost, respectively.

Finally, we are to analyze the effect of external factors (e.g. oil price, CO_2 price). To achieve these steps, some 'rules of thumb' are used to define the parameters needed to perform economic analysis of a CO_2 enhanced oil recovery process. In addition to the case of design basis, several real reservoir information are introduced to compare the results [148]. The adopted reservoirs are listed as follows:

Table 5.7 Reservoir information for ADP

Reservoir	EOR production (bbl/day)	Estimated ultimate EOR (million bbl)	Estimated ultimate CO_2 sequestrated (10^9 scm)	Estimated CO_2 effectiveness (scm/bbl)
Design basis	24,175	300	30	170
Wasson (Denver)	29,000	348	47	136
Rangely Weber Sand	11,208	136	17	127
SACROC	9,000	169	26	153

Also, we adopted the price values in Table 5.8 [148].

Table 5.8 Adopted cost parameters for EOR

	adopted value	unit
Wellhead oil price	50	\$/bbl
Power cost	0.044	\$/kWh
CO_2 cost	40	\$/tCO_2
Estimated capital cost (including compressor)	182 mil.	\$
Estimated O&M cost	27 mil.	\$

From the analysis of inventories and post-decision-state-based approximate dynamic programming, we can obtain the optimal decision of operating state for CO_2 enhanced oil recovery (Table 5.9[2]) and the value iterations (Figure 5.15). To approximate value function, we adopted a parameter estimation technique using a stochastic gradient algorithm. Value update was given by [35]

$$\bar{v}_a^n = \bar{v}_a^{n-1} - \alpha_{n-1}(\bar{v}_a^{n-1} - \hat{v}_a^n) \tag{5.59}$$

This update is a step to solve

$$\min_v \mathbb{E}\frac{1}{2}(v - \hat{v})^2 \tag{5.60}$$

[2]1: active, 2: inactive, 3: decommissioned

To parameterize the value function, we can introduce θ-function.

$$\min_{v} \mathbb{E}\frac{1}{2}(\bar{V}_a(\theta) - \hat{v})^2 \tag{5.61}$$

Applying stochastic gradient algorithm, we can update θ coefficients.

$$\bar{\theta}^n = \bar{\theta}^{n-1} - \alpha_{n-1}(\bar{V}_a(\bar{\theta}^{n-1}) - \hat{v}(\omega^n))\nabla_\theta \bar{V}_a(\theta^n) \tag{5.62}$$

Since a stochastic gradient algorithm requires the value of starting estimate, $\bar{\theta}^0$, we set $\theta^0 = 0$.

Table 5.9 Optimal decision of operating state

Time	Design basis	Wasson	Rangely Weber Sand	SACROC
Year 1	1	1	2	2
Year 2	1	1	2	2
Year 5	1	1	2	2
Year 10	1	1	1	1
Year 15	2	1	1	1
Year 20	2	2	2	1
Year 30	2	2	2	2

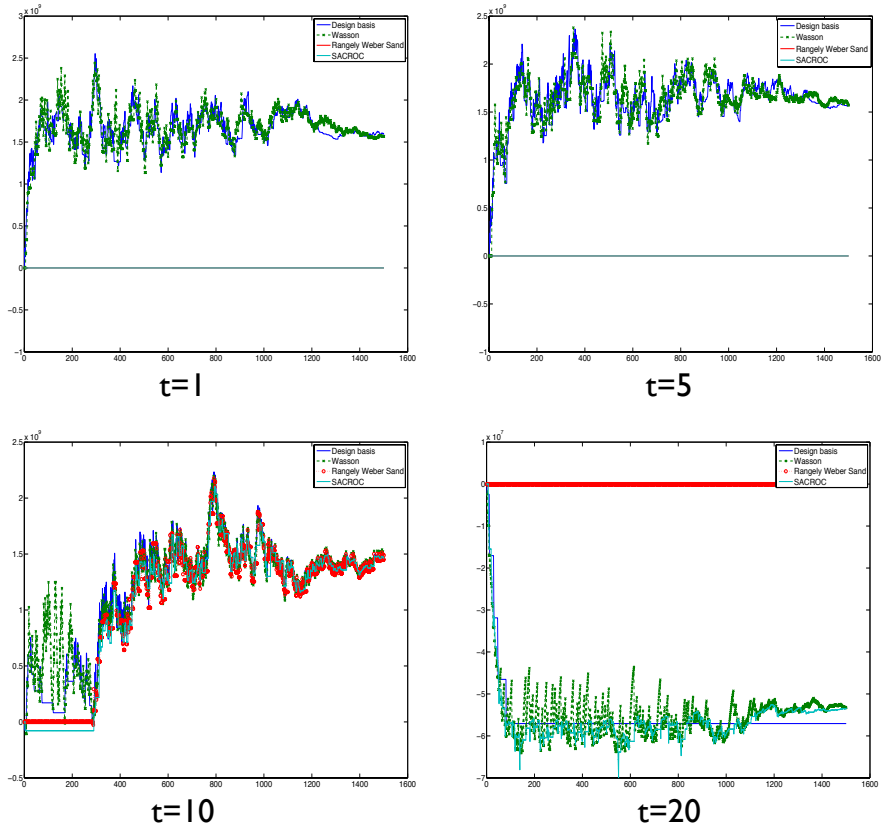

Figure 5.15 Value iterations of using post-decision-state-based approximate dynamic programming

Then, we analyze the effect of external factors (Figure 5.16 and Figure 5.17). The external factors which are considered in this study are CO_2 price and oil price. First, we fixed the CO_2 price as \$ 40/tCO_2 and made changes in oil price (\$ 50-200/bbl) in Figure 5.16. As the oil price increases, the duration of oil recovery increases and the CO_2 injection rate decreases slightly. Secondly, we fixed the oil price as \$ 100/bbl and made changes in CO_2 price (\$ 10-100/tCO_2) in Figure 5.17. As the CO_2 price increases, the duration of oil recovery decreases dramatically in case of \$ 100/tCO_2, and the CO_2 injection rate increases slightly.

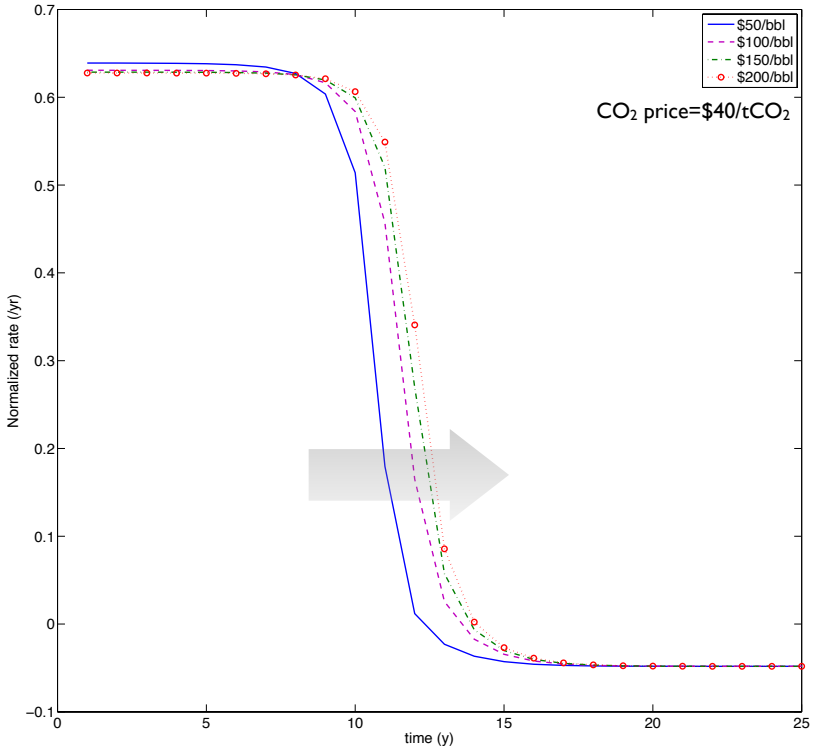

Figure 5.16 Change of optimal injection rate with respect to oil price

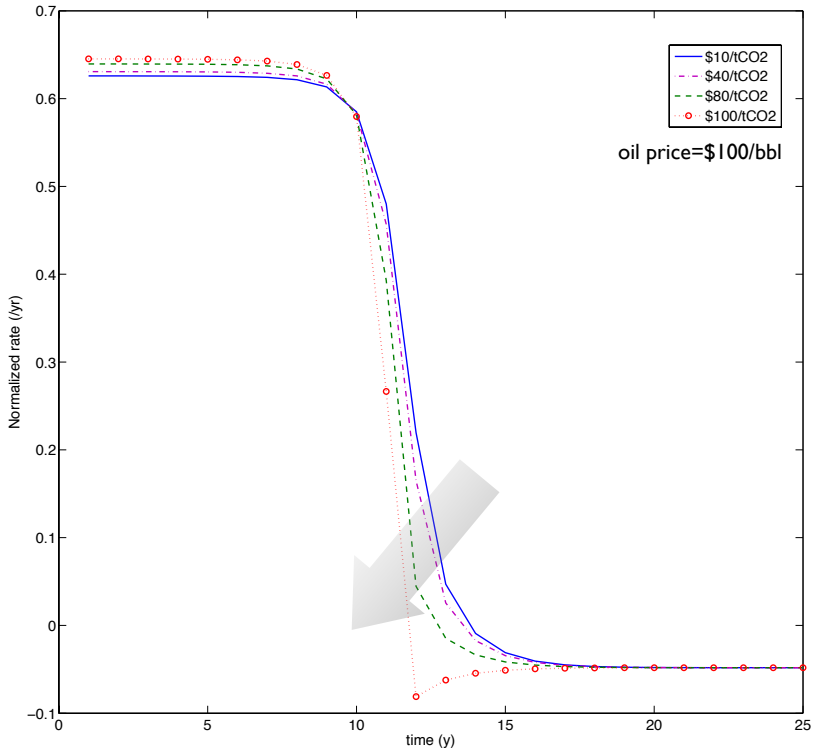

Figure 5.17 Change of optimal injection rate with respect to CO_2 price

Chapter 6

Conclusion

This thesis has presented the decision making procedures for mitigation of carbon dioxide emission and energy consumption of some case studies and their availability. The proposed procedures are based on life cycle assessment, which is an efficient methodology to identify environmental impact. Typical procedure of a life cycle assessment includes goal and scope definition, inventory analysis, impact assessment, and interpretation of result. Through the procedure, a decision maker would be able to improve production system and decide optimal planning or policy: the life cycle assessment would provide valuable information with respect to environmental effect, especially. The goal described in this thesis was the enhancement of process sustainability. The process sustainability in the thesis was defined as the reduction of CO_2 emission and energy consumption of the life cycle. Since handling the whole

scope of life cycle can be cumbersome works, the scopes and inventories of the life cycle of processes have been specified by proper viewpoints referring to the cases. Life cycle of processes consists of manifold inventories, and some methods have been introduced to analyze inventories of the process.

For process simulation, a commercial process simulator, ASPEN Plus, was introduced. This was used for the simulation case of dimethyl ether production system. Three of potential raw materials, natural gas, coal and waste wood, were selected for dimethyl ether production. Practical data and assumptions were adopted for the simulation. From the simulation results, the life cycle assessment could be performed. CO_2 intensity, energy intensity, and cost intensity were suggested to assess the sustainability of dimethyl ether production process. Through the assessment of the system, we can evaluate the sustainable competitiveness of each raw material for dimethyl ether production.

Next, the inventories which are difficult to be simulated by commercial process simulator have been modeled using mathematical and numerical modeling. In this thesis, the mathematical modeling with nonlinearity has been suggested for the case of energy planning including renewable energy systems. This is for estimation of the optimal energy planning. To optimize the capacities of energy systems, the minimization of total production cost was performed during the life cycle of energy systems. In addition to deterministic optimization, the uncer-

tain factors which can be varied with time or situations were considered for robust optimization of energy planning. The uncertain factors we adopted were learning rate, CO_2 price, and fuel cost. Monte Carlo simulation was introduced to handle these uncertainties. Through the simulation, we could estimate the range of total production cost and analyze the sensitivity of the uncertainties. With some practical constraints, the capacities of energy systems could be predicted in the future.

Finally, the numerical modeling has been proposed for the case of CO_2 enhanced oil recovery process. For calculation the amount of CO_2 of the process, we had to model the reservoir for enhanced oil recovery. Thus, the finite volume method has been introduced for the case of reservoir modeling. Based on Darcy's law and basic continuity equation, the transport phenomena of miscible flow of CO_2 and oil in the porous reservoir were modeled. The partial differential equations of pressure and saturation of miscible flow in porous media were derived. Since each partial differential equations were strongly coupled, we introduced two point flux approximation (of finite volume method) to solve the equations numerically. Using numerical results, we applied to life cycle assessment of CO_2 enhanced oil recovery. As an impact assessment, the amount of CO_2 emission and energy consumption were calculated to judge the state of feasible reservoirs in the future. There were a number of dimensions to decide the state of reservoirs. In this step, we used approximate dynamic programming to reduce dimensionality of

the proposed model.

In brief, this thesis suggested the revised method for improvement of process systems. Life cycle assessment-based procedures could contribute to decision making strategies for mitigation of CO_2 emission and energy consumption. Through three of practical case studies, which are for the promotion of energy security and mitigation of CO_2 emission, the availability of the proposed methods were shown and the valuable implications were drawn. Also, we introduced some proper techniques for analysis of various inventories. This would provide the solution method for complicated modeling of other cases (e.g. robust optimization, solving partial differential equation etc.).

Based on the proposed method in this thesis, there are several potentials for future work. Although we performed steady-state simulation for dimethyl ether production system, a dynamic simulation can increase the effectiveness of results in the case of using commercial process simulator. Because the life cycle assessment implies the flux of time as a 'life cycle' of process. Moreover the life cycle assessment can provide the optimal control strategies, if we simulate or model the process dynamically. In the case of CO_2 enhanced oil recovery, we made the dynamic model, however, the optimal control scheme is not obtained for reservoir management yet. Applying a model predictive control to reservoir modeling will be a appropriate approach for optimal operation of enhanced oil recovery process.

Bibliography

[1] US Environmental Protection Agency, Life cycle assessment. www.gdrc.org/uem/lca/lca-define.html.

[2] Web, Life-cycle assessment. en.wikipedia.org/wiki/Life-cycle_assessment.

[3] Scientific Applications International Corporation, Life Cycle Assessment: Principles and Practice, Tech. Rep. May (2006).

[4] L. Jacquemin, P.-Y. Pontalier, C. Sablayrolles, Life cycle assessment (LCA) applied to the process industry: a review, The International Journal of Life Cycle Assessment (2002). doi:10.1007/s11367-012-0432-9.

[5] ISO, ISO 14044, Tech. rep., International Organization for Standardization (2006).

[6] ISO, ISO 14040, Tech. rep., International Organization for Standardization (2006).

[7] EPD, The International EPD system - Environmental Product Declaration. www.environdec.com/en/The-EPD-system/.

[8] Ecomii, Cradle-to-Cradle definition. www.ecomii.com/ecopedia/cradle-to-cradle (2010).

[9] C. Jimenez-Gonzalez, S. Kim, M. Overcash, LCA Methodology Methodology for Developing Gate-to-Gate Life Cycle Inventory Information, Energy 5 (3) (2000) 153–159.

[10] C. Jimenez-Gonzalez, A. Curzons, D. Constable, V. Cunningham, LCA Case Studies LCA Case Studies Cradle-to-Gate Life Cycle Inventory and Assessment of Pharmaceutical Compounds, International Journal of Life Cycle Assessment 9 (2) (2004) 114–121.

[11] United Nations, Our Common Future. www.un-documents.net/ocf-02.htm (2010).

[12] United Nations, Report of the World Commission on Environment and Development. www.un-documents.net/wced-ocf.htm (2009).

[13] D. Botkin, Discordant Harmonies, a New Ecology for the 21st century, New York: Oxford University Press, 1990.

[14] CAPD, CAPD - Center for Advanced Process Decision-making. http://capd.cheme.cmu.edu/software.html (2012).

[15] M. R. Eden, A. Abdelhady, Introduction to Aspen Plus simulation.

[16] NETL, Carbon Dioxide Enhanced Oil Recovery, Tech. Rep. 4649 (May 2008). doi:10.1126/science.224.4649.563.

[17] J. Wittwer, Monte Carlo Simulation Basics. www.vertex42.com/ExcelArticles/mc/MonteCarloSimulation.html (2004).

[18] D. Hubbard, How to measure anything: Finding the value of intangibles in business, John Wiley & Sons., 2007.

[19] D. Hubbard, The failure of risk management: why it's broken and how to fix it, John Wiley & Sons., 2009.

[20] Web, Web data (Coal price), www.kocoal.or.kr/board/list.php?table=1038 (2011).

[21] B. D. Ripley, Stochastic simulation, John Wiley & Sons., 1987.

[22] S. S. Sawilowsky, You think you've got trivials?, Journal of Modern Applied Statistical Methods 2 (1) (2003) 218–225.

[23] S. S. Sawilowsky, G. C. Fahoome, Statistics via Monte Carlo simulation with Fortran, Rochester Hills, 2003.

[24] M. H. Kalos, Monte Carlo methods, Wiley, 2008.

[25] J. H. Davenport, Primality Testing Revisited, in: ISSAC '92, 1992, pp. 123–129.

[26] D. Vose, Risk Analysis, A Quantitative Guide, John Wiley & Sons., 2008.

[27] Web, Monte Carlo Simulation- What Is It and How Does It Work. www.palisade.com/risk/monte_carlo_simulation.asp.

[28] R. Eymard, T. R. Gallouet, R. Herbin, The finite volume method: Handbook of Numerical Analysis, 2000.

[29] J. r. E. Aarnes, T. Gimse, K. A. Lie, An Introduction to the Numerics of Flow in Porous Media using Matlab, Tech. rep.

[30] J. Ambrus, C. R. Maliska, F. S. V. Hurtado, A. F. C. da Silva, Finite volume methods with multi-point flux approximation with unstructured grids for diffusion problems, Defect and Diffusion Forum 297-301 (2010) 670–675.

[31] I. Aavatsmark, Multipoint flux approximation methods for quadrilateral grids, 9th International Forum on Reservoir Simulation (December).

[32] S. Dasgupta, C. H. Papadimitriou, U. V. Vazirani, Algorithms, McGraw-Hill, 2007.

[33] J. Rust, Dynamic Programming, no. 301, 2006.

[34] J. H. Lee, W. Wong, Approximate dynamic programming approach for process control, Journal of Process Control 20 (9) (2010) 1038–1048. doi:10.1016/j.jprocont.2010.06.007.

[35] W. B. Powell, Approximate dynamic programming: Solving the curses of dimensionality, Vol. 41, 2007. doi:10.1080/07408170802189500.

[36] T. J. Sargent, Dynamic Macroeconomic Theory, Vol. 2, 1987.

[37] T. H. Cormen, C. E. Leiserson, R. L. Rivest, C. Stein, Introduction to Algorithms, MIT press and McGraw-Hill, 2001.

[38] W. C. Wong, J. H. Lee, Postdecision-State-Based Approximate Dynamic Programming for Robust Predictive Control of Constrained Stochastic Processes, Industrial & Engineering Chemistry Research (2011) 1389–1399.

[39] H. Kim, A study on the sustainability of DME production system from various energy feedstocks (2011).

[40] Ministry of Knowledge Economy, National Energy Plan 2008-2030, Tech. rep., Ministry of Knowledge Economy (2008).

[41] T. a. Semelsberger, R. L. Borup, H. L. Greene, Dimethyl ether (DME) as an alternative fuel, Journal of Power Sources 156 (2) (2006) 497–511. doi:10.1016/j.jpowsour.2005.05.082.

[42] C. Arcoumanis, C. Bae, R. Crookes, E. Kinoshita, The potential of di-methyl ether (DME) as an alternative fuel for compression-ignition engines: A review, Fuel 87 (7) (2008) 1014–1030. doi:10.1016/j.fuel.2007.06.007.

[43] H. Kim, K. Han, E. S. Yoon, Development of Dimethyl Ether Production Process Based on Biomass Gasification by Using Mixed-Integer Nonlinear Programming, Journal of Chemical Engineering of Japan 43 (8) (2010) 671–681.

[44] E. S. Yoon, C. Han, A Review of Sustainable Energy – Recent Development and Future Prospects of Dimethyl Ether (DME), in: 10th International Symposium on Process Systems Engineering-PSE2009, Vol. 27, Elsevier Inc., 2009, pp. 169–175. doi:10.1016/S1570-7946(09)70249-4.

[45] E. G. Lindfeldt, M. Saxe, M. Magnusson, F. Mohseni, Strategies for a road transport system based on renewable resources – The case of an import-independent Sweden in 2025, Applied Energy 87 (6) (2010) 1836–1845. doi:10.1016/j.apenergy.2010.02.011.

[46] D. Song, W. Cho, G. Lee, D. K. Park, E. S. Yoon, Numerical Analysis of a Pilot-Scale Fixed-Bed Reactor for Dimethyl Ether (DME) Synthesis, Industrial & Engineering Chemistry Research 47 (13) (2008) 4553–4559. doi:10.1021/ie071589e.

[47] International Energy Agency, World Energy Outlook 2008, Tech. rep. (2008).

[48] Y. Ohno, N. Inoue, K. Okuyama, T. Yajima, D. M. E. Development, New Clean Fuel DME, in: International Petroleum Technology Conference, 2005, pp. 1–5.

[49] R. Vakili, E. Pourazadi, P. Setoodeh, R. Eslamloueyan, M. Rahimpour, Direct dimethyl ether (DME) synthesis through a thermally coupled heat exchanger reactor, Applied Energy 88 (4) (2011) 1211–1223. doi:10.1016/j.apenergy.2010.10.023.

[50] F. Cherubini, A. H. Strø mman, Life cycle assessment of bioenergy systems: state of the art and future challenges., Bioresource technology 102 (2) (2011) 437–51. doi:10.1016/j.biortech.2010.08.010.

[51] S. Soimakallio, J. Kiviluoma, L. Saikku, The complexity and challenges of determining GHG (greenhouse gas) emissions from grid electricity consumption and conservation in LCA (life cycle assessment) – A methodological review, Energy 36 (12) (2011) 6705–6713. doi:10.1016/j.energy.2011.10.028.

[52] K. Dowaki, Y. Genchi, Life cycle inventory analysis on Bio-DME and/or Bio-MeOH products through BLUE tower process, The International Journal of Life Cycle Assessment 14 (7) (2009) 611–620. doi:10.1007/s11367-009-0092-6.

[53] M. Higo, K. Dowaki, A Life Cycle Analysis on a Bio-DME production system considering the species of biomass feedstock in Japan and Papua New Guinea, Applied Energy 87 (1) (2010) 58–67. doi:10.1016/j.apenergy.2009.08.030.

[54] L. Zhang, Z. Huang, Life cycle study of coal-based dimethyl ether as vehicle fuel for urban bus in China, Energy 32 (10) (2007) 1896–1904. doi:10.1016/j.energy.2007.01.009.

[55] P. Gangadharan, A. Zanwar, K. Zheng, J. Gossage, H. H. Lou, Sustainability assessment of polygeneration processes based on syngas derived from coal and natural gas, Computers & Chemical Engineering 39 (2012) 105–117. doi:10.1016/j.compchemeng.2011.10.006.

[56] H. Hao, H. Wang, L. Song, X. Li, M. Ouyang, Energy consumption and GHG emissions of GTL fuel by LCA: Results from eight demonstration transit buses in Beijing, Applied Energy 87 (10) (2010) 3212–3217. doi:10.1016/j.apenergy.2010.03.029.

[57] X. Ou, Y. Xiaoyu, X. Zhang, Life-cycle energy consumption and greenhouse gas emissions for electricity generation and supply in China, Applied Energy 88 (1) (2011) 289–297. doi:10.1016/j.apenergy.2010.05.010.

[58] X. Ou, X. Yan, X. Zhang, Z. Liu, Life-cycle analysis on energy consumption and GHG emission intensities of alternative vehicle fuels in China, Applied Energy 90 (1) (2012) 218–224. doi:10.1016/j.apenergy.2011.03.032.

[59] S. Mangena, A. Brent, Application of a Life Cycle Impact Assessment framework to evaluate and compare environmental performances with economic values of supplied coal prod-

ucts, Journal of Cleaner Production 14 (12-13) (2006) 1071–1084. doi:10.1016/j.jclepro.2004.04.012.

[60] Y. Baek, W. Cho, H. C. Lee, The status of DME development and utilization as a fuel, Korean Industrial Chemistry News 13 (2) (2010) 1–11.

[61] US Environmental Protection Agency, Emission Facts, Tech. Rep. February, EPA (2005).

[62] International Energy Agency, World Energy Outlook 2010, Tech. rep. (2010).

[63] KOGAS, KOGAS, www.kogas.or.kr/kogas_kr/html/about/about_18.jsp (2011).

[64] PACE, Life Cycle Assessment of GHG Emissions from LNG and Coal Fired Generation Scenarios : Assumptions and Results, Tech. rep. (2009).

[65] I. H. Kim, S. Kim, W. Cho, E. Sup, Simulation of commercial dimethyl ether production plant, in: Computer Aided Chemical Engineering, Vol. 28, Elsevier B.V., 2010, pp. 799–804. doi:10.1016/S1570-7946(10)28134-8.

[66] M. Halabi, M. Decroon, J. Vanderschaaf, P. Cobden, J. Schouten, Modeling and analysis of autothermal reforming of methane to hydrogen in a fixed bed reformer, Chemical Engineering Journal 137 (3) (2008) 568–578. doi:10.1016/j.cej.2007.05.019.

[67] J. Lin, J. R. Lee, G. Wang, Dynamic Simulation for the Production of Dimethyl Ether from Natural Gas, in: AIChE proceedings, no. 2005, 2008, pp. 1–6.

[68] C. M. Silva, G. a. Gonçalves, T. L. Farias, J. M. C. Mendes-Lopes, A tank-to-wheel analysis tool for energy and emissions studies in road vehicles., The Science of the total environment 367 (1) (2006) 441–7. doi:10.1016/j.scitotenv.2006.02.020.

[69] D.-j. Sung, S.-h. Kang, Measurement of coal particle size and shape with concentrated coal-water mixtures, Korean Journal of Chemical Engineering 14 (1) (1997) 1–7.

[70] E. D. Larson, H. Yang, Dimethyl ether (DME) from coal as a household cooking fuel in China, Energy for Sustainable Development VIII (3) (2004) 115–126.

[71] K. Park, D. Shin, E. S. Yoon, The cost of energy analysis and energy planning for emerging, fossil fuel power plants based on the climate change scenarios, Energy 36 (5) (2011) 3606–3612. doi:10.1016/j.energy.2011.03.080.

[72] A. Schreiber, P. Zapp, W. Kuckshinrichs, Environmental assessment of German electricity generation from coal-fired power plants with amine-based carbon capture, The International Journal of Life Cycle Assessment 14 (6) (2009) 547–559. doi:10.1007/s11367-009-0102-8.

[73] X. Yan, R. J. Crookes, Life cycle analysis of energy use and greenhouse gas emissions for road transportation fuels in China, Renewable and Sustainable Energy Reviews 13 (9) (2009) 2505–2514. doi:10.1016/j.rser.2009.06.012.

[74] Korea Energy Economics Institute, KEEI annual report-2010, Tech. rep., KEEI (2010).

[75] E. Wetterlund, K. Pettersson, S. Harvey, Systems analysis of integrating biomass gasification with pulp and paper production – Effects on economic performance, CO2 emissions and energy use, Energy 36 (2) (2011) 932–941. doi:10.1016/j.energy.2010.12.017.

[76] B. Zaporowski, Analysis of energy-conversion processes in gas–steam power-plants integrated with coal gasification, Applied Energy 74 (3-4) (2003) 297–304. doi:10.1016/S0306-2619(02)00189-7.

[77] US Energy Information Administration, Natural gas price data, //205.254.135.7/naturalgas/weekly/ (2011).

[78] Web, Wood chip price data, www.daviddarling.info/encyclopedia (2011).

[79] Web, Select your Emission factor criteria, naei.defra.gov.uk/emissions/selection.php (2011).

[80] Web, Web data (DME price), price.alibaba.com/price/ (2011).

[81] K. E. E. Institute, Global energy changes and korean strategies for energy security, Tech. rep., Korea Energy Economics Institute (2008).

[82] S. Kim, J. Koo, C. J. Lee, E. S. Yoon, Optimization of Korean energy planning for sustainability considering uncertainties in learning rates and external factors, Energy Online (2012) 1–9.

[83] A. S. Kydes, J. Rabinowitz, Overview and special features of the time-stepped energy system optimization model, Resources and Energy 3 (1981) 65–92.

[84] A. Kanudia, R. Loulou, Robust responses to climate change via stochastic MARKAL : The case of Qufbec 1, European Journal Of Operational Research 7.

[85] D. Hill, V. L. Sailor, L. G. Fishbone, FUTURE U.S. ENERGY TECHNOLOGIES : COST AND OIL-IMPORT TRADEOFFS, Energy 6 (12) (1981) 1405–1431. doi:10.1016/0360-5442(81)90068-2.

[86] L. G. Fishbone, H. Abilock, Markal, a linear-programming model for energy systems analysis: Technical description of the bnl version, International Journal of Energy Research 5 (4) (1981) 353–375. doi:10.1002/er.4440050406.

[87] C. Cormio, A regional energy planning methodology including renewable energy sources and environmental constraints, Renewable and Sustainable Energy Reviews 7 (2) (2003) 99–130. doi:10.1016/S1364-0321(03)00004-2.

[88] Y. Cai, G. Huang, Z. Yang, Q. Lin, Q. Tan, Community-scale renewable energy systems planning under uncertainty—An interval chance-constrained programming approach, Renewable and Sustainable Energy Reviews 13 (4) (2009) 721–735. doi:10.1016/j.rser.2008.01.008.

[89] P. Krukanont, T. Tezuka, Implications of capacity expansion under uncertainty and value of information: The near-term energy planning of Japan, Energy 32 (10) (2007) 1809–1824. doi:10.1016/j.energy.2007.02.003.

[90] P. Viebahn, J. Nitsch, M. Fischedick, A. Esken, N. Supersberger, U. Zuberbu, Comparison of carbon capture and storage with renewable energy technologies regarding structural , economic , and ecological aspects in Germany, Solar Energy 1 (2007) 121–133. doi:10.1016/S1750-5836(07)00024-2.

[91] a. Chatzimouratidis, P. Pilavachi, Technological, economic and sustainability evaluation of power plants using the Analytic Hierarchy Process, Energy Policy 37 (2008) 778–787. doi:10.1016/j.enpol.2008.10.009.

[92] T. Kaya, C. Kahraman, Multicriteria renewable energy planning using an integrated fuzzy VIKOR & AHP methodology: The case of Istanbul, Energy 35 (6) (2010) 2517–2527. doi:10.1016/j.energy.2010.02.051.

[93] V. Krey, D. Martinsen, H.-J. Wagner, Effects of stochastic energy prices on long-term energy-economic scenarios, Energy 32 (12) (2007) 2340–2349. doi:10.1016/j.energy.2007.05.013.

[94] D. Streimikiene, Comparative assessment of future power generation technologies based on carbon price development, Renewable and Sustainable Energy Reviews 14 (4) (2010) 1283–1292. doi:10.1016/j.rser.2009.12.001.

[95] J. Koo, K. Han, E. S. Yoon, Integration of CCS, emissions trading and volatilities of fuel prices into sustainable energy planning,

and its robust optimization, Renewable and Sustainable Energy Reviews 15 (1) (2011) 665–672. doi:10.1016/j.rser.2010.07.050.

[96] H. T. Nguyen, I. T. Nabney, Short-term electricity demand and gas price forecasts using wavelet transforms and adaptive models, Energy 35 (9) (2010) 3674–3685. doi:10.1016/j.energy.2010.05.013.

[97] A. R. Brandt, R. J. Plevin, A. E. Farrell, Dynamics of the oil transition: Modeling capacity, depletion, and emissions, Energy 35 (7) (2010) 2852–2860. doi:10.1016/j.energy.2010.03.014.

[98] P. Kobos, J. Erickson, T. Drennen, Technological learning and renewable energy costs: implications for US renewable energy policy☆, Energy Policy 34 (13) (2006) 1645–1658. doi:10.1016/j.enpol.2004.12.008.

[99] F. Ferioli, K. Schoots, B. van der Zwaan, Use and limitations of learning curves for energy technology policy: A component-learning hypothesis, Energy Policy 37 (7) (2009) 2525–2535. doi:10.1016/j.enpol.2008.10.043.

[100] Y. Xie, Y. Li, G. Huang, Y. Li, An interval fixed-mix stochastic programming method for greenhouse gas mitigation in energy systems under uncertainty, Energy 35 (12) (2010) 4627–4644. doi:10.1016/j.energy.2010.09.045.

[101] J. Koo, K. Park, D. Shin, E. S. Yoon, Economic evaluation of renewable energy systems under varying scenarios and its implications to Korea's renewable energy plan, Applied Energy 88 (6) (2011) 2254–2260. doi:10.1016/j.apenergy.2010.12.063.

[102] J. M. Douglas, Conceptual design of chemical processes, 1988.

[103] P. Soderholm, T. Sundqvist, Empirical challenges in the use of learning curves for assessing the economic prospects of renewable energy technologies, Renewable Energy 32 (15) (2007) 2559–2578. doi:10.1016/j.renene.2006.12.007.

[104] a. McDonald, Learning rates for energy technologies, Energy Policy 29 (4) (2001) 255–261. doi:10.1016/S0301-4215(00)00122-1.

[105] U. K. Rout, M. Blesl, U. Fahl, U. Remme, A. Voß, Uncertainty in the learning rates of energy technologies: An experiment in a global multi-regional energy system model, Energy Policy 37 (11) (2009) 4927–4942. doi:10.1016/j.enpol.2009.06.056.

[106] E. Rubin, Learning curves for environmental technology and their importance for climate policy analysis, Energy 29 (9-10) (2004) 1551–1559. doi:10.1016/j.energy.2004.03.092.

[107] S. Yeh, E. S. Rubin, A centurial history of technological change and learning curves for pulverized coal-fired utility boilers, Energy 32 (10) (2007) 1996–2005. doi:10.1016/j.energy.2007.03.004.

[108] H. Winkler, A. Hughes, M. Haw, Technology learning for renewable energy : Implications for South Africa ' s long-term mitigation scenarios, Energy Policy 37 (11) (2009) 4987–4996. doi:10.1016/j.enpol.2009.06.062.

[109] J. Wang, Z. Zhou, A. Botterud, An evolutionary game approach to analyzing bidding strategies in electricity markets with elastic demand, Energy 36 (5) (2011) 3459–3467. doi:10.1016/j.energy.2011.03.050.

[110] US Energy Information Administration, Annual energy outlook 2011, Tech. rep. (2010).

[111] Korea Energy Management Corporation, Statistics on production and distribution of renewable energy in Korea during the year 2008, Tech. rep. (2009).

[112] R. Entriken, Decomposition and Importance Sampling for Stochastic Linear Models, Energy 15 (7) (1990) 645–659.

[113] P. J. Spinney, G. C. Watkins, Monte Carlo simulation techniques and electric utility resource decisions, Energy Policy 24 (2) (1996) 155–163. doi:10.1016/0301-4215(95)00094-1.

[114] S. Yu, J. Tao, Energy efficiency assessment by life cycle simulation of cassava-based fuel ethanol for automotive use in Chinese Guangxi context, Energy 34 (1) (2009) 22–31. doi:10.1016/j.energy.2008.10.004.

[115] S. H. Kim, T. H. Kim, Y. Kim, I.-g. Na, Korean energy demand in the new millenium : outlook and policy implications , 2000-2005, Energy Policy 29 (2001) (2005) 899–910.

[116] Web, Statistics of electric power in Korea, www.kepco.co.kr.

[117] International Energy Agency, World Energy Outlook 2011, Tech. rep. (2011).

[118] T. Ma, Y. Nakamori, Modeling technological change in energy systems – From optimization to agent-based modeling, Energy 34 (7) (2009) 873–879. doi:10.1016/j.energy.2009.03.005.

[119] S. Kim, C. Lee, Global Competitiveness Reinforcement of Korean Green Energy Industry, Tech. rep., Korea Energy Economics Institute (2011).

[120] W. J. Parkinson, G. F. Luger, R. E. Bretz, J. Osowski, Using an Expert system to explore enhanced oil recovery methods, Computers Electronic Engineering 20 (2) (1994) 181–197.

[121] E. G. Hertwich, M. Aaberg, B. Singh, A. H. Strø mman, Life-cycle Assessment of Carbon Dioxide Capture for Enhanced Oil Recovery, Chinese Journal of Chemical Engineering 16 (3) (2008) 343–353.

[122] A. Gaspar Ravagnani, E. Ligero, S. Suslick, CO2 sequestration through enhanced oil recovery in a mature oil field, Journal of Petroleum Science and Engineering 65 (3-4) (2009) 129–138. doi:10.1016/j.petrol.2008.12.015.

[123] M. Godec, V. Kuuskraa, T. Van Leeuwen, L. Stephen Melzer, N. Wildgust, CO2 storage in depleted oil fields: The worldwide

potential for carbon dioxide enhanced oil recovery, Energy Procedia 4 (2011) 2162–2169.

[124] F. van Bergen, J. Gale, K. Damen, A. Wildenborg, Worldwide selection of early opportunities for CO2-enhanced oil recovery and CO2-enhanced coal bed methane production, Energy 29 (9-10) (2004) 1611–1621. doi:10.1016/j.energy.2004.03.063.

[125] R. Booth, Miscible Flow Through Porous Media, Ph.D. thesis (2008).

[126] Electric Power Research Institute, Enhanced Oil Recovery Scoping Study, Tech. rep. (1999).

[127] Y. C. Yortsos, The relationship between immiscible and miscible displacement in porous media, AIChE Journal 33 (11) (1987) 1912–1915. doi:10.1002/aic.690331121.

[128] M. Bai, D. Elsworth, On the Modeling of Miscible Flow in Multi-Component Porous Media, Transport in Porous Media 21 (1995) 19–46.

[129] R. E. Ewing, NUMERICAL SIMULATION OF THE MULTI-PHASE.

[130] Z. Chen, G. Huan, Y. Ma, Computational Methods for Multiphase Flow in Porous Media, 2006.

[131] Web, en.wikipedia.org/wiki/Darcy's_law.

[132] M. Blunt, F. J. Fayers, F. M. Orr, Carbon dioxide in enhanced oil recovery, Energy Conversion and Management 34 (9) (1993) 1197–1204.

[133] A. Bourgeat, M. Jurak, Two phase partially miscible flow (2006).

[134] G. T. Eigestad, H. K. Dahle, B. Hellevang, F. Riis, W. T. Johansen, E. Ø ian, Geological modeling and simulation of CO2 injection in the Johansen formation, Computational Geosciences 13 (4) (2009) 435–450. doi:10.1007/s10596-009-9153-y.

[135] J. Douglas, J. E. Roberts, Numerical Methods for a Model for Compressible Miscible Displacement in Porous Media, Mathematics of Computation 41 (164) (1983) 441–459. doi:10.2307/2007685.

[136] W. Liu, Y. Yuan, Finite difference schemes for two-dimensional miscible displacement flow in porous media on composite triangular grids, Computers & Mathematics with Applications 55 (3) (2008) 470–484. doi:10.1016/j.camwa.2007.05.003.

[137] D. Yang, Simulation of Miscible Displacement in Porous Media by an Iterative Perturbation Algorithm Combined with a Characteristic Method, Computer methods in Applied Mechanics and Engineering 162 (1998) 359–368.

[138] R. M. Lansangan, M. Taylor, J. L. Smith, F. S. Kovarik, An improved viscosity correlation for CO2/reservoir oil systems, SPE Advanced Technology Series 1 (2) (1993) 134–141.

[139] M. K. Emera, H. K. Sarma, Prediction of CO 2 Solubility in Oil and the Effects on the Oil Physical Properties, Energy Sources, Part A: Recovery, Utilization, and Environmental Effects 29 (13) (2007) 1233–1242. doi:10.1080/00908310500434481.

[140] D. Gourgouillon, H. M. N. T. Avelion, J. M. N. A. Fareleira, M. Nunes da Ponte, Simultaneous viscosity and density measurement of supercritical CO -saturated PEG 400, The journal of supercritical fluids 13 (1998) 177–185.

[141] Advanced Resources International, Melzer Consulting, OPTIMIZATION OF CO 2 STORAGE IN CO 2 ENHANCED OIL RECOVERY, Tech. rep. (2010).

[142] C. Cooper, A technical basis for carbon dioxide storage, Energy Procedia 1 (1) (2009) 1727–1733. doi:10.1016/j.egypro.2009.01.226.

[143] F. J. Fayers, R. I. Hawes, J. D. Mathews, Some Aspects of the Potential Application of Surfactants or CO2 as EOR Processes in

North Sea Reservoirs, Journal of Petroleum Technology 9 (1981) 1617–1627.

[144] A. Leach, C. F. Mason, K. V. eld, Co-optimization of enhanced oil recovery and carbon sequestration, Resource and Energy Economics 33 (4) (2011) 893–912.

[145] E. Gilje, Simulation of viscous instabilities in miscible and immiscible displacement, Ph.D. thesis (2008).

[146] Web, CO2 properties, sfe.vemt.bme.hu/angol/supercritical.html.

[147] ZPlus, Oil Viscosity, Tech. rep. (2009).

[148] B. Bock, R. Rhudy, H. Herzog, M. Klett, J. Davison, D. De La Torre Ugarte, D. Simbeck, Economic evaluation of CO2 storage and sink enhancement options, Tech. rep. (2003).

[149] X. Guo, Z. Du, L. Sun, Y. Fu, Optimization of Tertiary Water-Alternate-CO 2 Flood in Jilin Oil Field of China : Laboratory and Simulation Studies, SPE International.

[150] C. J. Geankoplis, Transport Processes and Separation Process Principles, Prentice Hall, 2003.

[151] H. A. Kidd, H. F. Miller, Compression solutions for CO2 applications (Traditional centrifugal and supersonic technology), Engineer's notebook.

초 록

공정시스템의 탄소 배출 및 에너지 절감을 위한 의사결정 절차에 관한 연구

본 논문은 화학공정 시스템의 이산화탄소 배출과 에너지 소모 절감을 위한 의사결정 절차를 제안하고 여러 사례 연구를 다루고 있다. 지금까지 대부분의 화학공정은 비용의 효율 측면에서 최적화가 이루어졌고, 이를 바탕으로 설계, 개선되었다. 하지만 전 세계적으로 온실가스 규제, 에너지 사용절감 등 공정의 환경적인 측면의 제약이 많아짐에 따라, 화학공정의 운영은 더이상 비용이나 제품의 효율적인 측면만 중시할 수 없는 상황이 되었다. 그러므로 화학공정의 지속가능한 발전은 불가피한 것이 되었다. 지속가능한 발전을 위해 시스템 측면에서 의사결정이 필요한 몇 가지가 있는데, 원료의 선택, 공정 계획, 공정 운영 등을 들 수 있다. 그래서 도입할 수 있는 방법이 전과정 평가인데, 전과정 평가는 환경적으로 건전하고 지속가능한 발전을 실현하기 위해 원료, 제조, 유통, 소비, 폐기로 인한 자원, 에너지 소비 및 환경오염 부하를 최소화시키고 개선방안을 모색하는 방법이다. 기존의 전과정 평가는 하나의 제품에 국한되었던데 반해, 본 논문에서는 화학공정의 전과정을 범위로 설정하여 에너지 및 비용 뿐만 아니라 이산화탄소 배출과 같은 환경적인 요소를 고려할 수 있게 하였다.

먼저, 전과정 평가에 대한 설명 및 기본 구조를 살펴보도록 한다. 그리고 지속가능성을 위해 전과정 평가를 이용한 절차와 최적 의사결

정에 미치는 영향에 대해 살펴보았다. 전과정 평가는 목적과 범위의 설정이 중요한데, 본 논문에서 다루는 전과정 평가의 목적은 이산화탄소 배출량 에너지 사용의 최소화이다. 전과정의 범위는 각 사례 공정을 적절히 한정하였다. 그리고 전과정 평가의 범위에 포함되는 공정은 상용 공정 모사기와 수치해석적인 방법을 이용하여 구현하였다. 다음으로 공정의 전과정에 존재할 수 있는 불확실성을 고려하기 위해 몬테카를로 모사 기법을 적용하였다. 이는 전과정 평가의 신뢰성 있는 결과를 얻기 위해 수행되었다. 특히 화학공정에서의 의사결정은 불확실성을 자연적으로 내포하고 있기 때문에, 기존의 확정적인 모델과 달리 확률적 모델을 이용하는 것이 더 나은 결과를 얻을 수 있게 한다.

최적 운영 및 관리를 위한 접근방법으로는 근사 동적 계획법을 사용하였다. 기존의 동적 계획법이 차원수의 급격한 증가로 인해 계산하는데 어려움이 있는데 반해, 근사 동적 계획법은 계산해야할 차원수를 줄여 최적의 해를 찾는 방법으로 공정의 생산계획이나 일정관리, 원료의 배치 등에 유용하게 쓰일 수 있다. 특히 실제 화학공정에서는 차원수가 무한히 증가할 수 있으므로 근사 동적 계획법을 이용하여 차원수를 줄이는 것이 필요하다. 하지만 기본적인 근사 동적계획법 또한 각 상태의 값을 구하는 절차에서 다음 상태로의 기대값의 최적화를 수행해야하기 때문에 계산하기 힘든 단점을 갖고 있다. 이러한 단점을 극복하기 위해 결정 후 상태에 기반한 근사 동적 계획법을 이용하였다.

위 연구에서 제안된 절차는 사례 연구를 통해 그 효용성을 입증

한다. 첫번째 사례연구는 디메틸에테르 공정을 위한 원료 결정이다. 디메틸에테르는 전도유망한 신재생에너지로서 여러 원료를 이용해 합성할 수 있다. 이에 각 원료를 얻는 것으로부터 디메틸에테르를 합성하는 공정까지의 전과정을 상용 공정 모사기로 모사하였고, 그 전과정에 대해 이산화탄소와 에너지 효율 측면에서 영향평가를 수행하였다. 두번째 사례연구는 에너지 시스템의 생산계획 결이다. 불확실성을 가지는 미래 에너지 생산계획의 예측을 위해 확률적 모델을 기반으로 최적화를 수행하였다. 그 결과, 향후 각 에너지 생산계획의 범위를 제시하였고 불확실성 인자들의 민감도를 분석하였다. 세번째 사례연구는 이산화탄소 지중저장 및 원유 회수증진 공정 운영방법 결정이다. 이산화탄소 처리 방법 중 하나인 지중저장을 단순히 저장에 국한하지 않고 원유 회수증진에 이용하여 보다 지속가능한 발전을 모색하고자 한다. 여러 포집원에서 포집된 순도 높은 이산화탄소는 원유 회수증진에 매우 유용하게 사용될 수 있으며, 사례연구를 통해 원유 회수증진과 지중저장 사이에서 지속가능한 운영 전략을 제시하여 이산화탄소 처리 및 저장에 대한 의사결정을 지원하였다.

주요어: 최적 의사결정, 전과정 평가, 의사결정 절차, 지속가능성
학번: 2006-21334